Università degli Studi dell'Aquila
Dipartimento di Ingegneria e Scienze dell'Informazione e Matematica
Dottorato di Ricerca in Matematica e Modelli (XXXIV ciclo)

On a two-layers model of weakly coupled Kuramoto oscillators: Analysis and Dissipation theory

SSD MAT/05

Dottoranda

Astrid Herminia Correa Luces

Coordinatore del corso:
Prof. D. Gabrielli

Tutor:
Prof. D. Amadori
Prof. M. Colangeli

2023

This work is dedicated to Dr. Armando Brons for his constant support, wisdom and life reference.

Declaration

I hereby declare that except where specific reference is made to the work of others, the contents of this dissertation are original and have not been submitted in whole or in part for consideration for any other degree or qualification in this, or any other university. This dissertation is my own work and contains nothing which is the outcome of work done in collaboration with others, except as specified in the text and Acknowledgements.

Astrid Herminia Correa Luces
2023

Acknowledgements

First of all, I would like to express my sincere thanks to my supervisors Prof. Amadori and Prof. Colangeli for introducing me to the field of collective behavior and dissipation theory. I also thank them for their supervision, guidance and support during the research.

I would like to thank Prof. Rondoni for his fruitful collaboration that resulted in the results presented in Chapter 4. I also express my gratitude to Prof. Raluca Eftimie and Prof. Owen Jepps for accepting to be the reviewers of my manuscript. And to Prof. Corrado Lattanzio, Prof. Silvia Lorenzani, and Prof. Andrea Mentrelli for accepting to be members of the final Ph.D. Committee.

To the friends that helped me in every possible way: Elena De Dominicis, Jorge Guzman, Jon May, Nora Juhász, Maria Barrera and Monia Capanna. To all the people that brought a smile to my face during this Ph.D.: Alessandro, Alisbel, Diego, Danny, Filo, Ivan, Jose, Juan Pablo, Kwame, Roberto, Sandy, Shadi, Stas, Verča, Vidal and Yan.

To Davide and Richi those who have accompanied and supported me in this last stage of my theis.

I dedicate this thesis to my family. I am deeply indebted to my parents and my sister for their unconditional love. And finally to Dr. Brons, whose support and example have allowed me and my family to build a better life little by little.

Abstract

This thesis was written under a rather curious analytical eye on the behavior of Kuramoto oscillators. Note that ours are not the first eyes that fall on this type of oscillators, the good thing is that the dynamic system has multiple forms and questions, and, like the universe, mathematical theories continue to expand and give us more opportunities to analyze a problem in different ways, allowing us to cover every question we have. This is how we arrive at this thesis, where we work with two-layer oscillators, analyze their behavior and exploit their structure through the lens of dissipation theory.

In the first part of the thesis, we present the theory surrounding the Kuramoto model, from the first questions raised about the synchronization phenomenon, to the most significant properties of the model. We also establish the mathematical framework that will be used in the rest of the chapters of the thesis.

The second part of the thesis is focused on the proposed two-layer models, the work of systems over networks is quite popular nowadays since it allows us to apply them to a great variety of phenomena, such as human interactions, neuronal, electrical networks, among others. In general, they are studies focused on the general behavior of the system and not on the behavior of each layer, our interest goes beyond this uniform coupling and falls on the ability of each layer to achieve a synchronization state under a fairly weak coupling between layers, the study of the models under this perspective allows us to exploit the characteristics of its own topology. Thus, we analyze the stationary state of the system with identical oscillators and the behavior of the corresponding order parameters both analytically and via numerical simulations. Then, we study the case for non-identical oscillators, analyze the diameter of each layer and present the sufficient conditions to control the diameter. Moreover, our numerical results allow us to validate the presented theoretical derivation.

Finally, in the third part of the thesis, our focus is redirected to the study of dissipation theory. We make a review of the Dissipation Function and cast the Kuramoto model in the

framework of the exact response theory. We analyze the behavior of the Dissipation Function in the simplest case of two interactive oscillators as well in the presence of the N coupled oscillators. Then, we compare the predictions of linear response theory with those of the exact response theory. Finally, we extend our analysis to a model constituted by two sets (or "layers") of Kuramoto oscillators, interacting with one another via a small coupling constant ε. Our theoretical derivation is also complemented by numerical simulations of the Kuramoto dynamics.

Table of contents

Chapter 1

Introduction

This thesis is devoted to researching nonlinear systems of oscillators constrained to Kuramoto dynamics, the analysis of their behavior, and the exploration of the system in terms of the exact response theory.

This above sentence points out two of the three main topics of the thesis, the Kuramoto oscillators and the exact response theory. As a starting point, we consider the model introduced by Kuramoto [78] under a dynamic model to replicate the journey of these coupled self-sustained oscillators from their disarranged and isolated state to a coherent and connected state. This phenomenon is called synchronization and it is object of many books and monographs [12, 106, 123, 125]. It is persistently found in nature [17, 88, 129], in social science [95, 108] and in engineering [18, 92], among others. For this reason, different models have been proposed to describe this behavior [74, 89, 119, 134]; among them is the Kuramoto model, which since its formulation in 1975, has been widely studied [57, 91, 97, 120], modified [7, 140], extended [47, 55, 124] and applied to different phenomena [72]. One of the general forms of the model for N oscillators (see [36]) is given by:

$$\begin{cases} \dot{x}_i = \omega_i + K \sum_{j=1}^{N} W_{ij} \sin(x_j - x_i) \\ \sum_{j=1}^{N} W_{ij} = 1 \qquad\qquad \forall\, i = 1, \ldots, N, \\ x_i(0) = x_i^0 \end{cases} \tag{1.1}$$

where $x_i(t)$ represents the phase of the i oscillator at time t, $\omega_i \in \mathbb{R}$ is the natural frequency, K is the uniform coupling strength and $W_{ij} \in [0,1]$ is an element of the matrix encoding the topology of the network, in the classic Kuramoto model $W_{ij} = 1/N$. This generalization of the classic model is among many extensions in which networks are used to represent the oscillators' interaction [111]. This use is naturally justifiable in view of the advancement of the field of network sciences and the need to answer how the topology of the interaction influences the dynamic process and the possible patterns it can form.

This quest to understand how it affects the network structure led us to the study and analysis of oscillators under layered models, a pretty recent approach [68, 137] which represents the second main topic of the thesis. We mostly focused on models constituted by two groups of oscillators, in which each oscillator experiences a mean field interaction with the members of its own group and also a weaker interaction with all members of the other group. The presence of a coupling term between members of different groups can thus be regarded as a perturbation of the classical Kuramoto dynamics. This approach allows us to improve the modeling of real systems such as spreading processes [31], epidemic dynamics [52] and neuronal dynamics [10], in addition, consider a more complicated interaction that assumes an all to all connectivity, allow us to encounter other collective phenomena such as chimera states [2, 85], amplitude death [113], explosive synchronization [70], cluster synchronization [87] and so forth. Under this assumption, two types of connection between layers were considered. The first model follows the Singular Interlayer Connectivity, where each oscillator of one layer is connected with only one oscillator of the other layer, this type of configuration is called multiplex network, and the second model to be analyzed is with an Average Interlayer Connectivity where each oscillator weakly interacts with all the oscillators of the other layer. Under this type of connection, different oscillators' final states are studied depending on the natural frequency of each oscillator, in particular, the case where the oscillators have identical natural frequencies, the necessary conditions for the diameter between the oscillators of each layer to decrease and the behavior of the synchronization estimators proposed for the model. Then, we studied the case for nonidentical oscillators, and in the same way, we established the necessary conditions on the connection strengths of each layer to restrict the diameter of each layer. Different approaches [11, 22, 91] and techniques were used for these studies, from the differential diameter analysis [21, 34, 57] to the use of an energy function [61].

Finally, the exact response theory, based on the definition of the Dissipation Function and on the notion of transient mixing is the last topic of this thesis. Such theoretical framework makes it possible to study the Kuramoto dynamics both in its classical form and under

the connectivity frameworks presented above. This theory was developed with the aim of analyzing the response of particle systems to external perturbations [77, 86]. Such set-up fit nicely with the Kuramoto model if this is considered as a system in which each oscillator is initially driven only by its natural frequency until its dynamics gets suddenly perturbed by the classical Kuramoto-type of interaction with all the other oscillators. We start by reviewing the definition of the Dissipation Function [42], next we study the case of identical oscillators, and we then make a comparison with the standard linear response theory [41]. Finally, we adapt the system framework to consider the two-layer case with Average Interlayer Connectivity, from which we extract information about the divergence shape of the vector field and the dissipation function.

1.1 Outline of the thesis

In **Chapter 2**, we begin the introduction of Kuramoto oscillators with a summary of the history of the synchronization phenomenon, in it, we explain the first ideas that led to the creation of the Kuramoto model with its respective mathematical formulation and take as a practical example the behavior of fireflies. After this, we establish the mathematical concepts of synchronization and the different types of patterns that we will find in the dynamics of our model, and finally, we return to the classical Kuramoto model where we explain the main properties of the model which will be used in various demonstrations of the dynamics and compared with respect to the proposed layered models.

Chapter 3 presents the proposed layer models in detail, starting with their mathematical formulation; then, together with the proposed order parameters, we explain their properties and gradient flow formulation. Subsequently, we study the case for identical oscillators, where we present the form of their stationary solutions and the behavior of the order parameters with their respective numerical examples. Finally, we study the cases for non-identical natural frequencies, where we analyze the behavior of the oscillator diameters in each layer and of the system, in this analysis we present the sufficient conditions to control the diameters and we show different numerical results of the oscillator behavior under these conditions.

Finally, in **Chapter 4**, we review the essential elements and results of the exact response theory for the study of the classical Kuramoto model. There, we regard the Dissipation Function as the observable of interest and analyze its behavior both for the simplest case of two oscillators and for the case of N oscillators. After that, we present and compare the

linear response theory with respect to the exact response theory. At last, we use the exact response theory to study the onset of synchronization in a model made by two distinguished layers of oscillators, for different values of the interlayer coupling strength.

Chapter 2

General view of the Kuramoto model

2.1 Synchronization in a nutshell

> At the heart of the universe is a steady, insistent beat: the sound of cycles in sync (Strogatz, 2012).

It is evident that in the mind of a pattern seeker, such as a scientist, a phenomenon like synchronization will always stand out ([139],[104], [37],[109],[130]). Indeed, there are many natural and experimental phenomena associated with it. In the first recorded experiment of this phenomenon the components were expected to oscillate chaotically, but without looking for it, they began to influence each other and adjust the oscillation rate; this system was the Huygens's mechanical clocks described in his letters to the Royal Society in London [65] (Figure 2.1). After that, many phenomena of pulse-coupled oscillators have been studied [89], for instance, in the slime mold *Physarum polycephalum* has been observed synchronization phenomena in the cell's intrinsic cellular oscillation [129], in power grids [18, 92, 125], in social networks phenomena as waves of rhythmic applause [95] and in the opinion dynamics in a network of scientific collaborations [108]. However, in the same way that synchronization can be part of the behavior of the system and in some cases benefits it, its appearance like a stable state can push the system to an unwanted critical value, causing damage, as in the case of the pacemaker cells system in the heart generating heart attacks [88, 131] or epileptic seizures in our brain and neuronal system [94, 110, 117, 118, 126]. The last of our examples will be the flashing of fireflies studied by Buck and Buck [17]. We will use this example as a guide during the analysis of the construction of the most popular synchronization mathematical models.

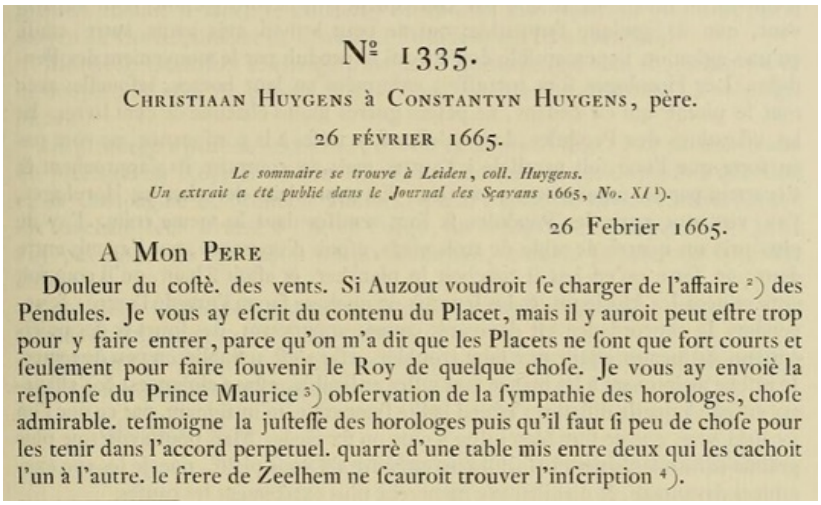

N^o 1335.

CHRISTIAAN HUYGENS à CONSTANTYN HUYGENS, père.

26 FÉVRIER 1665.

Le sommaire se trouve à Leiden, coll. Huygens.
Un extrait a été publié dans le Journal des Sçavans 1665, No. XI [1].

26 Febrier 1665.

A MON PERE

Douleur du coſtè. des vents. Si Auzout voudroit ſe charger de l'affaire [2]) des Pendules. Je vous ay eſcrit du contenu du Placet, mais il y auroit peut eſtre trop pour y faire entrer, parce qu'on m'a dit que les Placets ne ſont que fort courts et ſeulement pour faire ſouvenir le Roy de quelque choſe. Je vous ay envoiè la reſponſe du Prince Maurice [3]) obſervation de la ſympathie des horologes, choſe admirable. teſmoigne la juſteſſe des horologes puis qu'il faut ſi peu de choſe pour les tenir dans l'accord perpetuel. quarrè d'une table mis entre deux qui les cachoit l'un à l'autre. le frere de Zeelhem ne ſcauroit trouver l'inſcription [4]).

Fig. 2.1 Excerpt from Christian Huygens's letter to his father talking about the discovery of an "odd kind of sympathy" in the experiment carried out with two pendulum clocks and presented to the Royal Society of London. [65]

In 1968, an article on the behavior of fireflies was published describing how the fireflies flash in unison and at a constant tempo [17]. Even when the fireflies were isolated from one another, they still kept to a steady beat. This idea of a particular pulse can be traced back to: A. Winfree [134], one of the pioneers in the field of collective behavior. In this model, one looks at the phases of a system constituted by a large number of oscillators, in which each oscillator is equipped with its own natural frequency. Moreover, each oscillator has its mean of keeping time, some sort of internal clock, or in other words, a natural frequency. Then, setting the phase of the ith oscillator with θ_i, in a system where the oscillators do not interact with each other the dynamics of the phases can be described with their particular natural, which is usually taken as a random variable ω drawn from a probability distribution $g(\omega)$ and leads to having an initial description of the phase dynamical system with the form

$$\dot{\theta}_i = \omega_i \quad \forall i \in \{1,\dots,N\},$$

nevertheless, the works models developed after the Winfree model are so varied that today we have different studies where ω_i depends on time [29, 39, 105], the topology [80], and even the configuration of the system [28]. All these patterns start with something in common: they are, in principle, a self-sustaining periodic process which means that it has to be non-linear, and this implies that the oscillator must possess a limit cycle. The next element imposed for Winfree is related to the moment the fireflies start to connect in the same place, in other words, the system's interaction. Usually, at the moment of studying the state of an oscillator, it is considered both its phase and amplitude [136]. However, as was Winfree's one, our

interest only relies on the phase dynamics that we already started to describe before. Indeed, we will assume that the oscillators are weakly perturbed, which means that the orbital shape of the limit cycle is approximately inflexible under perturbations while the deviation on phase from his natural orbit is quite pronounced. Thus, the dynamics of the N-oscillators can be reduced to an N-dimensional vector field described with the phases of each oscillator with the nonlinear equation:

$$\dot{\theta}_i = \mathscr{F}_i(\theta_1, \ldots, \theta_N) = \omega_i + K g_i(\theta_1, \ldots, \theta_N),$$

where $g_i : R^N \to R$ contains all the coupling effects produced by the oscillators of the system to the i-oscillator, and $K \in \mathbb{R}^+$ indicates the overall coupling strength. In general, the vector field can explicitly depend on time t, in other words, we can have $\mathscr{F}_i(\theta_1, \ldots, \theta_N, t) = \omega_i(t) + K g_i(\theta_1, \ldots, \theta_N, t)$ but we are just going to consider autonomous systems that depend on phase. The reason why only the phase variable is considered can be understood with the iteration of fireflies, it has its maximum synchronization exponent when they flash, and then there is an interval of darkness while it recharges its light-emitting organs, so the influence is given by the moment in which the light is generated, ergo the phase of the light emitting organ and is not directly related to the time in which it is produced. The model designed by Winfree considered two functions: the *sensitivity function*, which encodes how an oscillator responds to the signals it receives, and the *influence function* that we already described. For simplicity, all the oscillators in a given population have the same influence and sensitivity functions. As a result, the Winfree model has the form

$$\dot{\theta}_i = \omega_i + \frac{K}{N} S(\theta_i) \sum_{j=1}^{N} I(\theta_j), \quad t > 0 \quad i = 1, 2, \ldots, N.$$

For more details about the Winfree model, examine his starters works [134, 135] and other works on the model [6, 58, 102]. Even though Winfree's model was the first successful attempt to model macroscopic synchronization, there were very few studies on the rigorous treatment for the emergent dynamics compared to the hundreds of literature studies made to a more tractable model, the Kuramoto model [78]. Kuramoto simplifies the view of interactions between oscillators with the symmetrical rule sets up the faster one slows down, and the slower one goes faster. This property of the motion is fundamental when the complete synchronization of the oscillators is analyzed [57]. The result pairwise structure is with the form

$$\dot{\theta}_i = \omega_i + \frac{K}{N}\sum_{j=1}^{N}\Gamma_{j,i}\left(\theta_j - \theta_i\right) \tag{2.1}$$

Then just like Winfree, Kuramoto decides to consider a sinusoidal dependency between the phases. He just considers the case where all oscillators affect each other without distinction (All-to-All)

$$\dot{\theta}_i = \omega_i + \frac{K}{N}\sum_{j=1}^{N}\sin(\theta_j - \theta_i).$$

The wide exploit of the model lies in the possibilities of carrying out a theoretical mathematical work, Kuramoto himself was able to demonstrate in a few pages the existence of a transition phase to synchronization. From this moment, the investigations carried out on the model have been quite numerous, so much that it is natural to go beyond the classical Kuramoto model and bring it closer to real problems with generalizations, like the use of inertia [47, 55, 124], delay coupling [140], noise [7], time-depending parameters [105] or the use of complex networks in the connectivity between the oscillators [36].

The study of the Kuramoto dynamics over complex networks was one of the first generalizations proposed by Watts and Strogatz [133], which work not only contributes to the synchronization field but also the modern theory of complex networks.

This merging between the field of synchronization with the field of complex networks was mutually beneficial since understanding the complex network topology allowed the analysis of synchronization processes, while these processes contributed to understanding the emergent properties in networks. To work with the Kuramoto oscillators over complex networks is necessary to consider the equation (2.1) modified as follows:

$$\dot{\theta}_i = \omega_i + K\sum_{j=1}^{N} W_{ij}\sin(\theta_j - \theta_i), \quad \sum_{j=1}^{N} W_{ij} = 1, \quad \forall i \in \{1,\ldots,N\}, \tag{2.2}$$

where $W_{ij} \in (0,1]$ if the oscillators i and j are connected and $W_{ij} = 0$ if are disconnected pairs. $W_{ij} = 1/N$ for all i and j recovered the original Kuramoto model. The use of complex networks requires a more rigorous treatment when establishing the coupling strength and the connectivity matrix to preserve at most the properties for the all-to-all case and provide some rigorous mathematical treatment from the phenomenology study to the stability analysis. The classic Kuramoto model shows that employing the coupling component $1/N$ sets a

perturbation over the average between the interaction with the whole system without a dependency on the number of oscillators. This disaffiliation is an essential asset for the system analysis in the thermodynamic limit $N \to \infty$. Reusing this coupling strength for a Kuramoto model on complex networks makes it dependent on N. Therefore, it is advisable to consider a more appropriate weight for the interaction of the system, such as a $W_{ij} = 1/k_i$ where k_i is the degree of the node i, in other words, is the number of connections that as the oscillator i, as has been used in [93]. Other possibilities are considering the average connectivity of the graph $\langle k \rangle$ [63] or the maximum degree $k_{\max}$ [50].

It can be observed that the selection of the appropriate coupling strength is directly connected with the topology of the connectivity matrix. In general, this matrix also present some rules, like connectedness and symmetry, in the sense that

- For any $i, j \in \{1, \ldots, N\}$ there exist a set of m distinct indices $k_1, k_2, \ldots, k_m \subset \{1, \ldots, N\}$ such that $i = k_1$, $j = k_m$ and $W_{k_l, k_{l+1}} > 0$ for $l \in \{1, m-1\}$,
- $W_{ij} = W_{ji} \geq 0$ for $1 \leq i, j \leq N$,

also, it is expected that their configuration can be translated from a finite set of oscillators $N \to \infty$ to their thermodynamic limit.

2.2 Synchronization patterns

Pikovsky et al. defined *synchronization* as the adjustment of rhythms of oscillating objects due to their weak interaction [106]; such a general concept opens the doors to different definitions and types of synchronization. For this reason, in this section, we provide a formal definition of the dynamics considered.

In terms of one to one oscillator, we said that:

Definition 2.2.1. *Two Kuramoto oscillators i and j are*

- *phase synchronized if*

$$\lim_{t \to \infty} \big(\theta_i(t) - \theta_j(t) \big) \equiv 0 \ (\ mod \ 2\pi) ;$$

- *antiphase if*

$$\lim_{t\to\infty}\big(\theta_i(t)-\theta_j(t)\big)\equiv\pi\ (\ mod\ 2\pi)\,; \tag{2.3}$$

- *phase-locked if*

$$\sup_{t>0}\big|\theta_i(t)-\theta_j(t)\big|<+\infty;$$

- *frequency synchronized if*

$$\lim_{t\to\infty}\big|\dot{\theta}_i(t)-\dot{\theta}_j(t)\big|=0$$

These concepts can be extended to the whole system in the following way:

Definition 2.2.2. *Let $\Theta(t)=\{\theta_i\}_{i=1}^N$ be the solution of a Kuramoto system. We say that the system has asymptotic complete phase synchronization if and only if the phase differences tend to zero asymptotically, i.e.*

$$\lim_{t\to\infty}(\theta_i(t)-\theta_j(t))\equiv 0\quad(\ mod\ 2\pi),\quad \forall\, i,j\in\{1,\dots,N\}\,; \tag{2.4}$$

it has an asymptotically phase-locked state if and only if each phase difference goes to a constant as $t\to\infty$, i.e.

$$\lim_{t\to\infty}\theta_i(t)-\theta_j(t)=\theta_{ij},\quad \forall\, i,j\in\{1,\dots,N\}\,; \tag{2.5}$$

And we said that, the system has asymptotic complete frequency synchronization if and only if the following condition holds,

$$\lim_{t\to\infty}(\dot{\theta}_i(t)-\dot{\theta}_j(t))=0,\quad \forall i,j\in\{1,\dots,N\}\ . \tag{2.6}$$

Notice that the equation (2.5) and (2.6) are not equivalent in general; for instance, condition (2.6) implies condition (2.5) under the assumption that $\dot{\theta}_i-\dot{\theta}_j$ decays at $+\infty$ in an integrable mode, but the implication may fail in general.

In the dynamic behavior of generalized Kuramoto oscillators given by (2.2), the presence of heterogeneous coupling forces makes the complete synchronization of the coupled system a rare phenomenon compared to other forms of synchrony. This is why weaker definitions of synchronization have been postulated, like for example, the concept of *practical synchronized* employed in [62, 71, 141]. The practical synchronization is set for generalized Kuramoto models (2.2) as follows:

Definition 2.2.3. *The solution* $\Theta(t) = (\theta_1, \ldots, \theta_N)$ *to the system* (2.2) *and initial condition* $\Theta(0) = \Theta^0$ *for* $t = 0$ *exhibits asymptotic practical synchronization if and only if the following conditions hold:*

$$\lim_{K\to\infty} \limsup_{t\to\infty} (\theta_i(t) - \theta_j(t)) = 0, \quad \forall i, j \in \{1, \ldots, N\} .$$

This definition allows the phase difference to be arbitrarily small instead of tending to zero as long as the coupling strength is large enough. This type of synchronization could be noted in a subgroup of oscillators with the same intrinsic dynamics. In fact, for Kuramoto models whose dynamics form homogeneous subgroups it is natural to introduce a local synchronization definition:

Definition 2.2.4. *A k-cluster state with* $k \geq 2$ *is defined as a partition of the set of oscillators* $(\theta_1, \ldots, \theta_N)$ *for which the entire set of their indices can be split into subsets in the following way*

$$A = \{1, \ldots, N\} = \bigcup_{j=1}^{k} A_j, \quad A_j \cap A_i = \emptyset \quad \text{for } j \neq i,$$

and $i_1, i_2 \in A_j \neq \emptyset$ *if they preserve any of the asymptotic dynamics defined in Definition 2.2.1.*

In addition, we will say that the system has a *splay state* Θ_{splay} if

$$|\theta_i(t) - \theta_j(t)| = 2\frac{m\pi}{N}, \quad i, j = 1, \ldots, N \quad \text{with} \quad i \neq j \text{ and } m = 1, \ldots, N-1. \tag{2.7}$$

Another form of the state is:

$$\Theta_{splay} = \left\{ \theta, \theta + m\frac{2\pi}{N}, \theta + m\frac{4\pi}{N}, \ldots, \theta + m\frac{2(N-1)\pi}{N} \right\},$$

for some $\theta \in [0, 2\pi)$.

2.3 Fundamentals of the Kuramoto model

Throughout this thesis, well-established mathematical concepts and properties are used and extended to study the behavior of the Kuramoto oscillators for the specific models that we will introduce. This section displays some basic formalism and properties of the classical Kuramoto model.

The Kuramoto dynamics is defined on the N-dimensional torus, $\mathscr{T}^N = (\mathbb{R}/(2\pi\mathbb{Z}))^N$, with $N \geq 1$, by the succeeding set of coupled first-order ODEs, for the phases $\theta_i(t)$:

$$\dot{\theta}_i = \omega_i + \frac{K}{N}\sum_{j=1}^{N}\sin(\theta_j - \theta_i) \qquad i = 1,\ldots,N, \tag{2.8}$$

where $K > 0$ is constant, and the natural frequencies $\omega_i \in \mathbb{R}$ are drawn from a given distribution $g(\omega)$. The N oscillators are represented by points rotating on the unit circle centered at the origin of the complex plane, more precisely by $e^{i\theta_j}$ with $j = 1,\ldots,N$. We introduce their barycenter expressed in polar coordinates R and Φ:

$$Re^{i\Phi} = \frac{1}{N}\sum_{j=1}^{N} e^{i\theta_j}. \tag{2.9}$$

It is clear that $0 \leq R \leq 1$ and $\Phi \in \mathscr{T}$ (defined if $R > 0$). The modulus $R = R(\theta(t))$ is called the *order parameter* and $\Phi = \Phi(\theta(t))$ the *collective phase*. One can rewrite Eq.(2.8) as follows:

$$\dot{\theta}_i = \omega_i + KR\sin(\Phi - \theta_i), \qquad i = 1,\ldots,N, \tag{2.10}$$

with $\theta = (\theta_1,...,\theta_N) \in \mathscr{M} = \mathscr{T}^N$, and $\mathscr{M}$ the phase space. This order parameter introduced by Kuramoto [79] has quite interesting properties and plays a key factor when measuring the degree of phase synchronization. The equation (2.9) implies the following identities:

$$R = \frac{1}{N}\sum_{i=1}^{N}\cos(\Phi - \theta_i), \tag{2.11}$$

$$0 = \frac{1}{N}\sum_{i=1}^{N}\sin(\Phi - \theta_i), \tag{2.12}$$

$$R\sin(\Phi - \theta_i) = \frac{1}{N}\sum_{j=1}^{N}\sin(\theta_j - \theta_i), \qquad i = 1,\ldots,N \tag{2.13}$$

$$R\cos(\Phi - \theta_i) = \frac{1}{N}\sum_{j=1}^{N}\cos(\theta_j - \theta_i), \qquad i = 1,\ldots,N. \tag{2.14}$$

Equations (2.11) and (2.14), further imply:

$$R^2 = \frac{1}{N^2}\sum_{i,j=1}^{N}\cos(\theta_j - \theta_i). \tag{2.15}$$

As was defined in Subsection 2.2, the *complete frequency synchronization* occurs as $t \to +\infty$, when the difference $\theta_i(t) - \theta_j(t)$ tends to a constant for all i and j. It has been proved by [3, 57, 120] that the Kuramoto model displays this behavior for large values of K over some specific configurations. Indeed, for $N \leq \infty$, Ha et al. [57] study the case in which the variations between the natural frequencies and the mean of the natural frequencies ω_c are zero:

$$\hat{\omega}_i := \omega_i - \omega_c = 0 \quad \text{with} \quad \omega_c := \frac{1}{N}\sum_{i=1}^{N} \omega_i$$

which is also called the case of identical oscillators. Over this condition, the dynamics for $\hat{\theta}_i = \theta_i - \theta_c$ becomes

$$\frac{d\hat{\theta}_i}{dt} = \frac{K}{N}\sum_{j=1}^{N} \sin(\hat{\theta}_j - \hat{\theta}_i) \tag{2.16}$$

since

$$\frac{d\theta_c}{dt} = \omega_c$$

where $\theta_c := 1/N\sum_{i=1}^{N} \theta_i$ is the center of mass of the oscillators.

Considering this setting, in [57] the authors prove that for the case of identical oscillators any smooth solution $\{\theta_i(t)\}_{i=1}^{N}$ of the system (2.8) with an initial configuration θ_i^0 satisfying the size condition

$$\max_{1\leq i,j\leq N} \left|\theta_j^0 - \theta_i^0\right| \leq \pi$$

undergoes an asymptotic complete *phase synchronization*. Moreover, $R(\theta(t))$ tends to $R^\infty \in (0,1]$, and the case in which $R^\infty = 1$ implies that all the N terms of the sum in (2.11) coincide with Φ. This work was extended by [34], proving that frequency synchronization can occur for all initial phase configurations distributed over the whole circle. In their work, they use the fact that the Kuramoto dynamics (2.10) can also be written as a gradient flow:

$$\dot{\theta} = -\nabla f(\theta) \tag{2.17}$$

with potential

$$f(\theta) = -\sum_{i=1}^{N} \omega_i\theta_i + \frac{K}{2N}\sum_{i,j=1}^{N} \Big(1 - \cos(\theta_j - \theta_i)\Big). \tag{2.18}$$

that is analytic in θ.

After this, Benedetto et al. in 2015 [11] continued the study of N identical oscillators for any initial condition and proved the complete frequency synchronization with a different

method concerning [34] indeed several of their results will be used in conjoint with this thesis.

We are going to define when a set of N oscillators is of type $(N-k,k)_\varphi$:

Definition 2.3.1. *Given $\varphi \in [0,2\pi)$, $N \in \mathbb{N}$ and $k \in \{0,\dots,N/2\}$, a set $\{\alpha_i\}_{i=1}^N \subset \mathbb{R}$ is of type $(N-k,k)_\varphi$ if there exists $I \subset \{1,\dots,N\}$ of cardinality $N-k$ such that*

$$\alpha_i = \begin{cases} \varphi \mod 2\pi & i \in I \\ (\varphi+\pi) \mod 2\pi & i \in I^c \end{cases}$$

In other words, if a set of oscillators is of type $(N-k,k)_\varphi$ then have a complete synchronization state when $k=0$ or a bi-polar state when $k>0$.

Proposition 2.3.2. *$\{\theta_i^*\}_{i=1}^N$ is a stationary solution of* (2.16) *iff one of the following properties hold:*

- $R \equiv 0$
- *$\{\theta_i^*\}_{i=1}^N$ is of type $(N-k,k)_{\varphi^*}$*

The first possible state of the stationary solution correspond to an incoherent state, meanwhile, in the second case, we will have that $R^\infty = 1-2k/N$ which corresponds to a complete frequency synchronized state for $k \geq 1$, and complete phase synchronized state for $k=0$. Benedetto et al. also studies the asymptotic behavior of R and φ, proving that:

Proposition 2.3.3. *If $\{\theta_i(t)\}_{i=1}^N$ is not a stationary solution, then*

- $\dot{R}(t) > 0$, $\forall t > 0$
- $R(t) \to R^\infty \in (0,1]$
- *$\varphi(t)$ is well defined $\forall t > 0$*

We can present the main result of [11].

Theorem 2.3.4. *If $\theta_i(t)$, $i = 1,\dots,N$ is not a stationary solution, then it converges to a complete frequency synchronized state of type $(N-k,k)_\varphi$. Moreover, if $\theta_i(0) \neq \theta_j(0) \mod 2\pi$ when $i \neq j$, the solution converges to a stationary solution of type $(N,0)$ or $(N-1,1)$.*

The theory developed over the classic Kuramoto model is quite extensive, and we limited ourselves in this chapter to just recovering the properties used in our work. As we established before, thinking in a collection of oscillators with just an all to all connectivity is relatively restricted when we are trying to describe real collective behaviors, for this reason we exploit the most important features of the generalized Kuramoto model moreover we focus on the branch of multilayer networks.

A first instance of a multilayer Kuramoto model can be found in Okuda and Kuramoto and was later developed e.g. in [3, 56, 111]. The last comprehensive summary covers the recent development of synchronization of the Kuramoto oscillator model in multilayer networks from a numerical approach and also offers a survey on the stability analysis [137]. Primarily, the work developed until now and presented in this review from a rigorous stability analysis focuses on the classical Kuramoto model and on sufficient conditions leading to asymptotic complete phase-frequency synchronization and bounded synchronization [21, 23, 57]. More general structures of the network have been addressed in Montbrió et al.[90], where synchronization between two interacting populations is investigated and a rich dynamic behavior is outlined. Moreover the interplay of coupling, noise and phase asymmetries in coupled oscillators is discussed by Sheeba et al.[116], where also the continuum limit of the model is studied. In Ha et al.[61] the author discuss the formation of phase-locked states for local Kuramoto oscillators that are locally connected and symmetric instead of having an all-to. Dong and Xue[34] besides studying the original Kuramoto oscillators, works also with the generalized Kuramoto and shows sufficient conditions to obtain frequency synchronization. The focus of the work of Kawamura et al.[69] is the study, in the continuum limit, of the synchronization of two groups of nonidentical weakly interacting oscillators. Ha and Li[60] studies the asymptotic emergence of full synchronization with hierarchical driving. Panaggio and Abrams[99] finds chimeral states in systems with a finite number of oscillators organized in two groups. Schaub et al. [114] exploits graph-theoretical concepts to study the synchronization in Kuramoto networks and Tiberi et al.[127] uses a geometric approach for the synchronization patterns. While studies of the multilayer Kuramoto model are numerous, most of the studies concern the continuum limit of the model. The study of synchronization mechanisms in multilayer Kuramoto models with a finite numer of oscillators is, hence, still open.

Chapter 3

Kuramoto oscillators on two-layers networks

In the last decades, the work conducted in synchronization has been expanding and focused on increasingly complex phenomena. A recent research line pointed towards the investigation of multilayer networks [67, 68, 128, 137, 142], these studies differ from formal proposals for complex networks in the fact that complex networks have focused mainly on cases in which the topology of the system is mapped in a network, and each unit-unit interaction is represented under a number that quantifies its weight in the connection of the graph. However, the multilayer approach has a particular interest in the interplay between the structure of the networks and their dynamics since can provide a solid foundation for modeling, controlling, and simulating dynamical behaviors of real work networks such as spreading processes [31], epidemic synchronization [52], social [33] or brain [10].

Even when is a quite recent approach, if we consider a two populations system as a two-layer system, one of the first works in this direction would be by Okuda and Kuramoto [96]. His real-life example was motivated by the investigations conducted between 1988 and 1989 on the oscillatory responses of functional columns in the visual cortex of cats; these are spatially separated and synchronized under certain conditions [38, 54]. Other more modern examples can be found in the analysis of social networks, where each group of people seems as if the connections between its members occur at the same level, that is, the interactions that are made with each person are uniform. However, either because of the way we connect with people or because of the algorithms developed in social networks, the strongest relationships occur within specific groups formed by our offline relationships, common ideals, lifestyles,

and so on [33]. More examples of multilayer networks can refer to surveys [13, 73]. The majority of the studies in this field meanly relies on numerical investigations of the onset of different synchronization patters, such as the explosive synchronization [68, 142] and the chimera states [85] letting behind the stability analysis that until now has been mostly covered in the continuum limit [69, 116]. Our particular interest is studying the two most common multilayer networks from a stability analysis approach and covering problems in which the connection between the layers is weak. To better understand the importance of this hypothesis, it is significant to mention that in most of the works carried out so far, the necessary conditions to obtain some type of synchronization depended directly on the minimum coupling force [34, 61, 83, 138], considering that ours is already weak, we focus in the other forces capable of establishing these conditions and studying the different types of synchronization.

3.1 The SIC and AIC Kuramoto Models

Let us consider a system of nonlinear oscillators, formed by two layers of N oscillators in each layer, the positions of them can be represented in a unitary circle on the complex plane:

$$\left\{x_j = e^{i\theta_j}\right\}_{j=1}^{N} \quad \text{and} \quad \left\{\bar{x}_j = e^{i\xi_j}\right\}_{j=1}^{N} \tag{3.1}$$

in function of the phases:

$$\Theta = \left\{\theta_j\right\}_{j=1}^{N}, \quad \Xi = \left\{\xi_j\right\}_{j=1}^{N}.$$

During the work over two-layer model, we will use the notation above to differentiate the characteristics of each layer and the following notation when we emphasize the properties of the $2N$-system:

$$X = (\Theta, \Xi) \quad O = (\Omega, \bar{\Omega}) = (\omega_1, \ldots, \omega_N, \bar{\omega}_1, \ldots \bar{\omega}_N) \in \mathbb{R}^{2N},$$

with components X_i, O_i, respectively. The study of the temporal dynamics of the phases described by a Kuramoto model is pursued, i.e., the behavior of each oscillator θ_j (ξ_j) governed by a stationary natural frequency $\omega_j \in \mathbb{R}$ ($\bar{\omega}_j \in \mathbb{R}$) and a sinusoidal coupling where ψ_{ij} is an element of the adjacency matrix Ψ that represents the coupling strength connection encoding the topology of the network:

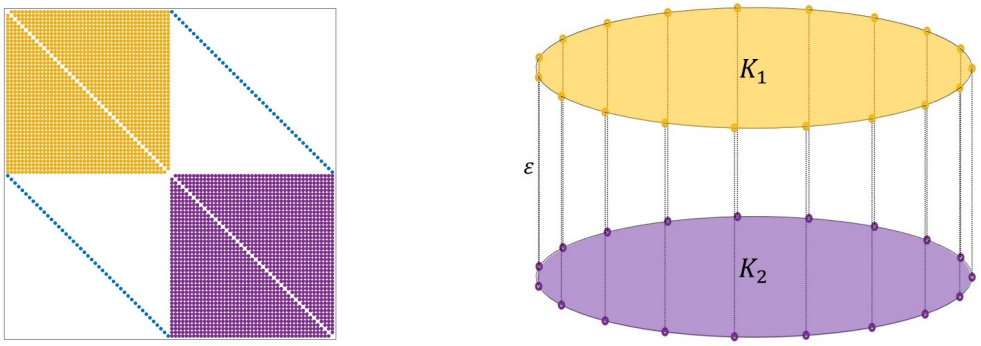

(a) Matrix scheme (b) Graph scheme

Fig. 3.1 Visualization of the network of 2-layer with weak singular interconnection (SIC)

$$\dot{X}_i = O_i + \sum_{j=1}^{2N} \psi_{ij} \sin(X_j - X_i), \qquad i = 1, \ldots, 2N \tag{3.2}$$

Our interest goes beyond the uniform coupling of the system and lies in the weak interlayer coupling; this means that the coupling strength between layers is considered to be relatively small. This study is divided into two possible types of interlayer connectivity; the first model follows Singular Interlayer Connectivity (SIC), in which each oscillator will be connected with just one oscillator of the other counterpart. This model is represented by:

$$\begin{cases} \dot{\theta}_j = \omega_j + \dfrac{K_1}{N} \displaystyle\sum_{l=1}^{N} \sin(\theta_l - \theta_j) + \varepsilon \sin(\xi_j - \theta_j), \\ \\ \dot{\xi}_j = \bar{\omega}_j + \dfrac{K_2}{N} \displaystyle\sum_{l=1}^{N} \sin(\xi_l - \xi_j) + \varepsilon \sin(\theta_j - \xi_j), \end{cases} \tag{3.3}$$

where $K_1 > K_2 > 0$ are the intralayer coupling strengths between the oscillators of the same layer, and $\varepsilon > 0$ is the weakly coupling strength between two oscillators of different layers. It is assumed that:

$$K_1, K_2 \geqslant \varepsilon > 0. \tag{3.4}$$

The model is described by a graph whose matrix is represented in Figure 3.1 a. Note that this configuration forms a particular type of multilayer network called a *multiplex network*, where, like in the SIC model, different layers have the same number of nodes, and the only

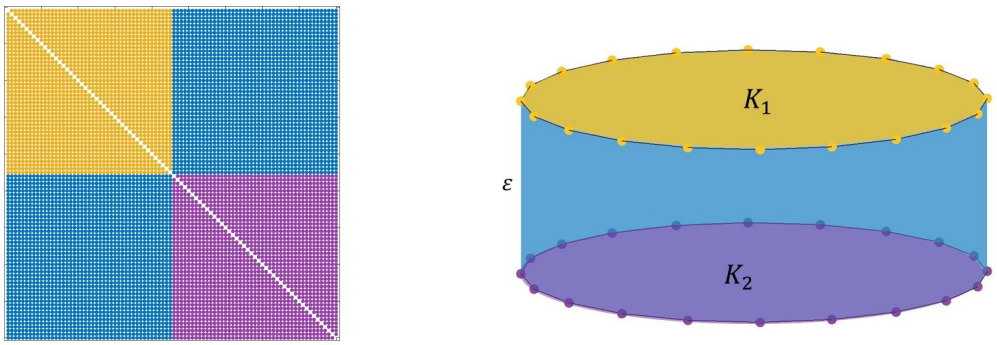

(a) Matrix scheme (b) Graph scheme

Fig. 3.2 Visualization of the network of 2-layer with weak average interconnection (AIC)

possible type of inter-layer connections are those in which a given node is only connected to its counterpart nodes in the rest of the layers [73]. Multiplex networks have attracted much attention as they allow us to divide the different layers into distinct types of interactions; indeed, we can find works in the evolution of cooperation [51], the interplay between awareness and epidemic spreading [53], social structures [75] and in particular in social networks [81, 132]. Other examples include the real-world network of user ratings for films, namely, the Netflix data set [64], the European Air Transport Network [19], coupled power grids [16], and coupled climate networks [35].

Similarly, the second model to study follows Average Interlayer Connectivity (AIC), in which each oscillator interacts weakly with all the oscillators from the other layer:

$$\begin{cases} \dot{\theta}_j = \omega_j + \dfrac{K_1}{N}\displaystyle\sum_{l=1}^{N}\sin(\theta_l - \theta_j) + \dfrac{\varepsilon}{N}\sum_{k=1}^{N}\sin(\xi_k - \theta_j) \\ \\ \dot{\xi}_j = \bar{\omega}_j + \dfrac{K_2}{N}\displaystyle\sum_{l=1}^{N}\sin(\xi_l - \xi_j) + \dfrac{\varepsilon}{N}\sum_{k=1}^{N}\sin(\theta_k - \xi_j)\,, \end{cases} \tag{3.5}$$

Models with the AIC shape are popular because the discrete average connections are easily translatable to a continuous form [96, 122]. Moreover, thanks to the Ott and Antonsen ansatz for models with global sinusoidal coupling [97, 98], the analytical treatment of coupled phase oscillators in the continuum limit has been rapidly developed [1, 9, 90, 99, 101, 107]. Besides, the idea of two populations of phase oscillators asymmetrically interacting is likely to occur since it can be related to a difference between the type of oscillators and not just the capacity of connectivity as it is in the case of the SIC Model.

Taken $t = 0$ as the initial time of the system's state each phase is represented by:

$$\theta_j(0) = \theta_j^0 \quad \xi_j(0) = \xi_j^0 \quad X_j(0) = X_j^0, \tag{3.6}$$

Moreover, any of the systems can be written in the general form given by the equation (3.2), where the capacity matrix $\psi = (\psi_{ij})$ is described by:

$$\psi_{ij} = \begin{cases} \frac{K_1}{N} & \text{if } i,j \in [N] \\ \frac{K_2}{N} & \text{if } i,j \in [N]+N \\ \varepsilon & \text{if } i \in [N],\ j = i+N \\ \varepsilon & \text{if } j \in [N]+N,\ i = j-N \\ 0 & \text{otherwise.} \end{cases}, \psi_{ij} = \begin{cases} \frac{K_1}{N} & \text{if } i,j \in [N] \\ \frac{K_2}{N} & \text{if } i,j \in [N]+N \\ \frac{\varepsilon}{N} & \text{if } i \in [N],\ j \in [N]+N \\ \frac{\varepsilon}{N} & \text{if } i \in [N]+N,\ j \in [N] \end{cases}, \tag{3.7}$$

or

$$\psi_{ij} = \frac{K}{N},$$

where we used the notation $[N] = \{1,\ldots,N\}$. The final form of ψ_{ij} depends on what type of model we are working on: All-to-All, SIC or AIC. As we have already mentioned, there are numerous works where the system is analyzed as a complex system where the possibility of dividing the oscillators into different capacities is ignored, the fact of showing the form of the SIC and AIC models as other complex systems implies that many of the results obtained can be applied in the models.

3.2 Fundamentals of the SIC and AIC models

As in the classical model, most of the essential features of each layer's dynamics and of the system can be measured with the macro-variables that we will define in this section.

We propose the following order parameters for the interlayer and intralayer analysis

$$z_1 = r_1 e^{i\varphi_1} = \frac{1}{N}\sum_{j=1}^{N} e^{i\theta_j} \quad z_2 = r_2 e^{i\varphi_2} = \frac{1}{N}\sum_{j=1}^{N} e^{i\xi_j} \tag{3.8}$$

$$z_3 = r_3 e^{i\varphi_3} = \frac{1}{N}\sum_{j=1}^{N} e^{i(\xi_j-\theta_j)} \quad \text{and} \quad z = re^{i\varphi} = \frac{1}{2N}\sum_{j=1}^{N} e^{i\theta_j} + e^{i\xi_j} \tag{3.9}$$

Notice that the order parameter preserves the identities analogous to (2.11), (2.12) for the order parameter (2.9), i.e.:

$$r_1 = \frac{1}{N}\sum_{j=1}^{N} \cos(\varphi_1 - \theta_j) \tag{3.10}$$

$$0 = \frac{1}{N}\sum_{j=1}^{N} \sin(\varphi_1 - \theta_j) \tag{3.11}$$

$$r_2 = \frac{1}{N}\sum_{j=1}^{N} \cos(\varphi_2 - \xi_j) \tag{3.12}$$

$$0 = \frac{1}{N}\sum_{j=1}^{N} \sin(\varphi_2 - \xi_j). \tag{3.13}$$

Indeed, it is sufficient to take the real and imaginary part of the two identities

$$r_1 = \frac{1}{N}\sum_{j=1}^{N} e^{i(\theta_j-\varphi_1)} \quad \text{and} \quad r_2 = \frac{1}{N}\sum_{j=1}^{N} e^{i(\xi_j-\varphi_2)}.$$

to get the expressions (3.10)- (3.13). Using these parameters the SIC system (3.3) can be rewritten as

$$\begin{cases} \dot{\theta}_i = \omega_i + K_1 r_1 \sin(\varphi_1 - \theta_i) + \varepsilon \sin(\xi_i - \theta_i) \\ \\ \dot{\xi}_i = \bar{\omega}_i + K_2 r_2 \sin(\varphi_2 - \xi_i) + \varepsilon \sin(\theta_i - \xi_i), \end{cases} \tag{3.14}$$

and in the same way the AIC system (3.5) transforms into:

$$\begin{cases} \dot{\theta}_i = \omega_i + K_1 r_1 \sin(\varphi_1 - \theta_i) + \varepsilon r_2 \sin(\varphi_2 - \theta_i) \\ \\ \dot{\xi}_i = \bar{\omega}_i + K_2 r_2 \sin(\varphi_2 - \xi_i) + \varepsilon r_1 \sin(\varphi_1 - \xi_i). \end{cases} \tag{3.15}$$

Another important feature is the center of mass of the phases and the average of the natural frequencies in each layer given by:

$$\theta_c(t) = \frac{1}{N}\sum_{i=1}^{N}\theta_i(t)\,, \quad \xi_c(t) = \frac{1}{N}\sum_{i=1}^{N}\xi_i(t), \quad \omega_c = \frac{1}{N}\sum_{i=1}^{N}\omega_i\,, \quad \bar{\omega}_c = \frac{1}{N}\sum_{i=1}^{N}\bar{\omega}_i \tag{3.16}$$

Similarly, we can define the average phase and frequency for the whole system,

$$X_c = \frac{1}{2N}\sum_{i=1}^{2N}X_i\,, \qquad \Omega_c = \frac{1}{2N}\sum_{i=1}^{2N}O_i\,.$$

Lemma 3.2.1. *Let $X = (\Theta, \Xi)$ be a phase vector which dynamics is governed by* (3.3)*, then the quantity X_c moves with a constant velocity, while θ_c and ξ_c preserve a sinusoidal motion over the interlayer-perturbation.*

Proof. It is easy to check that

$$X_c = \frac{1}{2}\left(\theta_c + \xi_c\right), \qquad \Omega_c = \frac{1}{2}\left(\omega_c + \bar{\omega}_c\right).$$

While the dynamics of each center of mass considering (3.3) is

$$\begin{aligned}\dot{\theta}_c &= \frac{1}{N}\frac{d}{dt}\sum_{i=1}^{N}\theta_i = \frac{1}{N}\sum_{i=1}^{N}\omega_i + \frac{K_1}{N^2}\underbrace{\sum_{i,j=1}^{N}\sin\left(\theta_j - \theta_i\right)}_{=0} + \frac{\varepsilon}{N}\sum_{i=1}^{N}\sin\left(\xi_i - \theta_i\right)\\ &= \omega_c + \frac{\varepsilon}{N}\sum_{i=1}^{N}\sin\left(\xi_i - \theta_i\right)\end{aligned}$$

and similarly

$$\dot{\xi}_c = \bar{\omega}_c + \frac{\varepsilon}{N}\sum_{i=1}^{N}\sin\left(\theta_i - \xi_i\right)$$

Then we have that the perturbation of the connectivity between each layer neutralizes, preserving a setting up a constant dynamic:

$$\dot{X}_c(t) = \dot{\theta}_c(t) + \dot{\xi}_c(t) = \omega_c + \bar{\omega}_c \ = \Omega_c,$$

This property is a consequence of the symmetry of the coefficients in (3.7). □

By a change of variables ($\hat{\theta}_i = \theta_i - \Omega_c$ and $\hat{\xi}_i = \xi_i - \Omega_c$), we can assume:

$$\Omega_c = \omega_c + \bar{\omega}_c = 0 \tag{3.17}$$

and therefore the mean phases of the whole system is conserved over time:

$$X_c(t) = X_c(0) \qquad \forall\, t > 0 \tag{3.18}$$

that implies that $\theta_c(t) + \xi_c(t) = \theta_c(0) + \xi_c(0)$.

By another change of variables, we can fix the value of $X_c(0)$; for instance we can assume that

$$X_c(0) = 0 \qquad \sum_{i=1}^{N} \theta_i(0) + \sum_{i=1}^{N} \xi_i(0) = 0\,. \tag{3.19}$$

3.2.1 A gradient flow formulation

Here, we present new formulations of the SIC (3.3) and AIC (3.5) models as gradient systems. For the classic Kuramoto model and in a population of locally interacting Kuramoto oscillators, such a gradient flow formulation was first introduced in [11] and in [61] respectively. Now, consider the function $U(X) : \mathbb{R}^{2N} \to \mathbb{R}$ for the SIC model we have

$$\begin{aligned} U(X) = \sum_{k=1}^{N} \Bigg\{ & -(\omega_k \theta_k + \bar{\omega}_k \xi_k) + \varepsilon\,(1 - \cos(\xi_k - \theta_k)) \\ & + \sum_{j=1}^{N} \left[\frac{K_1}{2N} \left(1 - \cos(\theta_j - \theta_k)\right) + \frac{K_2}{2N} \left(1 - \cos(\xi_j - \xi_k)\right) \right] \Bigg\} \end{aligned} \tag{3.20}$$

Our analytic potential satisfies

$$\partial_{\theta_i\theta_j} U(X) = \partial_{\theta_j\theta_i} U(X), \quad \partial_{\theta_i\xi_i} U(X) = \partial_{\xi_i\theta_i} U(X), \quad \partial_{\theta_i\xi_j} U(X) = \partial_{\xi_j\theta_i} U(X)$$
$$\text{and} \quad \partial_{\xi_i\xi_j} U(X) = \partial_{\xi_j\xi_i} U(x) \quad i \neq j\,.$$

Then is clear that

$$\begin{aligned}\partial_{\theta_i} U(X) &= -\omega_i - \frac{K_1}{2N}\sum_{j=1}^{N}\sin(\theta_j-\theta_i) + \frac{K_1}{2N}\sum_{k=1}^{N}\sin(\theta_i-\theta_k) - \varepsilon\sin(\xi_i-\theta_i)\\ &= -\dot{\theta}_i.\end{aligned}$$

In the same way, $\partial_{\xi_i} U(X) = -\dot{\xi}_i$. This shows that the system (3.3) is a gradient system with the form

$$\dot{X} = -\nabla U(X),$$

for the AIC system, we have that a suitable function that meets the properties presented above for the SIC model is:

$$U(X) = \sum_{k=1}^{N}\left\{-(\omega_k\theta_k + \bar{\omega}_k\xi_k) + \sum_{j=1}^{N}\left[\frac{K_1}{2N}\left(1-\cos(\theta_j-\theta_k)\right) + \frac{K_2}{2N}\left(1-\cos(\xi_j-\xi_k)\right) + \frac{\varepsilon}{N}\left(1-\cos(\xi_j-\theta_k)\right)\right]\right\}. \quad (3.21)$$

The fact that the SIC and AIC model are gradient flow systems with analytic potentials is an expected characteristic given the symmetry of the coupling system.

3.3 Identical Oscillators

In this part, we present complete phase and frequency synchronization estimates for identical oscillators with the same natural frequency, i.e.

$$\omega_j = \bar{\omega}_j = \omega \quad \forall j = 1,\dots N. \quad (3.22)$$

Without loss of generally is possible to take $\omega = 0$ since we can subtract ωt from the phases. To analyze of the patterns of synchronization, we study the stationary solutions, the dynamics of the order parameters, and the diameter of the phases. For the following analysis, we introduce the definitions of phase diameters:

$$D(\Theta(t)) := \max_{1\le i,j\le N}\left|\theta_i(t)-\theta_j(t)\right|, \quad D(\Xi(t)) := \max_{1\le i,j\le N}\left|\xi_i(t)-\xi_j(t)\right|,$$

$$D(X(t)) := \max_{1\leq i,j\leq 2N} \left|X_i(t) - X_j(t)\right|.$$

3.3.1 SIC

The SIC model with identical oscillators (3.22) and simplified with the proposed order parameters (3.8) reads as

$$\begin{cases} \dot{\theta}_i = \dfrac{K_1}{N}\displaystyle\sum_{j=1}^{N} \sin(\theta_j - \theta_i) + \varepsilon \sin(\xi_i - \theta_i) = K_1 r_1 \sin(\varphi_1 - \theta_i) + \varepsilon \sin(\theta_i - \xi_i) \\ \dot{\xi}_i = \dfrac{K_2}{N}\displaystyle\sum_{j=1}^{N} \sin(\xi_j - \xi_i) + \varepsilon \sin(\theta_i - \xi_i) = K_2 r_2 \sin(\varphi_2 - \xi_i) + \varepsilon \sin(\xi_i - \theta_i) \\ \theta_i(0) = \theta_{i0} \quad \xi_i(0) = \xi_{i0} \end{cases} \tag{3.23}$$

Moreover, thanks to the properties (3.10)-(3.13) of the order parameters (3.9), we have that

$$\frac{1}{N^2}\sum_{j,k=1}^{N} \cos(\theta_j - \theta_k) = r_1^2 \quad \text{and} \quad \frac{1}{N^2}\sum_{j,k=1}^{N} \cos(\xi_j - \xi_k) = r_2^2.$$

The equation above gives us the final form of the gradient function (3.20):

$$U(X) = N\left[\frac{K_1}{2}\left(1 - r_1^2\right) + \frac{K_2}{2}\left(1 - r_2^2\right) + \varepsilon\left(1 - r_3\cos(\varphi_3)\right)\right].$$

The final form shows that an absolute minimum of the function U is achieved by a complete synchronizations state of the whole system, that is when $r_1 = 1$ and $r_2 = 1$, $r_3 = 1$, and $\varphi_3 = 2n\pi$ with $n \in \mathbb{N}$. And the maximum of energy will be reached when $r_1 = 0$,$r_2 = 0$ and $r_3 = 1$ with $\varphi_3 = (2n+1)\pi$ which means that each couple θ_i and ξ_i are antipodal for all $i \in [N]$.

Definition 3.3.1. *Given $\varphi \in [0, 2\pi)$, $N \in \mathbb{N}$ and $k \in \mathbb{N}_0 := \mathbb{N}\bigcup\{0\}$ with $N - k \geq k$, a set $\{\alpha_i\}_{i=1}^N \subset \mathbb{R}$ is of type $(N-k,k)_\varphi$ if there exists $I \subset \{1,\ldots,N\}$ of cardinality $N-k$ such that*

$$\alpha_i = \begin{cases} \varphi \mod 2\pi & i \in I \\ (\varphi + \pi) \mod 2\pi & i \in I^c \end{cases}$$

Considering the above definitions, we can classify the stationary solutions of the SIC system into two main types.

Proposition 3.3.2. *$\{\theta_i^\infty, \xi_i^\infty\}_{i=1}^N$ is a stationary solution of (3.3) iff one of the following properties holds*

1. *$r_1 = 0$ and $r_2 = 0$ and each pair $\theta_i = \xi_i + k_i\pi$ for $k_i \in \mathbf{Z}$*
2. *There exist $\bar{\varphi}_1^\infty$ and $\bar{\varphi}_2^\infty$ such that $\{\theta_i^\infty\}_{i=1}^N$ is of type $(N-k_1, k_1)_{\varphi_1}$, $\{\xi_i^\infty\}_{i=1}^N$ is of type $(N-k_2, k_2)_{\varphi_2}$ and $\varphi_1 = \varphi_2 - K\pi$ for any $K \in \mathbf{Z}$.*

Proof. The first case corresponds to an incoherent state in each layer with a balance phase and antiphase synchronization between pairs i of inter-layer connections. In the second case, we have that

$$\begin{cases} K_1 r_1 \sin(\varphi_1 - \theta_i) + \varepsilon \sin(\xi_i - \theta_i) = 0 \\ \\ K_2 r_2 \sin(\varphi_2 - \xi_i) + \varepsilon \sin(\theta_i - \xi_i) = 0 \end{cases}$$

Notice that thanks to (3.11) and (3.13), summing the equations over θ_i and ξ_i we obtain that

$$\sin(\varphi_1 - \xi_i) = 0 \quad \text{and} \quad \sin(\varphi_2 - \theta_i) = 0$$

summing the equations above again over ξ_i and θ_i respectively, we obtain that $\sin(\varphi_1 - \varphi_2) = 0$ then we have that $\varphi_1 = \varphi_2 + K\pi$ and each oscillator $\theta_i = \varphi_2 - k_i\pi$ and $\xi_i = \varphi_1 - \bar{k}_i\pi$ which by transitivity means that $\{\theta_i^\infty\}_{i=1}^N$ is of type $(N-k_1, k_1)_{\varphi_1}$, and $\{\xi_i^\infty\}_{i=1}^N$ is of type $(N-k_2, k_2)_{\varphi_2}$. □

The last proposition proved that the only stationary states of the SIC model are either incoherent, bipolar or complete synchronization states. Like in the classical Kuramoto model [56], for an ensemble of identical oscillators with $N \geq 4$, it is possible to construct a continuum of phase-locked states with zero-order parameters.

Example. *For $\mu_1, \mu_2 \in [0, 2\pi]$ and $N \geq 4$, we can have a state $X^{\mu_1,\mu_2} = \{\Theta^{\mu_1}, \Xi^{\mu_2}\}$ such that it is a permutation of:*

$$\sigma(\Theta^{\mu_1})_i := \begin{cases} \dfrac{2i\pi}{N-2} + \mu_1, & i = 1, \ldots, N-2, \\ 0, & i = N-1, \\ \pi, & i = N. \end{cases}$$

and

$$\sigma(\Xi^{\mu_2})_i := \begin{cases} \dfrac{2i\pi}{N-2} + \mu_2, & i = 1,\dots,N-2, \\ 0, & i = N-1, \\ \pi, & i = N. \end{cases}$$

where the bijection σ implies the same ordered arrangements of the vectors Θ^{μ_1} and Ξ^{μ_2} and $\mu_1 - \mu_2 = k\pi$ with $k \in \mathbb{Z}$.

Moreover, since we have the form of every possible equilibrium point, it is also possible to perform a linear stability analysis at an equilibrium point $\bar{X} = \{\theta_i^\infty, \xi_i^\infty\}_{i=1}^N$, with $\dot{\delta}_X(t) = J(\bar{X})\delta_X(t)$ where $\delta_X = X - \bar{X}$ and $J(\bar{X})$ is the Jacobian matrix of V with components:

$$\begin{aligned}
J_{ii} = &\quad -K_1 r_1 \cos(\varphi_1^\infty - \theta_i^\infty) - \varepsilon\cos(\xi_i^\infty - \theta_i^\infty) \\
J_{(N+i)(N+i)} = &\quad -K_2 r_2 \cos(\varphi_2^\infty - \xi_i^\infty) - \varepsilon\cos(\theta_i^\infty - \xi_i^\infty) \\
J_{ih} = &\quad -\frac{K_1}{N}\cos(\theta_h^\infty - \theta_i^\infty) \qquad i,h \in [1,N] \quad i \neq h \\
J_{(N+i)(N+h)} = &\quad -\frac{K_2}{N}\cos(\xi_h^\infty - \xi_i^\infty) \\
J_{i(N+i)} = &\quad -\varepsilon\cos(\xi_i^\infty - \theta_i^\infty) \\
J_{(N+i)i} = &\quad -\varepsilon\cos(\theta_i^\infty - \xi_i^\infty) \\
J_{ih} = &\quad 0 \qquad\qquad\qquad\qquad \text{o/w}
\end{aligned}$$

Notice that J is a symmetric $2N \times 2N$ matrix with zero row-sums; this implies that it always has a zero eigenvalue with the $\mathbf{1}$ eigenvector. For the incoherent states, if at least one of the pairs $\theta_i - \xi_i = k_i\pi$ is with k_i odd we will have that the equilibrium points is unstable, this claim is proved by Monzón and Paganini in [91] for the classic Kuramoto model but can be easily used for the J matrix since both share the same properties, and if there is an odd k_i, then an element of the diagonal will be positive, and J can not be negative definite nor semi-definite.

Due to the connectivity of the oscillators, we have that the dynamics of the order parameter that measure the level of synchrony of the system and the layers are not monotonic; indeed,

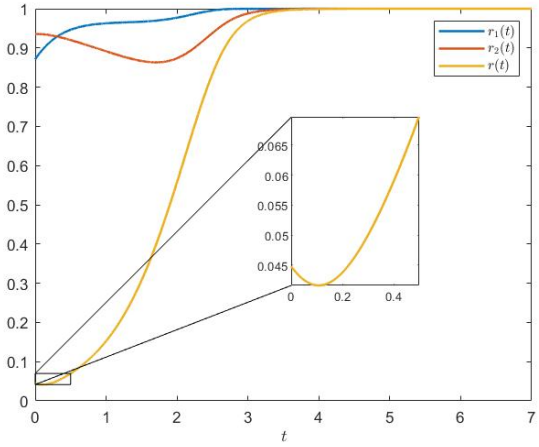

Fig. 3.3 Dynamics of the order parameter r_1, r_2 and r, for $\{\theta_i(t), \xi_(t)\}_{i=1}^N$ following the equation (3.23) and $r_1(t)$, $r_2(t)$ and $r(t)$ given by (3.8) and (3.9) with $\{\theta_i^0\}_{i=1}^N \in [0,(2\pi+1)/4]$, $\{\xi_i^0\}_{i=1}^N \in [\pi,(3\pi)/2]$, with $K_1 = 2.5$, $K_2 = 1.2$ and $\varepsilon = 1$ for $t \in [0,7]$.

the final form of the r dynamics is given by

$$\begin{aligned}\dot{r} = \frac{1}{4rN}\Bigg\{ & K_1 r_1^2 \sum_{j=1}^{N} \sin^2(\varphi_1 - \theta_j) + K_2 r_2^2 \sum_{j=1}^{N} \sin^2(\varphi_2 - \theta_j) \\ & + N(K_1+K_2) r_1 r_2 \left[\frac{\cos(\varphi_1 - \varphi_2)}{2} - r_1 \cos(\varphi_1) - r_2 \cos(\varphi_2) \right] \\ & + 2\varepsilon \sum_{j=1}^{N} \sin^2(\xi_j - \theta_j) \left[r_1 \cos\left(\varphi_1 - \frac{\xi_j + \theta_j}{2}\right) + r_2 \cos\left(\varphi_2 - \frac{\xi_j + \theta_j}{2}\right) \right] \Bigg\}.\end{aligned}$$

3.3.2 AIC

The system (3.5) reduced with the order parameters (3.8) and natural frequencies given by (3.22) reads:

$$\begin{cases} \dot{\theta}_i = K_1 r_1 \sin(\varphi_1 - \theta_i) + \varepsilon r_2 \sin(\varphi_2 - \theta_i) \\ \\ \dot{\xi}_i = K_2 r_2 \sin(\varphi_2 - \xi_i) + \varepsilon r_1 \sin(\varphi_1 - \xi_i) \end{cases} \tag{3.24}$$

The following lemma can be proved in the same way as in [57] and [34] and will be valuable in the analysis of phase collisions and stationary solutions for (3.5).

Lemma 3.3.3. *(Uniform boundedness of X,Θ and Ξ) Let $X(t) = \{\theta_i(t), \xi_i(t)\}_{i=1}^N$ be the solution of system* (3.24) *with initial conditions $D(\Theta^0) < 2\pi$ and $D(\Xi^0) < 2\pi$. Then we have that $D(\Theta(t)) < 2\pi$ and $D(\Xi(t)) < 2\pi$ for $t \geq 0$. Moreover, if $D(X^0) := D_{X^0} \leq \pi$, the diameter of the phases of the total system satisfies $D(X(t)) \leq D_{X^0}$ for $t \geq 0$*

Proof. For the intralayer bound, assume that the initial conditions are $D(\Theta^0) < 2\pi$ and $D(\Xi^0) < 2\pi$. Now, we are going to prove that $D(\Theta(t)) < 2\pi$ for $t \geq 0$. Assume the contrary. Then there exist i and j such that

$$\theta_i(t) < \theta_j(t) + 2\pi, \text{ for } t \in [0, t_0) \quad \text{and} \quad \theta_i(t_0) = \theta_j(t_0) + 2\pi. \tag{3.25}$$

For (3.24) follows that

$$\begin{aligned}
\frac{d\theta_i}{dt}(t_0) &= K_1 r_1 \sin(\varphi_1 - \theta_i(t_0)) + \varepsilon r_2 \sin(\varphi_2 - \theta_i(t_0)) \\
&= K_1 r_1 \sin(\varphi_1 - \theta_j(t_0) - 2\pi) + \varepsilon r_2 \sin(\varphi_2 - \theta_j(t_0) - 2\pi) \\
&= K_1 r_1 \sin(\varphi_1 - \theta_j(t_0)) + \varepsilon r_2 \sin(\varphi_2 - \theta_j(t_0)) \\
&= \frac{d\theta_j}{dt}(t_0),
\end{aligned}$$

with $r_1, r_2, \varphi_1, \varphi_2$ at time t_0, then $\dot{\theta}_i(t_0) = \dot{\theta}_j(t_0)$. Moreover, by the successive differentiation of the system (3.24), we have

$$\begin{aligned}
\frac{d^2\theta_i}{dt^2}(t_0) &= K_1 \left[\dot{r}_1 \sin(\varphi_1 - \theta_i(t_0)) + r_1 \cos(\varphi_1 - \theta_i(t_0)) \left(\dot{\varphi}_1 - \dot{\theta}_i\right)\right] \\
&+ \varepsilon \left[\dot{r}_2 \sin(\varphi_2 - \theta_i(t_0)) + r_2 \cos(\varphi_2 - \theta_i(t_0)) \left(\dot{\varphi}_2 - \dot{\theta}_i\right)\right] \\
&= K_1 \left[\dot{r}_1 \sin(\varphi_1 - \theta_j(t_0)) + r_1 \cos(\varphi_1 - \theta_j(t_0)) \left(\dot{\varphi}_1 - \dot{\theta}_j\right)\right] \\
&+ \varepsilon \left[\dot{r}_2 \sin(\varphi_2 - \theta_j(t_0)) + r_2 \cos(\varphi_2 - \theta_j(t_0)) \left(\dot{\varphi}_2 - \dot{\theta}_j\right)\right] \\
&= \frac{d^2\theta_j}{dt^2}(t_0),
\end{aligned}$$

thanks to the periodicity of cosine and sine. Similarly, we can obtain

$$\frac{d^n\theta_i}{dt^n}(t_0) = \frac{d^n\theta_j}{dt^n}(t_0), \text{ for } n \geq 2, \tag{3.26}$$

hence, combining this fact with the analyticity of θ_i and θ_j, and Corollary A.1.3 [76] we have that

$$\theta_i(t) < \theta_j(t) + 2\pi, \quad t \in (0,T) \quad T > t_0.$$

This equality contradicts the assumption (3.25).

For the boundedness of X, let $T \in (0,\infty]$ be any number. Suppose that the phase-diameter $D(X(t)) < \pi$ with $t \in [0,T)$. Then the dynamics will depend on whether the extreme indices belong to the same layer or not. In the first case, we have:

$$\begin{aligned}
\frac{dD(X(t))}{dt} &= \frac{d\left(\theta_M - \theta_m\right)}{dt} \\
&= \frac{K_1}{N}\left(\sum_{j=1}^{N} \underbrace{\sin(\theta_j - \theta_M)}_{\leq 0} - \underbrace{\sin(\theta_j(t) - \theta_m)}_{\geq 0}\right) \\
&+ \frac{\varepsilon}{N}\left(\sum_{j=1}^{N} \underbrace{\sin(\xi_j - \theta_M)}_{\leq 0} - \underbrace{\sin(\xi_j(t) - \theta_m)}_{\geq 0}\right) \\
&\leq 0,
\end{aligned}$$

in the second case:

$$\begin{aligned}
\frac{dD(X(t))}{dt} &= \frac{d\left(\theta_M - \xi_m\right)}{dt} \\
&= \frac{K_1}{N}\sum_{j=1}^{N} \underbrace{\sin(\theta_j - \theta_M)}_{\leq 0} - \frac{K_2}{N}\sum_{j=1}^{N} \underbrace{\sin(\xi_j(t) - \xi_m)}_{\geq 0} \\
&+ \frac{\varepsilon}{N}\left(\sum_{j=1}^{N} \underbrace{\sin(\xi_j - \theta_M)}_{\leq 0} - \underbrace{\sin(\theta_j(t) - \xi_m)}_{\geq 0}\right) \\
&\leq 0.
\end{aligned}$$

□

Several things change from the AIC model with respect to the SIC model. One of the many properties that the classic Kuramoto has is that in the set of solutions, there will be finite-time phase collisions between two identical oscillators [57]; this property is not preserved in the SIC case; indeed, if $\theta_i = \theta_j$ unless $\xi_i = \xi_j$, the oscillators will be detached, the same will happen if two oscillators in the Ξ layer collide. On the other hand, for the AIC case, we will have this property preserved between oscillators from the same layer, i.e., if $\theta_i(t_0) = \theta_j(t_0)$, then they will remain attached for $t \geq t_0$, and the same will happen for $\xi_i(t_0) = \xi_j(t_0)$. Following a similar argument that when we prove that $D(\Theta) \leq 2\pi$ it is easy to see that if two oscillators θ_i and θ_j collide at $t = t_0 \in (0,\infty)$ then the equality $\dot{\theta}_i = \dot{\theta}_j$ and equation (3.26) will be satisfied, and thanks to Corollary 1.2.5 in [76] (rewritten for completeness in A.1.3) $\theta_i(t) = \theta_j(t)$ for $t \geq t_0$, clearly if $t_0 = 0$ then $\theta_i(t) = \theta_j(t)$ for $t \geq 0$. This property is not preserved between oscillators from different layers. Also, notice that for the dynamics of $D(X(t))$, the only condition for the diameter decrease in time is that the initial diameter of the system D_{X^0} is less than π. Since the topology does not interfere with this dynamic, this property is easily transferable to the SIC model.

Based on the last Lemma 3.3.3 and eqs. (3.18) and (3.19), it follows that for $t \geq 0$, $i = 1,\ldots,N$, if $D_{X^0} < \pi$ then

$$|\theta_i(t)| = |\theta_i(t) - X_c(t)| \leq \frac{1}{2N}\sum_{j=1}^{N}|\theta_i(t) - \theta_j(t)| + \frac{1}{2N}\sum_{j=1}^{N}|\theta_i(t) - \xi_j(t)| < \pi,$$

in the same way $\xi_i(t) < \pi$ for all $i = 1,\ldots,N$.

Since the system can be rewritten in a gradient form and our solution $X(t)$ is bounded, it implies that there exists a vector $X^\infty = (\theta_1^\infty,\ldots,\xi_N^\infty)$ and some sequence $t_n \to \infty$ such that $X(t_n) \to X^\infty$ as $N \to \infty$. Then using theorem A.1.5, we conclude that $X(t) \to X_\infty$ as $t \to \infty$, which implies that there exists X_{ij} such that $X_j(t) - X_i(t) \to X_{ij}^\infty$ as $t \to \infty$ and in particular exist a θ_{ij} such that $\theta_i(t) - \theta_j(t) \to \theta_{ij}^\infty$ and a ξ_{ij} such that $\xi_i(t) - \xi_j(t) \to \xi_{ij}^\infty$.

Moreover, following the same approach as Choi et al., Monzón and Paganini [22, 91], since each of the oscillators can be represented in a unitary circle on the complex plane just like we describe in (3.1), for the critical point X^∞, we can make use their positions $\{x_j^\infty = e^{i\theta_j^\infty}\}_{j=1}^N$ and $\{\bar{x}_j^\infty = e^{i\xi_j^\infty}\}_{j=1}^N$ to define the numbers:

$$\alpha_i := K_1\sum_{j=1}^{N}\frac{x_j^\infty}{x_i^\infty} + \varepsilon\sum_{j=1}^{N}\frac{\bar{x}_j^\infty}{x_i^\infty}$$

$$
\begin{aligned}
&= K_1 \sum_{j=1}^{N} e^{i\theta_j^\infty - \theta_i^\infty} + \varepsilon \sum_{j=1}^{N} e^{i\xi_j^\infty - \theta_i^\infty} \\
&= K_1 \sum_{j=1}^{N} \cos(\theta_j^\infty - \theta_i^\infty) + \varepsilon \sum_{j=1}^{N} \cos(\xi_j^\infty - \theta_i^\infty) \\
&+ i \left[K_1 \sum_{j=1}^{N} \sin(\theta_j^\infty - \theta_i^\infty) + \varepsilon \sum_{j=1}^{N} \sin(\xi_j^\infty - \theta_i^\infty) \right]
\end{aligned}
$$

and

$$
\begin{aligned}
\bar{\alpha}_i &:= K_2 \sum_{j=1}^{N} \frac{\bar{x}_j^\infty}{\bar{x}_i^\infty} + \varepsilon \sum_{j=1}^{N} \frac{x_j^\infty}{\bar{x}_i^\infty} \\
&= K_2 \sum_{j=1}^{N} e^{i\xi_j^\infty - \xi_i^\infty} + \varepsilon \sum_{j=1}^{N} e^{i\theta_j^\infty - \xi_i^\infty} \\
&= K_2 \sum_{j=1}^{N} \cos(\xi_j^\infty - \xi_i^\infty) + \varepsilon \sum_{j=1}^{N} \cos(\theta_j^\infty - \xi_i^\infty) \\
&+ i \left[K_2 \sum_{j=1}^{N} \sin(\xi_j^\infty - \xi_i^\infty) + \varepsilon \sum_{j=1}^{N} \sin(\theta_j^\infty - \xi_i^\infty) \right]
\end{aligned}
$$

Since X^∞ is an equilibrium point, we have that:

$$
\begin{cases}
K_1 \sum_{j=1}^{N} \sin(\theta_j^\infty - \theta_i^\infty) + \varepsilon \sum_{j=1}^{N} \sin(\xi_j^\infty - \theta_i^\infty) = 0, \quad i = 1, \dots N \\
K_2 \sum_{j=1}^{N} \sin(\xi_j^\infty - \xi_i^\infty) + \varepsilon \sum_{j=1}^{N} \sin(\theta_j^\infty - \xi_i^\infty) = 0, \quad i = 1, \dots N
\end{cases}
\tag{3.27}
$$

By (3.27), α_i and $\bar{\alpha}_i$ are real numbers that obey

$$
\begin{cases}
K_1 \sum_{j=1}^{N} x_j^\infty + \varepsilon \sum_{j=1}^{N} \bar{x}_j^\infty = \alpha_i x_i^\infty \\
\\
K_2 \sum_{j=1}^{N} \bar{x}_j^\infty + \varepsilon \sum_{j=1}^{N} x_j^\infty = \bar{\alpha}_i \bar{x}_i^\infty.
\end{cases}
$$

These equations imply that the weighted sum of angles of each layer in the complex plane must be parallel to the angle of the i-oscillator in their layer. On the other hand, according to the last lemma, the phases $\{X_i^\infty\}_{i=1}^{2N}$ are distributed in an open half-circle. Then

$$\theta_i^\infty = \theta_j^\infty \quad \text{and} \quad \xi_i^\infty = \xi_j^\infty \quad \text{for any} \quad i,j = 1,2,\dots N.$$

Otherwise, we can find an oscillator whose angle cannot be parallel to the weighted sum of angles influencing it. Therefore, the phases are asymptotically synchronized.

In Lemma 3.3.3, we discussed the existence of phase-locked states as solutions of the Kuramoto dynamics, with general initial conditions, in the large time limit. Moreover, we show the final structure of the oscillators if the initial configuration is bounded by π. So far, the structure of the phase-locked states for the AIC model is given by the following proposition.

Proposition 3.3.4. *The set* $\{\theta_i^\infty, \xi_i^\infty\}_{i=1}^N$ *is a stationary solution of* (3.24) *iff one of the following properties hold*

- $r_1 = 0$ *and* $r_2 = 0$
- *There exist* φ_1^∞ *and* φ_2^∞ *such that*

$$\varphi_1^\infty = \varphi_2^\infty + k\pi \mod 2\pi$$

where $\{\theta_i^\infty\}_{i=1}^N$ *is of type* $(N-k_1,k_1)_{\varphi_1^\infty}$ *or* $\{\xi_i^\infty\}_{i=1}^N$ *is of type* $(N-k_2,k_2)_{\varphi_2^\infty}$

Proof. The first case corresponds to the state in which each center of mass θ_c and ξ_c are at the origin and, φ_1 and φ_2 are undefined. In the second case from the equation (3.24), we use the trivial case in which each stationary solution $\{\theta_i^\infty, \xi_i^\infty\}$ follows $\sin(\varphi_1^\infty - \theta_i) = 0$ and $\sin(\varphi_2^\infty - \xi_i) = 0$ then $\varphi_1^\infty = \theta_i^\infty + k_i\pi = \varphi_2^\infty = \xi_i^\infty + k_i\pi \,(\text{mod } 2\pi)$. If $\sin(\varphi_1^\infty - \theta_i^\infty) \neq 0$ then we have that considering the sum of (3.24) over i we have that:

$$K_1 r_1 \sum_{i=1}^N \sin(\varphi_1^\infty - \theta_i^\infty) = -\varepsilon r_2 \sum_{i=1}^N \sin(\varphi_2^\infty - \theta_i^\infty) \tag{3.28}$$

then by (3.11) and (3.13):

$$0 = \varepsilon r_2 \sum_{i=1}^N \sin(\varphi_2^\infty - \theta_i^\infty) = \varepsilon N r_2 r_1 \sin(\varphi_2^\infty - \varphi_1^\infty)$$

then $\sin(\varphi_2^\infty - \varphi_1^\infty) = 0$, so we have that $\varphi_1^\infty = \varphi_2^\infty + k\pi$ for any $k \in \mathrm{N}$ then we have that (3.28) is

$$\sin(\varphi_1^\infty - \theta_i^\infty)\,(K_1 r_1 + \varepsilon r_2) = 0$$

for k even, but since $\sin(\varphi_1^\infty - \theta_1^\infty) \neq 0$ and $K_1, K_2, r_1, r_2 > 0$, we arrive at a contradiction. For k odd, if any of the oscillators is of type $(N-k_1,k_1)_{\varphi_1^\infty}$ for the Θ layer or type $(N-k_2,k_2)_{\varphi_2^\infty}$ for the Ξ layer we need $K_1 r_1 = \varepsilon r_2$ and in the same way, $K_2 r_2 = \varepsilon r_1$ but since $K_1 > \varepsilon$ and $K_2 > \varepsilon$, then $r_2 > r_1$ and $r_1 > r_2$ at the same time then we arrive again to a contradiction. Therefore, the oscillators of the layer must be of type $(N-k_1,k_1)_{\varphi_1^\infty}$ for the Θ layer or type $(N-k_2,k_2)_{\varphi_2^\infty}$ for the Ξ layer. □

Next, we prove that the order parameter of the system r is a monotonically non-decreasing function while the interlayer order parameters r_1 and r_2 are not necessarily monotone.

Proposition 3.3.5. *If $X(t) = \{\theta_i(t), \xi_i(t)\}_{i=1}^N$ is not a stationary solution then*

1. $\dot{r} > 0$, $\forall t > 0$
2. *The dynamics of the order parameters r_1 and r_2 are given by:*

$$\begin{cases} \dot{r}_1(t) = r_1 \dfrac{K_1}{N} \displaystyle\sum_{j=1}^{N} \sin\left(\varphi_1 - \theta_j\right)^2 + \dfrac{\varepsilon r_2}{N} \sum_{j=1}^{N} \sin\left(\varphi_1 - \theta_j\right) \sin\left(\varphi_2 - \theta_j\right), & \text{(3.29a)} \\ & \text{(3.29b)} \\ \dot{r}_2(t) = r_2 \dfrac{K_2}{N} \displaystyle\sum_{j=1}^{N} \sin\left(\varphi_2 - \xi_j\right)^2 + \dfrac{\varepsilon r_1}{N} \sum_{j=1}^{N} \sin\left(\varphi_2 - \xi_j\right) \sin\left(\varphi_1 - \xi_j\right), & \text{(3.29c)} \end{cases}$$

Proof. To prove point 2, we consider the first equation in (3.8) and deriving with respect to t

$$\dot{r_1} e^{i\varphi_1} + i r_1 \dot{\varphi_i} e^{i\varphi_1} = \frac{i}{N} \sum_{i=1}^{N} e^{i\theta_i} \dot{\theta}_i,$$

multiplying both sides of the equation by $e^{-i\varphi_1}$ and separating the real part from the imaginary part, we obtain the system:

$$\begin{cases} \dot{r_1} = -\dfrac{1}{N} \displaystyle\sum_{i=1}^{N} \sin(\theta_i - \varphi_1)\dot{\theta}_i, \\ \\ \dot{\varphi}_1 = \dfrac{1}{N r_1} \displaystyle\sum_{i=1}^{N} \cos(\theta_i - \varphi_1)\dot{\theta}_i, \end{cases} \tag{3.30}$$

in the same way, for z_2, we reach the following identity

$$\begin{cases} \dot{r_2} = -\dfrac{1}{N}\displaystyle\sum_{i=1}^{N} \sin(\xi_i - \varphi_2)\dot{\xi}_i \\ \\ \dot{\varphi}_2 = \dfrac{1}{Nr_2}\displaystyle\sum_{i=1}^{N} \cos(\xi_i - \varphi_2)\dot{\xi}_i \end{cases} \tag{3.31}$$

then from the equation (3.30) and (3.31), we obtain

$$\begin{cases} \dot{r_1} = \dfrac{K_1}{N}\displaystyle\sum_{i=1}^{N} \sin(\varphi_1 - \theta_i)^2 + \varepsilon \sum_{i=1}^{N} \sin(\varphi_1 - \theta_i)\sin(\varphi_2 - \theta_i) \\ \\ \dot{r_2} = \dfrac{K_2}{N}\displaystyle\sum_{i=1}^{N} \sin(\varphi_2 - \xi_i)^2 + \varepsilon \sum_{i=1}^{N} \sin(\varphi_2 - \xi_i)\sin(\varphi_1 - \xi_i) \end{cases} \tag{3.32}$$

Now back to point 1, notice that from (3.9) we have that

$$z = re^{i\varphi} = \frac{1}{2}\left(r_1 e^{\varphi_1} + r_2 e^{\varphi_2}\right)$$

then we have that for any $x_i \in \mathbb{R}$

$$re^{i\varphi - x_i} = \frac{1}{2}\left(r_1 e^{\varphi_1 - x_i} + r_2 e^{\varphi_2 - x_i}\right)$$

which give us for $r > 0$

$$\sin(\varphi - x_i) = \frac{1}{2r}\left(r_1 \sin(\varphi_1 - x_i) + r_2 \sin(\varphi_2 - x_i)\right) \tag{3.33}$$

considering the equation above, we have that differentiating z in (3.9) with respect to time and multiplying for $e^{-i\varphi}$ both sides we obtain the system

$$\begin{cases} \dot{r} = -\dfrac{1}{2N}\left[\displaystyle\sum_{j=1}^{N} \sin(\theta_j - \varphi)\dot{\theta}_j + \sum_{j=1}^{N} \sin(\xi_j - \varphi)\dot{\xi}_j\right] \\ \\ r\dot{\varphi} = \dfrac{1}{2N}\left[\displaystyle\sum_{j=1}^{N} \cos(\theta_j - \varphi)\dot{\theta}_j + \sum_{j=1}^{N} \cos(\xi_j - \varphi)\dot{\xi}_j\right] \end{cases} \tag{3.34}$$

Then using the equation (3.33) with x_i equal to θ_i and ξ_i in the dynamics of (3.34)

$$\begin{aligned}
\dot{r} &= \frac{1}{2N}\left[\sum_{i=1}^{N}\frac{1}{2r}\left(r_1\sin(\varphi_1-\theta_i)+r_2\sin(\varphi_2-\theta_i)\right)\left(K_1 r_1\sin(\varphi_1-\theta_i)+\varepsilon r_2\sin(\varphi_2-\theta_i)\right.\right.\\
&\left.\left.+\sum_{i=1}^{N}\frac{1}{2r}\left(r_1\sin(\varphi_1-\xi_i)+r_2\sin(\varphi_2-\xi_i)\right)\left(K_2 r_2\sin(\varphi_2-\xi_i)+\varepsilon r_1\sin(\varphi_1-\xi_i)\right)\right]\right.\\
&= \frac{1}{4Nr}\left[\sum_{i=1}^{N}K_1 r_1^2\sin^2(\varphi_1-\theta_i)+\varepsilon r_2^2\sin^2(\varphi_2-\theta_i)\right.\\
&+(K_1+\varepsilon)\,r_1 r_2\sum_{i=1}^{N}\sin(\varphi_1-\theta_i)\sin(\varphi_2-\theta_i)+K_2 r_2^2\sin^2(\varphi_2-\xi_i)+\varepsilon r_1^2\sin^2(\varphi_1-\xi_i)\\
&\left.+(K_2+\varepsilon)\,r_1 r_2\sum_{i=1}^{N}\sin(\varphi_1-\xi_i)\sin(\varphi_2-\xi_i)\right]
\end{aligned}$$

since $K_1 > K_2 > \varepsilon$, we have that

$$\begin{aligned}
\dot{r} &\geq \frac{\varepsilon}{4Nr}\left[\sum_{i=1}^{N}\left(r_1\sin(\varphi_1-\theta_i)-r_2\sin(\varphi_2-\theta_i)\right)^2\right.\\
&\left.+\left(r_2\sin(\varphi_2-\xi_i)-r_1\sin(\varphi_1-\xi_i)\right)^2\right]\\
&> 0
\end{aligned}$$

□

It is not possible to exclude the possibility in which $\dot{r}_1$ and $\dot{r}_2$ can take negative values even though r always increases. In fact, if we take randomly initial states with $\{\theta_i^0\}_{i=1}^N \in [3\pi/2, 2\pi]$ and $\{\xi_i^0\}_{i=1}^N \in [0,\pi]$, we can observe that for $K_1 = 3$, $K_2 = 2$ and $\varepsilon = 1$, the order parameters tend to 1, but given the initial configuration, r_1 and r_2 decrease at the beginning while r increases until it reaches a steady state, as shown in Figure 3.4.

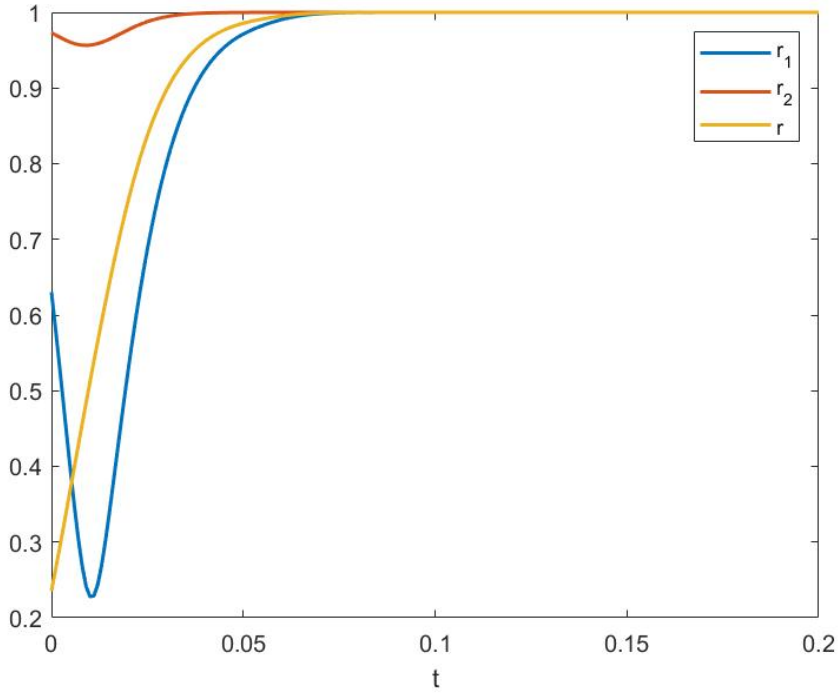

Fig. 3.4 Dynamics of the order parameters r_1, r_2 and r following the equations (3.32) and (3.34) for $\{\theta_i^0\}_{i=1}^N \in [3\pi/2, 2\pi]$ and $\{\xi_i^0\}_{i=1}^N \in [0,\pi]$ with $K_1 = 3$, $K_2 = 2$ and $\varepsilon = 1$ in the time $t \in [0, 0.2]$.

3.4 Asymptotic formation of a 2-cluster locked state for the SIC Model

Consider the system (3.3)-(3.6), with a natural frequency ω_i randomly chose from a generic frequency distribution $g(\omega)$. We now introduce the natural frequency diameter between oscillators of the same layer and the whole network:

$$D(\Omega) := \max_{1\le i,j\le N} \left|\omega_i - \omega_j\right|, \quad D(\bar{\Omega}) := \max_{1\le i,j\le N} \left|\bar{\omega}_i - \bar{\omega}_j\right|,$$
$$d(\Omega) := \min_{\substack{1\le i,j\le N \\ i\neq j}} \left|\omega_i - \omega_j\right|, \quad d(\bar{\Omega}) := \min_{\substack{1\le i,j\le N \\ i\neq j}} \left|\bar{\omega}_i - \bar{\omega}_j\right|,$$
$$\text{and} \quad D(\Omega,\bar{\Omega}) := \max\left\{D(\Omega), D(\bar{\Omega}), \max_{1\le i,j\le N} |\omega_i - \bar{\omega}_i|\right\}$$

The diameter of the natural frequencies is an important measure since it is directly related to the variations of the frequencies. Indeed, the larger the frequency's diameter, the higher the variation of the frequencies.

Also, let us set the dual angles D_1^∞ and D_2^∞ of the initial phase diameters $D(\Theta^0)$ and $D(\Xi^0)$ under the assumption that the initial phase diameters are in the range $(0,\pi)$:

$$D_1^\infty, D_2^\infty \in \left(0, \frac{\pi}{2}\right), \quad \sin(D_1^\infty) = \sin(D(\Theta^0)), \quad \sin(D_2^\infty) = \sin(D(\Xi^0)).$$

Then is clear that for an $D(\Theta^0) \in \left[0, \frac{\pi}{2}\right]$, the dual angle D_1^∞ coincides with $D(\Theta^0)$, the same would be for $D(\Xi^0) \in \left[0, \frac{\pi}{2}\right]$ and D_2^∞.

As in the case of identical oscillators, we can use the phase diameter of each layer as a Lyapunov functional, and study the temporal evolution of each layer via Grönwall's inequalities

Lemma 3.4.1. *Suppose $N \geq 2$ and that the system* (3.3)-(3.6) *has a global smooth solution $X(t) = (\Theta, \Xi)$ with the initial phases satisfying $D(\Theta^0), D(\Xi^0) \in (0,\pi)$, and the coupling strengths $K_1 > K_1^c$ and $K_2 > K_2^c$ where*

$$K_1^c = \frac{D(\Omega) + 2\varepsilon}{\sin(D(\Theta^0))} \quad \text{and} \quad K_2^c = \frac{D\left(\bar{\Omega}\right) + 2\varepsilon}{\sin(D(\Xi^0))}. \tag{3.35}$$

Then the phase diameters $D(\Theta(t))$ and $D(\Xi(t))$ are uniformly bounded by $D(\Theta^0)$ and $D(\Xi^0)$ respectively:

$$D(\Theta(t)) \leq D(\Theta^0), \quad D(\Xi(t)) \leq D(\Xi^0), \quad t \neq 0.$$

Moreover, we have the following linear Grönwall's inequality for $D(\Theta(t))$ and $D(\Xi(t))$:

$$\frac{dD(\Theta)}{dt} \leq D(\Omega) + 2\varepsilon - K_1 \frac{\sin\left(D(\Theta^0)\right)}{D(\Theta^0)} D(\Theta)$$
$$\frac{dD(\Xi)}{dt} \leq D(\bar{\Omega}) + 2\varepsilon - K_2 \frac{\sin\left(D(\Xi^0)\right)}{D(\Xi^0)} D(\Xi)$$

Proof. First, let us define the extremal indexes M_1, M_2, m_1 and m_2 as

$$M_1 = \arg\max_{1\leq i\leq N} |\theta_i|, \qquad M_2 = \arg\max_{1\leq i\leq N} |\xi_i|, \tag{3.36}$$

$$m_1 = \arg\min_{1\leq i\leq N} |\theta_i|, \quad \text{and} \quad m_2 = \arg\min_{1\leq i\leq N} |\xi_i|. \tag{3.37}$$

Considering the initial setup, we have that since $D(\Theta^0) < \pi$:

$$\begin{aligned}
\left.\frac{dD(\Theta(t))}{dt}\right|_{t=0} &= \dot{\theta}_{M_1}(0) - \dot{\theta}_{m_1}(0) \\
&= \omega_{M_1} - \omega_{m_1} + \frac{K_1}{N}\sum_{j=1}^{N}\left[\underbrace{\sin\left(\theta_j^0 - \theta_{M_1}^0\right)}_{<0} - \underbrace{\sin\left(\theta_j^0 - \theta_{m_1}^0\right)}_{>0}\right] \\
&+ \varepsilon\left[\sin\left(\xi_{M_1} - \theta_{M_1}\right) - \sin\left(\xi_{m_1} - \theta_{m_1}\right)\right] \\
&\leq D(\Omega) + 2\varepsilon + \frac{K_1 \sin(D(\Theta^0))}{ND(\Theta^0)}\sum_{j=1}^{N}\left[\left(\theta_j^0 - \theta_{M_1}^0\right) - \left(\theta_j^0 - \theta_{m_1}^0\right)\right] \\
&\leq D(\Omega) + 2\varepsilon - K_1 \sin(D(\Theta^0)) < 0. \qquad (3.38)
\end{aligned}$$

Where we used that if $-\pi < -D(\Theta^0) \leq x \leq 0$, then

$$\sin(x) \leq \frac{\sin(D(\Theta^0))}{D(\Theta^0)}x, \qquad (3.39)$$

and if $\pi > D(\Theta^0) \geq x \geq 0$:

$$\sin(x) \geq \frac{\sin(D(\Theta^0))}{D(\Theta^0)}x. \qquad (3.40)$$

Therefore, $D(\Theta(t))$ starts to strictly decrease at $t = 0_+$. Then as the functional $D(\Theta(t))$ is continuous, it follows that the set

$$\mathscr{T}_1 := \left\{t \in [0,\infty], 0 \leq \tau \leq t : D\left(\Theta(\tau)\right) < D(\Theta^0)\right\}, \text{ and } T_1 := \sup \mathscr{T}_1,$$

$\mathscr{T}_1$ is not empty, and $T_1 > 0$ is well-defined. Then let us suppose that there exists a time $t = T_1 < \infty$ such that $D\left(\Theta\left(T_1\right)\right) = D(\Theta^0)$, we are going to work on the derivative of $D(\Theta(t))$ at time $t = T_1$, following the same argument above is easy to see that:

$$\left.\frac{dD(\Theta(t))}{dt}\right|_{t=T_1} \leq D(\Omega) + 2\varepsilon - K_1 \sin(D(\Theta^0)) < 0.$$

Therefore, $\dot{D}(\Theta)|_{t=T_1} < 0$ which is a contradiction, since if $T_1 < \infty$ then $\dot{D}(\Theta)|_{t=T_1} \geq 0$, which means that $T_1 = \infty$. Furthermore, we apply the standard Grönwall's lemma to obtain,

$$D(\Theta) \leq \frac{(D(\Omega)+2\varepsilon)D(\Theta^0)}{K_1 \sin(D(\Theta^0))}\left[1-e^{-\frac{K_1\sin(D(\Theta^0))}{D(\Theta^0)}t}\right]+D(\Theta^0)e^{-\frac{K_1\sin(D(\Theta^0))}{D(\Theta^0)}t} = Z(t) \tag{3.41}$$

The behavior of the diameter of Ξ group is analogous since the phase-diameter $D(\Xi^0) < \pi$ we are going to have

$$\left.\frac{dD(\Xi(t))}{dt}\right|_{t=0} \leq D(\bar{\Omega}) + 2\varepsilon - K_2 \sin(D(\Xi^0))) < 0,$$

let $T_2 \in (0,\infty]$ be any number. Suppose that the phase-diameter $D(\Xi)(t) < D(\Xi^0)$ for $t \in [0,T_2)$, then in this time interval, we have that

$$\begin{aligned}
\frac{dD(\Xi(t))}{dt} &= \dot{\xi}_{M_2} - \dot{\xi}_{m_2} \\
&= \bar{\omega}_{M_2} - \bar{\omega}_{m_2} + \frac{K_2}{N}\sum_{j=1}^{N}\left[\sin\left(\xi_j - \xi_{M_2}\right) - \sin\left(\xi_j - \xi_{m_2}\right)\right] \\
&+ \varepsilon\left[\sin\left(\theta_{M_2} - \xi_{M_2}\right) - \sin\left(\theta_{m_2} - \xi_{m_2}\right)\right] \\
&\leq D(\bar{\Omega}) + 2\varepsilon - K_2\frac{\sin(D^\infty)}{D^\infty}D(\Xi(t)) \\
&\leq 0.
\end{aligned}$$

Defining again a set $\mathscr{T}_2$ and a time T_2 such that:

$$\mathscr{T}_2 := \left\{t \in [0,\infty], 0 \leq \tau \leq t : D\left(\Xi(\tau)\right) < D(\Xi^0)\right\}, \text{ and } T_2 := \sup \mathscr{T}_2 = \bar{Z}(t)$$

if $T_2 < \infty$ then

$$\lim_{t\to T_2^-} D(\Xi(t)) = D(\Xi^0), \tag{3.42}$$

but from the differential inequality, we know that

$$D(\Xi(t)) < D(\Xi^0), \quad t \in [0,T_2).$$

This inequality implies that

$$\lim_{t\to T_2^-} D(\Xi(t)) < D(\Xi^0),$$

which is a contradiction to (3.42) then $T_2 = \infty$ and $D(\Xi(t))$ is bound for any $t \geq 0$ by:

$$D(\Xi) \leq \frac{\left(D(\bar{\Omega}) + 2\varepsilon\right) D(\Xi^0)}{K_2 \sin(D(\Xi^0))} \left[1 - e^{-\frac{K_2 \sin(D(\Xi^0))}{D(\Xi^0)} t}\right] + D(\Xi^0) e^{-\frac{K_2 \sin(D(\Xi^0))}{D(\Xi^0)} t}. \tag{3.43}$$

□

Notice that the last lemma gives us sufficient conditions under which we can bound the diameter of each later without depending on the size of ε, in the sense that even for a significantly small value of ε the diameter of each layer can be locked.

In the same way that we calculate an upper bound, we can estimate a positive lower bound, which depends on the minimum possible distance between the natural frequencies and the values of the intralayer coupling strength.

Lemma 3.4.2. *Let $X(t) = (\{\theta_i(t)\}_{i=1}^N, \{\xi_i(t)\}_{i=1}^N)$, be the smooth solution to the system with initial configuration $\{\theta_i^0\}_{i=1}^N$ and $\{\xi_i^0\}_{i=1}^N$ satisfying $D_{X^0} \leq \pi/2$ then*

$$D(\Theta(t)) \geq \frac{d(\Omega)}{K_1} - \left(\frac{d(\Omega) - 2}{K_1} - D(\Theta^0)\right) e^{-K_1 t}$$
$$D(\Xi(t)) \geq \frac{d(\bar{\Omega})}{K_2} - \left(\frac{d(\bar{\Omega}) - 2}{K_2} - D(\Theta^0)\right) e^{-K_2 t}$$

Proof. We estimate the evolution of the minimal phase following similar arguments to those made for the proof of Lemma 3.4.1 and the elementary inequalities

$$\sin(x) \geq x, \quad x \leq 0, \quad sin(x) \leq x, \quad x \geq 0$$

to obtain

$$\begin{aligned}
\frac{dD(\Theta)}{dt} &\geq d(\Omega) - 2\varepsilon + \frac{K_1}{N} \sum_{j=1}^{N} \sin(\theta_j - \theta_{M_1}) - \sin(\theta_j - \theta_{m_1}) \\
&\geq d(\Omega) - \frac{K_1}{N} \sum_{j=1}^{N} (\theta_j - \theta_{M_1}) - (\theta_j - \theta_{m_1}) \\
&\geq d(\Omega) - K_1 D(\Theta),
\end{aligned}$$

this yields the desired result. The same procedure gives us the inequality for $D(\Xi)$. □

For the following statement, we will use Lemma A.1.1, given by [21]. In this proposition, we estimate the time in which the diameter of the layers is reduced until entering the range of D_1^∞ and D_2^∞, respectively.

Proposition 3.4.3. *Let $X(t) = (\Theta, \Xi)$ be the global solution to the system* (3.3)-(3.6) *satisfying*

$$D(\Theta^0), D(\Xi^0) \in (0,\pi), \quad K_1 > K_1^c \quad \text{and} \quad K_2 > K_2^c$$

Then there exists $t_1, t_2 > 0$ such that

$$D(\Theta(t)) \leq D_1^\infty \quad \text{for } t \geq t_1, \quad D(\Xi(t)) \leq D_2^\infty \quad \text{for } t \geq t_2.$$

Proof. We will only work on the Θ case since the proof is quite long and Ξ is analogous. For the case $D(\Theta^0) < \frac{\pi}{2}$, we have $D_1^\infty = D(\Theta^0)$, and it follows from Lemma 3.4.1 that $D(\Theta(t)) \leq D(\Theta^0) = D^\infty$, for any $t \geq 0$.

Next, for any $D(\Theta^0) \in (0,\pi)$, it follows from the assumptions and Lemma 3.4.1 that $D(\Theta(t)) \leq D(\Theta^0) < \pi$ and

$$\begin{aligned}
\dot{D}(\Theta(t)) &= \dot{\theta}_{M_1} - \dot{\theta}_{m_1} = \omega_{M_1} - \omega_{m_1} - \frac{K_1}{N}\sum_{j=1}^{N}\left(\sin(\theta_j - \theta_{M_1}) - \sin(\theta_j - \theta_{m_1})\right) \\
&\quad + \varepsilon\left(\sin(\xi_{M_1} - \theta_{M_1}) - \sin(\xi_{m_1} - \theta_{m_1})\right) \\
&= \omega_{M_1} - \omega_{m_1} + \varepsilon\left(\sin(\xi_{M_1} - \theta_{M_1}) - \sin(\xi_{m_1} - \theta_{m_1})\right) \\
&\quad + \frac{K_1}{N}\left[-2\sin(\theta_{M_1} - \theta_{m_1}) + \sum_{j\neq M_1, m_1}^{N}\left(\sin(\theta_j - \theta_{M_1}) - \sin(\theta_j - \theta_{m_1})\right)\right] \\
&= \omega_{M_1} - \omega_{m_1} - K_1\sin(\theta_{M_1} - \theta_{m_1}) + \varepsilon\left(\sin(\xi_{M_1} - \theta_{M_1}) - \sin(\xi_{m_1} - \theta_{m_1})\right) \\
&\quad + \frac{K_1}{N}\sum_{j\neq M_1, m_1}^{N}\left(\sin(\theta_j - \theta_{M_1}) + \sin(\theta_{m_1} - \theta_j) + \sin(\theta_{M_1} - \theta_{m_1})\right).
\end{aligned}$$

We use the result of Lemma A.1.1:

$$\sin(\chi_M - \chi_m) + \sin(\chi_l - \chi_M) + \sin(\chi_m - \chi_l) \leq 0,$$

and $K > K_1^c$ to get

$$\dot{D}(\Theta(t)) \leq D(\Omega) + 2\varepsilon - K_1\sin(D(\Theta(t))). \tag{3.44}$$

Hence, we have that in the case of $D(\Theta^0) = \pi/2$ we get

$$\dot{D}(\Theta^0) \leq D(\Omega) + 2\varepsilon - K_1 \sin(D(\Theta^0)) = D(\Omega) + 2\varepsilon - K_1 < 0,$$

thus, there exists a time $t_1 > 0$ such that $D(\Theta(t_1)) < \frac{\pi}{2}$, moreover, we can designate a constant γ such that

$$K_1 > \frac{D(\Omega) + 2\varepsilon}{\sin(\gamma)} > D(\Omega) + \varepsilon \quad \text{and} \quad D(\Theta(t_1)) < \gamma < D(\Theta^0),$$

then using the same arguments as the case $D(\Theta^0) \in (0, \pi/2)$ we found that $D(\Theta(t)) \leq \gamma \leq D^\infty$ after a time $t \geq 0$.

To conclude, consider the case where $D(\Theta^0) \in (\pi/2, \pi)$ and suppose that $D^\infty \leq D(\Theta(t)) \leq D(\Theta^0)$ for $t \geq 0$. Since $\sin(D(\Theta(t))) \geq \sin(D_1^\infty) = \sin(D(\Theta^0))$ for $t \geq 0$ and from (3.44) precedes

$$\begin{aligned}
\dot{D}(\Theta(t)) &\leq D(\Omega) + 2\varepsilon - K_1 \sin(D(\Theta(t))) \\
&\leq D(\Omega) + 2\varepsilon - K_1 \sin(D_1^\infty) \\
&= D(\Omega) + 2\varepsilon - K_1 \sin(D(\Theta^0)) \\
&= \left(1 - \frac{K_1}{K_1^c}\right)(D(\Omega) + 2\varepsilon) < 0.
\end{aligned}$$

Integrating the above differential inequality, we get

$$D(\Theta(t)) \leq D(\Theta^0) + \left(1 - \frac{K_1}{K_1^c}\right)(D(\Omega) + 2\varepsilon)t$$

then with

$$t_1 := \frac{D(\Theta^0) - D_1^\infty}{\left(\frac{K_1}{K_1^c} - 1\right)(D(\Omega) + 2\varepsilon)},$$

we have that for $t > t_1$

$$D(\Theta^0) + \left(1 - \frac{K}{K_1^c}\right) D(\Omega)t \leq D_1^\infty.$$

Hence, at $t = t_1$, we have that $D(\Theta(t))$ leaves the interval $\left[D_1^\infty, D(\Theta^0)\right]$. The next step is to prove that after $t \leq t_1$, the dynamics $D(\Theta(t))$ remains bounded to D_1^∞, this proof follows the same procedure given by 3.4.1, where instead of being $D(\Theta^0)$, our upper bound it is D_1^∞. □

The last lemma gives us sufficient conditions to bound the diameter of each layer for all $t > 0$. After this, it is reasonable to analyze whether the given conditions also imply that the entire system is bound. Only considering the above conditions, this behavior cannot be guaranteed; in effect, if, for example, we consider a state in which the extremes of the system are given by oscillators in different groups, we are going to see in the following lemma that the influence of the intralayer strength over the dynamics of the diameter of the system is inversely proportional to the diameter of each layer, in other words, the greater the intralayer synchronization is, the lower the influence of the intralayer forces on the dynamics of the system diameter.

Lemma 3.4.4. *Suppose that the initial configuration X^0 and coupling strengths satisfy:*

- $D(\Theta^0)$, $D(\Xi^0) \in (\frac{\pi}{2}, \pi)$
- $K_1 > K_1^c$, $K_2 > K_2^c$ *and*

$$\varepsilon > \frac{D\left(\Omega, \bar{\Omega}\right) - \left(D(\Omega) + D(\bar{\Omega})\right)}{2}, \tag{3.45}$$

where K_1^c and K_2^c are defined in (3.35)*. Then, there exists a finite time $t_\varepsilon \in (0, \infty)$ such that $\dot{D}(X(t_\varepsilon)) \leq 0$.*

Proof. We are going to work over the derivative of $D(X(t))$ at time $t = 0$, in connection with the membership of the extremal phases of the whole system $X = \{\Theta, \Xi\}$. Let M and m be indices such that

$$X_M(t) := \max\{\theta_{M_1}, \xi_{M_2}\}, \quad X_m(t) := \min\{\theta_{m_1}, \xi_{m_2}\}, \tag{3.46}$$

then we will have two cases: when the maximum and the minimum belong to the same layer and when not.

The first case: *(Maximal and minimal from the same layer)* For this case it is clear that there are two possibilities, either $X_M = \theta_M$ and $X_m = \theta_m$ or $X_M = \xi_M$ and $X_m = \xi_m$, in any of the cases, thanks to the result of Lemma 3.4.1 we have that $\dot{D}(X(0)) < 0$.

The second case*(Maximal and minimal from different layers).* Assume that $X_M = \theta_{M_1}$ and $X_m = \xi_{m_2}$, then

$$\left.\frac{d^+ D(X(t))}{dt}\right|_{t=0} = \omega_M - \bar{\omega}_m + \frac{K_1}{N}\sum_{j=1}^{N}\sin(\theta_j^0 - \theta_M^0) - \frac{K_2}{N}\sum_{j=1}^{N}\sin(\xi_j^0 - \xi_m^0)$$

$$+2\varepsilon\left[\sin(\xi_M-\theta_M)-\sin(\theta_m-\xi_m)\right].$$

By Lemma 3.4.1, and considering the initial setup, we have

$$\begin{aligned}\left.\frac{d^+D(X(t))}{dt}\right|_{t=0} &\leq D(\Omega,\bar{\Omega})+2\varepsilon-K_1\sin(D(\Theta(t)))-K_2\sin(D(\Xi(t)))\\ &\leq D(\Omega,\bar{\Omega})+2\varepsilon-K_1\sin(D(\Theta^0))-K_2\sin(D(\Xi^0))\\ &\leq D(\Omega,\bar{\Omega})+2\varepsilon-\frac{D(\Omega)+2\varepsilon}{\sin(D(\Theta^0))}\sin(D(\Theta^0))-\frac{D(\bar{\Omega})+2\varepsilon}{\sin(D(\Xi^0))}\sin(D(\Xi^0))\\ &\leq D(\Omega,\bar{\Omega})-\big(D(\Omega)+D(\bar{\Omega})\big)-2\varepsilon\\ &\leq 0,\end{aligned}$$

due to the condition (3.45). Therefore, $\dot{D}(X)|_{t=0}<0$ and for the continuity of $D(X(t))$ there exist a t_ε such that $\dot{D}(X)|_{t=t_\varepsilon}\leq 0$.

□

Note that Lemma 3.4.4 establishes sufficient conditions so that in a finite time we can control the total distance of the oscillators of the system. In general to control this diameter, it is required that the initial configuration of the system is within the range $[0,\pi]$, but the conditions of Lemma 3.4.4 allow us to relax this restriction and to know the behavior of the system for cases outside the range in a finite time. An example of the behavior of the diameters of the system under these conditions can be seen in Figure 3.6, note that this plot not only allows us to observe how the diameter of the oscillators in the system is shortened for a while and then grow but also how under the same conditions the diameter of each layer is maintained at a constant distance, highlighting the importance of analyzing the system as a layered structure. Moreover, if we consider a system with more restricted initial conditions we can restrict in a finite time the diameter of the system under a linear equation:

Lemma 3.4.5. *Suppose that the initial configuration $D_{X^0}\in(\frac{\pi}{2},\pi)$ and the coupling strengths satisfy:*

$$K_1>K_1^c=\frac{D(\Omega)+D(\Omega,\bar{\Omega})}{2\sin(D(\Theta^0))},\quad K_2>K_2^c=\frac{D(\bar{\Omega})+D(\Omega,\bar{\Omega})}{2\sin(D(\Xi^0))},\quad \textit{and}\quad \varepsilon>0.$$

Then, exists a finite time $t_\varepsilon\in(0,\infty)$ such that $\dot{D}(X(t_\varepsilon))\geq 0$. And $D(X(t))\leq D^\infty$ for $t\in(0,t_\varepsilon)$.

$$D(X(t))\leq D_{X^0}.$$

Proof. Suppose that

$$\begin{aligned} D^{\infty} \leq D(X(t)) \leq D_{X^0} \\ D_1^{\infty} \leq D(\Theta(t)) \leq D(\Theta^0) \\ \text{and} \quad D_2^{\infty} \leq D(\Xi(t)) \leq D(\Xi^0), \end{aligned}$$

for $t \geq 0$. Consider the definitions of extremal phases given in (3.46) and the two possible extremal phase states.

The first case: *(Maximal and minimal from the same layer)*

Assume that $X_M = \theta_M$ and $X_m = \theta_m$ then

$$\begin{aligned} \left.\frac{d^+ D(X(t))}{dt}\right|_{t=0} &= \omega_M - \omega_m + \frac{K_1}{N}\sum_{j=1}^{N} \sin(\theta_j^0 - \theta_M^0) - \sin(\theta_j^0 - \theta_m^0) \\ &\quad + \varepsilon \underbrace{\left[\sin(\xi_M^0 - \theta_M^0) - \sin(\xi_m^0 - \theta_m^0)\right]}_{\leq 0} \\ &\leq D(\Omega) - K_1 \sin(D_{X^0}) \\ &\leq D(\Omega) - K_1 \sin(D(\Theta^0)) \\ &= -\frac{1}{2}\left[D(\Omega)\left(\frac{K_1}{K_1^c} - 1\right) + \left(\frac{K_1}{K_1^c} D(\Omega, \bar{\Omega}) - D(\Omega)\right)\right] \\ &< 0. \end{aligned}$$

Notice that we use the same approach for the calculations on Lemma 3.4.1, and the case $X_M = \xi_M$ and $X_m = \xi_m$ is analogous. Moreover, if we integrate the above inequality to get

$$D(X(t)) \leq D_{X^0} - \frac{1}{2}\left[D(\Omega)\left(\frac{K_1}{K_1^c} - 1\right) + \left(\frac{K_1}{K_1^c} D(\Omega, \bar{\Omega}) - D(\Omega)\right)\right] t.$$

Note that after

$$t_1 := \frac{2\left(D_{X^0} - D^{\infty}\right)}{D(\Omega)\left(\frac{K_1}{K_1^c} - 1\right) + \left(\frac{K_1}{K_1^c} D(\Omega, \bar{\Omega}) - D(\Omega)\right)},$$

we have that $D(X(t_1)) \leq D^{\infty}$, which means that $D(X(t))$ leaves the interval $[D^{\infty}, D_{X^0}]$ at the time $t = t_1$. In the case that maximal and minimal are in the layer of Ξ, we have that the time

in which $D(X(t))$ leaves $[D^\infty, D_{X^0}]$ is given by:

$$t_2 := \frac{2\left(D_{X^0} - D^\infty\right)}{D(\bar{\Omega})\left(\frac{K_2}{K_2^c} - 1\right) + \left(\frac{K_2}{K_2^c} D(\Omega, \bar{\Omega}) - D(\bar{\Omega})\right)}.$$

Second case *(Maximal and minimal from different layers)* Set $X_M = \theta_M$ and $X_m = \xi_m$

$$\begin{aligned}
\left.\frac{d^+ D(X(t))}{dt}\right|_{t=0} &= \omega_M - \bar{\omega}_m + \frac{K_1}{N}\sum_{j=1}^{N}\sin(\theta_j^0 - \theta_M^0) - \frac{K_2}{N}\sum_{j=1}^{N}\sin(\xi_j^0 - \xi_m^0) \\
&\quad + \varepsilon\left[\sin(\xi_M^0 - \theta_M^0) - \sin(\theta_m^0 - \xi_m^0)\right] \\
&\leq D(\Omega, \bar{\Omega}) - K_1 \sin(D(\Theta^0)) - K_2 \sin(D(\Xi^0)) \\
&\leq D(\Omega, \bar{\Omega}) - \frac{K_1}{2K_1^c}(D(\Omega, \bar{\Omega}) + D(\Omega)) - \frac{K_2}{2K_2^c}(D(\Omega, \bar{\Omega}) + D(\bar{\Omega})) \\
&\leq -\frac{1}{2}\left[D(\Omega, \bar{\Omega})(\frac{K_1}{K_1^c} + \frac{K_2}{K_2^c} - 2) + \frac{K_1}{K_1^c} D(\Omega) + \frac{K_2}{K_2^c} D(\bar{\Omega})\right] \\
&< 0,
\end{aligned}$$

in the same way as before, if we integrate the inequality, we get

$$D(X(t)) \leq D_{X^0} - \frac{1}{2}\left[D(\Omega, \bar{\Omega})(\frac{K_1}{K_1^c} + \frac{K_2}{K_2^c} - 2) + \frac{K_1}{K_1^c} D(\Omega) + \frac{K_2}{K_2^c} D(\bar{\Omega})\right] t.$$

□

3.5 Asymptotic formation of a 2-cluster locked state for the AIC Model

In this subsection, we provide sufficient conditions for reaching a 2-cluster configuration on the AIC model.

Lemma 3.5.1. *Suppose that the system* (3.5)-(3.6) *has* $N \geq 2$ *and a global smooth solution* $X(t) = (\Theta, \Xi)$ *with the initial phases satisfying* $D(\Theta^0), D(\Xi^0) \in (0, \pi)$*, and the coupling strengths* $K_1 > K_1^c$ *and* $K_2 > K_2^c$ *where*

$$K_1^c = \frac{D(\Omega) + 2\varepsilon \sin(\frac{D(\Theta^0)}{2})}{\sin(D(\Theta^0))} \quad \textit{and} \quad K_2^c = \frac{D\left(\bar{\Omega}\right) + 2\varepsilon \sin(\frac{D(\Xi^0)}{2})}{\sin(D(\Xi^0))}. \tag{3.47}$$

Then the phase diameters $D(\Theta(t))$ and $D(\Xi(t))$ are uniformly bounded by $D(\Theta^0)$ and $D(\Xi^0)$ respectively:

$$D(\Theta(t)) \leq D(\Theta^0), \quad D(\Xi(t)) \leq D(\Xi^0), \quad t \neq 0$$

Proof. Let $T_1 \in (0,\infty]$ be any number. Suppose that the phase-diameter $D(\Theta(t))$ satisfies $D(\Theta(t)) < \pi$ for all $t \in [0,T_1)$. Considering the extremal indexes defined in eqs. (3.36) and (3.37) over the time interval $[0,T_1)$ and the AIC dynamics (3.5), we have

$$\begin{aligned}
\frac{dD(\Theta(t))}{dt} &= \dot{\theta}_{M_1}(t) - \dot{\theta}_{m_1}(t) \\
&= \omega_{M_1} - \omega_{m_1} + \frac{K_1}{N}\sum_{j=1}^{N}\left[\underbrace{\sin\left(\theta_j - \theta_{M_1}\right)}_{<0} - \underbrace{\sin\left(\theta_j - \theta_{m_1}\right)}_{>0}\right] \\
&+ \frac{\varepsilon}{N}\sum_{j=1}^{N}\left[\sin\left(\xi_j - \theta_{M_1}\right) - \sin\left(\xi_j - \theta_{m_1}\right)\right] \\
&\leq D(\Omega) + \frac{K_1 \sin(D(\Theta^0))}{N D(\Theta^0)}\sum_{j=1}^{N}\left[\left(\theta_j - \theta_{M_1}\right) - \left(\theta_j - \theta_{m_1}\right)\right] \\
&+ \frac{2\varepsilon}{N}\sin\left(\frac{\theta_{m_1} - \theta_{M_1}}{2}\right)\sum_{j=1}^{N}\cos\left(\xi_j - \frac{\theta_{M_1} + \theta_{m_1}}{2}\right),
\end{aligned}$$

where we use eqs. (3.39) and (3.40). This yields

$$\frac{dD(\Theta(t))}{dt} \leq D(\Omega) + 2\varepsilon\sin\left(\frac{D(\Theta(t))}{2}\right) - \frac{K_1\sin(D(\Theta^0))}{D(\Theta^0)}D(\Theta(t)). \tag{3.48}$$

Moreover, a time $t = 0$ we have

$$\frac{dD(\Theta(t))}{dt} \leq D(\Omega) + 2\varepsilon\sin\left(\frac{D(\Theta^0)}{2}\right) - K_1\sin(D(\Theta)^0) < 0.$$

Therefore, $D(\Theta(t))$ starts to strictly decrease at $t = 0_+$. Then, since the functional $D(\Theta(t))$ is continuous, it follows that the set

$$\mathscr{T}_1 := \left\{t \in [0,\infty], 0 \leq \tau \leq t : D\left(\Theta(\tau)\right) < D(\Theta^0)\right\}, \text{ and } \quad T_1 := \sup \mathscr{T}_1,$$

is not empty, and $T_1 > 0$ is well-defined. Then let us suppose that there exists a time $t = T_1 < \infty$ such that $D(\Theta(T_1)) = D(\Theta^0)$, then we are going to work over the derivative of $D(\Theta(t))$ at time $t = T_1$, following the same problem as earlier, it is easy to see that:

$$\left.\frac{dD(\Theta(t))}{dt}\right|_{t=T_1} \leq D(\Omega) + 2\varepsilon \sin\left(\frac{D(\Theta^0)}{2}\right) - K_1 \sin(D(\Theta^0))) < 0.$$

Therefore, $\dot{D}(\Theta)|_{t=T_1} < 0$ which is a contradiction, since if $T_1 < \infty$ then $\dot{D}(\Theta)|_{t=T_1}| \geq 0$, which means that $T_1 = \infty$.

The behavior of the diameter of the Ξ group is analogous. Since the phase-diameter $D(\Xi^0) < \pi$, we have

$$\left.\frac{dD(\Xi(t))}{dt}\right|_{t=0} \leq D(\bar{\Omega}) + 2\varepsilon \sin\left(\frac{D(\Xi^0)}{2}\right) - K_2 \sin(D(\Xi^0))) < 0, \tag{3.49}$$

Defining again a set $\mathscr{T}_2$ and a time T_2 such that:

$$\mathscr{T}_2 := \left\{t \in [0,\infty], 0 \leq \tau \leq t : D(\Xi(\tau)) < D(\Xi^0)\right\}, \quad \text{and} \quad T_2 := \sup \mathscr{T}_2 = \bar{Z}(t),$$

From the equation (3.49) we know that $\mathscr{T}_2 \neq \emptyset$, assume $T_2 < \infty$ then

$$\lim_{t \to T_2^-} D(\Xi(t)) = D(\Xi^0), \tag{3.50}$$

let $T_2 \in (0,\infty]$ be any number. Suppose that the phase-diameter $D(\Xi)(t) < D(\Xi^0)$ for $t \in [0, T_2)$, then in this time interval, we have that

$$\frac{dD(\Xi(t))}{dt} \leq D(\bar{\Omega}) + 2\varepsilon \sin\left(\frac{D(\Xi(t))}{2}\right) - K_2 \frac{\sin(D(\Xi^0)}{D(\Xi^0)} D(\Xi(t))$$

from the differential inequality, we know that

$$D(\Xi(t)) < D(\Xi^0), \quad t \in [0, T_2).$$

This implies that

$$\lim_{t \to T_2^-} D(\Xi(t)) < D(\Xi^0),$$

which is a contradiction to (3.50) then $T_2 = \infty$. □

Below, we show that the diameter of each layer will collapse exponentially fast. For this, we propose bigger lower bounds for the intralayer coupling strength:

$$\bar{K}_1^c = \frac{D(\Omega) + \varepsilon D(\Theta^0)}{\sin(D(\Theta^0))} \quad \text{and} \quad \bar{K}_2^c = \frac{D(\bar{\Omega}) + \varepsilon D(\Xi^0)}{\sin(D(\Xi^0))}. \tag{3.51}$$

The following lemma states that the diameter of each layer exponentially decrease for any of the coupling strengths bounds given by (3.47) or (3.51).

Lemma 3.5.2. *Let $X(t) = (\Theta(t), \Xi(t))$ be a solution to the system* (3.5)-(3.6) *with initial data $D(\Theta^0)$, $D(\Xi^0) \in (0, \pi)$. For a K_1 and K_2 large enough, there exist positive constants C_1, C_2, Λ_1 and Λ_2 such that*

$$D(\Theta(t)) \leq C_1 \left(1 - e^{-\Lambda_1 t}\right) + D(\Theta^0) e^{-\Lambda_1 t} \quad \text{and}$$
$$D(\Xi(t)) \leq C_2 \left(1 - e^{-\Lambda_2 t}\right) + D(\Xi^0) e^{-\Lambda_2 t},$$

where the constant estimates will depend on the lower bound, dependent on K_1 and K_2.

Proof. We use the estimates made in Lemma 3.5.1, in particular, for the Θ layer, we use the equation (3.48)

$$\frac{d}{dt} D(\Theta) \leq D(\Omega) + 2\varepsilon \sin\left(\frac{D(\Theta(t))}{2}\right) - \frac{K_1 \sin(D(\Theta^0))}{D(\Theta^0)} D(\Theta(t)). \tag{3.52}$$

If we consider $K_1 > K_1^c$, since $D(\Theta(t)) \in (0, \pi)$ and $D(\Theta(t)) \leq D(\Theta^0)$ for Lemma 3.5.1 we have

$$\sin\left(\frac{D(\Theta(t))}{2}\right) \leq \sin\left(\frac{D(\Theta^0)}{2}\right), \quad \forall t \geq 0,$$

then the equation (3.52) takes the Grönwall-type inequality:

$$\frac{d}{dt} D(\Theta) \leq D(\Omega) + 2\varepsilon \sin\left(\frac{D(\Theta^0)}{2}\right) - \frac{K_1 \sin(D(\Theta^0))}{D(\Theta^0)} D(\Theta(t)),$$

which leads to

$$D(\Theta) \leq \frac{\left(D(\Omega) + 2\varepsilon \sin\left(\frac{D(\Theta^0)}{2}\right)\right) D(\Theta^0)}{K_1 \sin(D(\Theta^0))} \left[1 - e^{-\frac{K_1 \sin(D(\Theta^0))}{D(\Theta^0)} t}\right] + D(\Theta^0) e^{-\frac{K_1 \sin(D(\Theta^0))}{D(\Theta^0)} t},$$

On the other side, if we consider $K_1 > \bar{K}_1^c$, we can consider the Grönwall inequality

$$\frac{d}{dt}D(\Theta) \leq D(\Omega) - \left[\frac{K_1 \sin(D(\Theta^0))}{D(\Theta^0)} - \varepsilon\right] D(\Theta(t)),$$

where we use the fact that $\sin(x) < x$ for $x > 0$. Then we arrive to the form

$$D(\Theta(t)) \leq D(\Theta^0)\left\{\frac{D(\Omega)}{K_1 \sin(D(\Theta^0)) - \varepsilon D(\Theta^0)}\left[1 - e^{-\left(\frac{K_1 \sin(D(\Theta^0))}{D(\Theta^0)} - \varepsilon\right)t}\right] + e^{-\left(\frac{K_1 \sin(D(\Theta^0))}{D(\Theta^0)} - \varepsilon\right)t}\right\}.$$

The case for the Ξ layer is analogous considering K_2^c and $\bar{K}_1^c$. This leads to the desired result. □

We present sufficient conditions for a 2-cluster bounded synchronization. Moreover, notice that when $D(\Omega) = 0$, for a $K_1 > \bar{K}_{c_1}$, $D(\Theta) \to 0$ when $t \to \infty$, the same behavior can happen to the Ξ layer if $D(\bar{\Omega}) = 0$ and $K_2 > \bar{K}_{c_2}$.

Now we will present the conditions for the complete synchronization of the system giving an *AIC* topology. Primarily, there is a work done for symmetric matrix coupling given by [61] and [59]. Our work aims to exploit the AIC structure for giving conditions over the intralayer strengths and not over the interlayer strength. Consider the total variance of the natural frequencies

$$\sigma(\Omega, \bar{\Omega}) := \frac{1}{\sqrt{N}}\left(\sum_{i=1}^{N} |\omega_i|^2 + |\bar{\omega}_i|^2\right)^{\frac{1}{2}}.$$

and the total difference between the intracoupling strengths $\Delta_{K_{12}} = |K_1 - K_2|$

Then give it the energy function:

$$\mathscr{E}(X(t)) := \frac{1}{N}\sum_{i=1}^{2N} |X_i(t)|^2 = \frac{1}{N}\sum_{i=1}^{N} |\theta_i(t)|^2 + \frac{1}{N}\sum_{i=1}^{N} |\xi_i(t)|^2,$$

Lemma 3.5.3. *Let $\lambda_0 \in (0,\pi)$, and $X(t) = \{\Theta(t), \Xi(t)\}$ be the smooth solution to the system* (3.5) *and* (3.6) *with coupling strength and initial data satisfying:*

$$\varepsilon > \frac{1}{2}\left[\frac{\sqrt{2}\sigma(\Omega,\bar{\Omega})}{\sin(\lambda_0)} + \frac{\Delta_{K_{12}}}{2}\right] \quad \textit{and} \quad \mathscr{E}(X^0) \leq \frac{\lambda_0^2}{2N}. \tag{3.53}$$

Then we have:

$$D(X(t)) \leq \lambda_0 < \pi \quad \forall t \geq 0.$$

where the energy function $\mathscr{E}(X(t))$ satisfies:

$$\frac{d\mathscr{E}(X(t))}{dt} \leq 2\sigma\left(\Omega,\bar{\Omega}\right)\sqrt{\mathscr{E}(X(t))} - (4\varepsilon - \Delta_{K_{12}})\frac{\sin(\lambda_0)}{\lambda_0}\mathscr{E}(X(t)). \tag{3.54}$$

Proof. First define the time set:

$$\mathscr{T} := \{T : D(X(t)) < \lambda_0, \quad \forall t \in [0,T)\} \text{ and } T_* := \sup \mathscr{T}.$$

Since

$$\left|X_i^0 - X_j^0\right|^2 \leqslant 2\left(|X_i^0|^2 + |X_j^0|^2\right) \leqslant 2N\mathscr{E}(X^0) < \lambda_0^2, \quad i,j = 1,\ldots,N, \tag{3.55}$$

thanks to the upper bound give it to the energy function in (3.53). By continuity, there exists a $\delta > 0$ such that

$$|X_i(t) - X_j(t)| < \lambda_0, \quad t \in [0,\delta), \quad i,j = 1,\ldots,N.$$

Therefore $\delta \in \mathscr{T}$ and $\mathscr{T} \neq \emptyset$. Suppose that there exists a $T_* < \infty$, then we have

$$\max_{t\in[0,T_*]} D(X(t)) \leqslant \lambda_0. \tag{3.56}$$

we use the dynamics of the AIC system given by (3.5) to find

$$\begin{aligned}\frac{d\mathscr{E}(X(t))}{dt} &= \frac{2}{N}\sum_{i=1}^{N}\dot{\theta}_i\theta_i + \frac{2}{N}\sum_{i=1}^{N}\dot{\xi}_i\xi_i \\ &= \frac{2}{N}\left[\sum_{i=1}^{N}\omega_i\theta_i + \sum_{i=1}^{N}\bar{\omega}_i\xi_i + \frac{K_1}{N}\sum_{i,j=1}^{N}\sin\left(\theta_j - \theta_i\right)\theta_i + \frac{K_2}{N}\sum_{i,j=1}^{N}\sin\left(\xi_j - \xi_i\right)\xi_i\right]\end{aligned}$$

$$
\begin{aligned}
&+2\frac{\varepsilon}{N^2}\sum_{i,j=1}^{N}\sin(\xi_j-\theta_i)\theta_i+2\frac{\varepsilon}{N^2}\sum_{i,j=1}^{N}\sin\left(\theta_j-\xi_i\right)\xi_i\\
&\overset{i\leftrightarrow j}{\leq}\frac{2}{N}\sum_{j=1}^{N}|\omega_j\theta_j|+|\bar{\omega}_j\xi_j|+\frac{2K_1}{N^2}\sum_{i,j=1}^{N}\sin\left(\theta_i-\theta_j\right)\theta_j\\
&+\frac{2K_2}{N^2}\sum_{i,j=1}^{N}\sin\left(\xi_j-\xi_i\right)\xi_j+2\frac{\varepsilon}{N^2}\left[\sum_{i,j=1}^{N}\sin(\xi_i-\theta_j)\theta_j+\sum_{i,j=1}^{N}\sin(\theta_i-\xi_j)\xi_j\right].
\end{aligned}
$$

Then for Hölder inequality and since $\sin(x)$ is odd we have

$$
\begin{aligned}
\frac{d\mathscr{E}(X(t))}{dt}&\leq\frac{2}{N}\left(\sum_{i=1}^{N}|\omega_i|^2+|\bar{\omega}_i|^2\right)^{\frac{1}{2}}\left(\sum_{i=1}^{N}|\theta_i|^2+\sum_{i=1}^{N}|\xi_i|^2\right)^{\frac{1}{2}}\\
&-\frac{K_1}{N^2}\sum_{i,j=1}^{N}\sin(\theta_j-\theta_i)(\theta_j-\theta_i)-\frac{K_2}{N^2}\sum_{i,j=1}^{N}\sin(\xi_j-\xi_i)(\xi_j-\xi_i)\\
&-2\frac{\varepsilon}{N^2}\sum_{i,j=1}^{N}\sin(\xi_j-\theta_i)(\xi_j-\theta_i).
\end{aligned}
$$

Considering that we are working in the time $t\in[0,T^*)$ and the elementary inequality

$$
\frac{\sin(x)}{x}\geq\frac{\sin(\lambda_0)}{\lambda_0},\quad\forall x\in[-\lambda_0,\lambda_0],\tag{3.57}
$$

that implies

$$
x\sin(x)\geq\frac{\sin(\lambda_0)}{\lambda_0}x^2\quad\forall x\in[-\lambda_0,\lambda_0].\tag{3.58}
$$

we apply the above inequality to derive

$$
\begin{aligned}
\frac{d\mathscr{E}(X(t))}{dt}&=2\frac{\sigma\left(\Omega,\bar{\Omega}\right)}{\sqrt{N}}\left(\sum_{i=1}^{N}|\theta_i|^2+\sum_{i=1}^{N}|\xi_i|^2\right)^{\frac{1}{2}}-\frac{K_1}{N^2}\frac{\sin(\lambda_0)}{\lambda_0}\sum_{i,j=1}^{N}\left|\theta_j-\theta_i\right|^2\\
&-\frac{K_2}{N^2}\frac{\sin(\lambda_0)}{\lambda_0}\sum_{i,j=1}^{N}\left|\xi_j-\xi_i\right|^2-2\frac{\varepsilon}{N^2}\frac{\sin(\lambda_0)}{\lambda_0}\sum_{i,j=1}^{N}\left|\xi_j-\theta_i\right|^2\\
&=\frac{\sigma\left(\Omega,\bar{\Omega}\right)}{\sqrt{N}}\left(\sum_{i=1}^{N}|\theta_i|^2+\sum_{i=1}^{N}|\xi_i|^2\right)^{\frac{1}{2}}-2\frac{K_1}{N}\frac{\sin(\lambda_0)}{\lambda_0}\sum_{i=1}^{N}|\theta_i|^2\\
&+2\frac{K_1}{N^2}\frac{\sin(\lambda_0)}{\lambda_0}\sum_{i,j=1}^{N}\theta_i\theta_j-2\frac{K_2}{N}\frac{\sin(\lambda_0)}{\lambda_0}\sum_{i=1}^{N}|\xi_i|^2
\end{aligned}
$$

$$
\begin{aligned}
&+2\frac{K_2}{N^2}\frac{\sin(\lambda_0)}{\lambda_0}\sum_{i,j=1}^{N}\xi_i\xi_j-2\frac{\varepsilon}{N}\frac{\sin(\lambda_0)}{\lambda_0}\sum_{i=1}^{N}\left(|\xi_i|^2+|\theta_i|^2\right)\\
&+4\frac{\varepsilon}{N^2}\frac{\sin(\lambda_0)}{\lambda_0}\sum_{i,j=1}^{N}\xi_j\theta_i\\
&=2\frac{\sigma\left(\Omega,\bar{\Omega}\right)}{\sqrt{N}}\left(\sum_{i=1}^{N}|\theta_i|^2+\sum_{i=1}^{N}|\xi_i|^2\right)^{\frac{1}{2}}-2(K_1+\varepsilon)\frac{\sin(\lambda_0)}{N\lambda_0}\sum_{i=1}^{N}|\theta_i|^2\\
&-2(K_2+\varepsilon)\frac{\sin(\lambda_0)}{N\lambda_0}\sum_{i=1}^{N}|\xi_i|^2\\
&\underbrace{+2\frac{K_1}{N^2}\frac{\sin(\lambda_0)}{\lambda_0}\sum_{i,j=1}^{N}\theta_j\theta_i+2\frac{K_2}{N^2}\frac{\sin(\lambda_0)}{\lambda_0}\sum_{i,j=1}^{N}\xi_i\xi_j+4\varepsilon\frac{\sin(\lambda_0)}{N^2\lambda_0}\sum_{i,j=1}^{N}\xi_j\theta_i}_{:=E}.
\end{aligned}
$$

Focusing on the components in E of the last inequality and noticing that since $P_c=0$, we have that $\theta_c=-\xi_c$, which means:

$$
\sum_{i,j=1}^{N}\theta_j\theta_i=\sum_{i,j=1}^{N}\xi_i\xi_j=-\sum_{i,j=1}^{N}\theta_i\xi_j, \tag{3.59}
$$

and

$$
\left(\sum_{i=1}^{N}\theta_i\right)^2+\left(\sum_{i=1}^{N}\xi_i\right)^2=-2\sum_{i,j=1}^{N}\theta_i\xi_j, \tag{3.60}
$$

considering the equalities (3.59), (3.60) and that $K_1>K_2>\varepsilon$, we have

$$
\begin{aligned}
E&=2\frac{\sin(\lambda_0)}{\lambda_0N^2}\left[K_1\sum_{i,j=1}^{N}\theta_j\theta_i+K_2\sum_{i,j=1}^{N}\xi_i\xi_j+2\varepsilon\sum_{i,j=1}^{N}\xi_j\theta_i\right]\\
&=2\frac{\sin(\lambda_0)}{\lambda_0N^2}\left[-K_1\sum_{i,j=1}^{N}\theta_i\xi_j-K_2\sum_{i,j=1}^{N}\xi_i\theta_j+2\varepsilon\sum_{i,j=1}^{N}\xi_i\theta_j\right]\\
&=\frac{\sin(\lambda_0)}{\lambda_0N^2}(K_1+K_2-2\varepsilon)\left[\left(\sum_{i=1}^{N}\theta_i\right)^2+\left(\sum_{i=1}^{N}\xi_i\right)^2\right].
\end{aligned}
$$

using the above equality over the estimates for the dynamics of the energy function and the Callebaut's inequality, we have

$$
\frac{d\mathscr{E}(X(t))}{dt}\leq 2\left\{\sigma\left(\Omega,\bar{\Omega}\right)\sqrt{\mathscr{E}(X(t))}-\frac{\sin(\lambda_0)}{\lambda_0}\left[\frac{K_1+\varepsilon}{N}\sum_{i=1}^{N}|\theta_i|^2+\frac{K_2+\varepsilon}{N}\sum_{i=1}^{N}|\xi_i|^2\right]\right\}
$$

$$
\begin{aligned}
&-\frac{2\varepsilon-(K_1+K_2)}{2N^2}\frac{\sin(\lambda_0)}{\lambda_0}\left[\left(\sum_{i=1}^{N}\theta_i\right)^2+\left(\sum_{i=1}^{N}\xi_i\right)^2\right]\\
&\leq 2\sigma\left(\Omega,\bar{\Omega}\right)\sqrt{\mathscr{E}(X(t))}-2\frac{K_1+\varepsilon}{N}\frac{\sin(\lambda_0)}{\lambda_0}\sum_{i=1}^{N}|\theta_i|^2\\
&-2\frac{K_2+\varepsilon}{N}\frac{\sin(\lambda_0)}{\lambda_0}\sum_{i=1}^{N}|\xi_i|^2-\frac{2\varepsilon-(K_1+K_2)}{2N}\frac{\sin(\lambda_0)}{\lambda_0}\left(\sum_{i=1}^{N}\theta_i^2+\sum_{i=1}^{N}\xi_i^2\right)\\
&\leq 2\sigma\left(\Omega,\bar{\Omega}\right)\sqrt{\mathscr{E}(X(t))}-(4\varepsilon+(K_1-K_2))\frac{\sin(\lambda_0)}{N\lambda_0}\sum_{i=1}^{N}|\theta_i|^2\\
&-(4\varepsilon-(K_1-K_2))\frac{\sin(\lambda_0)}{N\lambda_0}\sum_{i=1}^{N}|\xi_i|^2.
\end{aligned}
$$

Setting $\Delta_{K_{12}}=K_1-K_2$ yields the differential inequality

$$
\frac{d\mathscr{E}(X(t))}{dt}\leq 2\sigma\left(\Omega,\bar{\Omega}\right)\sqrt{\mathscr{E}(X(t))}-(4\varepsilon-\Delta_{K_{12}})\frac{\sin(\lambda_0)}{\lambda_0}\mathscr{E}(X(t)). \tag{3.61}
$$

In the next step, we will prove that $T=\infty$.

For simplicity, we can rewrite the differential inequality (3.61) setting

$$
y(t):=\sqrt{\mathscr{E}(X(t))},\quad t\geq 0. \tag{3.62}
$$

For the inequality (3.61) we can see that $y(t)$ satisfies

$$
\frac{dy(t)}{dt}\leq\sigma(\Omega,\bar{\Omega})-\left(2\varepsilon-\frac{\Delta_{K_{12}}}{2}\right)\frac{\sin(\lambda_0)}{\lambda_0}y(t),\quad t\in[0,T^*].
$$

Moreover, analyzing the ODE:

$$
\begin{cases}
\dfrac{dz(t)}{dt}=\sigma(\Omega,\bar{\Omega})-\left(2\varepsilon-\dfrac{\Delta_{K_{12}}}{2}\right)\dfrac{\sin(\lambda_0)}{\lambda_0}z(t)\\
z(0)=\sqrt{\mathscr{E}(X^0)}
\end{cases},
$$

we have that it has a unique stable equilibrium point in

$$
z_*:=\frac{2\sigma(\Omega,\bar{\Omega})}{4\varepsilon-\Delta_{K_{12}}}\left(\frac{\lambda_0}{\sin(\lambda_0)}\right),
$$

moreover since

$$\varepsilon > \frac{\sqrt{2N}\sigma(\Omega)}{2\sin(\lambda_0)} + \frac{\Delta_{K_{12}}}{4} \longleftrightarrow z_* < \frac{\lambda_0}{\sqrt{2N}},$$

and the ODE solution is:

$$z(t) = \frac{2\sigma(\Omega,\bar{\Omega})}{4\varepsilon - \Delta_{K_{12}}} \frac{\lambda_0}{\sin(\lambda_0)} \left(1 - e^{-\frac{(4\varepsilon+\Delta_{K_{12}})\sin(\lambda_0)}{2\lambda_0}t}\right) + \sqrt{\mathscr{E}(X^0)} e^{-\frac{(4\varepsilon+\Delta_{K_{12}})\sin(\lambda_0)}{2\lambda_0}t}.$$

From the last equation, we can see that the trajectory of $z(t)$ increases to z_* if $z(0) < z_*$ and decreases to z_* in the contrary case. Therefore, z_* is an asymptotically stable point, and $z(t) \leq \max\{z_*, z(0)\}$. Then for comparison principle we have that

$$\sqrt{\mathscr{E}(t)} = y(t) \leq z(t) \leq \max\{z(0), z_*\} \leq \frac{\lambda_0}{\sqrt{2}}, \quad t \in [0, T_*].$$

in particular

$$y(T_*) < \frac{\lambda_0}{\sqrt{2}}, \quad \text{for} \quad t \in [0, T^* + \delta_1],$$

and subsequently for the continuity of y, there exist a $\delta_1 > 0$ such that

$$y(t) < \frac{\lambda_0}{\sqrt{2}},$$

and by (3.62) and the relation give it in (3.55) , we have that

$$\left|X_i^0 - X_j^0\right| \leqslant \sqrt{2\mathscr{E}(X^0)} < \lambda_0, \quad i, j = 1, \ldots, N \quad \text{and} \quad t \in [0, T_* + \delta_1).$$

Therefore, $T_* + \delta_1 \in \mathscr{T}$ which contradicts $T_* = \sup \mathscr{T}$. Therefore, $T_* = \infty$. □

Then since we assume that the initial center of mass of the system is zero (3.19), the last theorem guarantees the uniform boundedness of X:

$$|X_i| = |X_i - X_c| = \left|\frac{1}{2N}\sum_{j=1}^{2N} X_i - X_j\right| \leq \frac{1}{2N}\sum_{j=1}^{2N} \left|X_i - X_j\right| < \lambda_0.$$

Since the system can be formulated as a gradient system (3.21) and we give sufficient conditions such that the fluctuations around the phase in time are uniformly bounded, we can use the Theorem 3.5.4 given by [61] for systems of the general form (3.2) to prove that this boundedness leads to a steady state via Łojasiewicz's inequality.

Theorem 3.5.4. *Let $X(t)$ be the global solution to* (3.2) *with* (3.6). *If X(t) satisfies a priori uniformly boundedness condition:*

$$\max_{1\leq i\leq N}\sup_{t>0}|X_i(t)|<\infty,$$

then the frequency of the oscillators $\dot{X}$ converges to zero as $t\to+\infty$.

Proof. See Theorem 3.1, [61]. □

With the previous theorem, we obtain the necessary conditions for use the Theorem 3.5.4 and prove the complete frequency synchronization of the system. Furthermore, this completes the proof of the following theorem

Theorem 3.5.5. *Let $\lambda_0\in(0,\pi)$, and $X(t)=\{\Theta(t),\Xi(t)\}$ be the smooth solution to the system* (3.5) *and* (3.6) *with coupling strength and initial data satisfying:*

$$\varepsilon>\frac{1}{2}\left[\frac{\sqrt{2}\sigma(\Omega,\bar{\Omega})}{\sin(\lambda_0)}+\frac{\Delta_{K_{12}}}{2}\right]\quad\text{and}\quad\mathscr{E}(X^0)\leq\frac{\lambda_0^2}{2N}.\tag{3.63}$$

Then we have $D(X(t))<\lambda_0$,

$$\lim_{t\to\infty}\left|\dot{\theta}_i(t)\right|=0\quad\text{and}\quad\lim_{t\to\infty}\left|\dot{\xi}_i(t)\right|=0,\quad i=1,\ldots,N.$$

3.6 Numerical simulations

In this section, we provide several numerical examples of the results of sections 3.4 and 3.5.

Starting with the SIC model (3.1), for the simulations, we selected the fourth-order Runge-Kutta method with a time step of $h=10^{-3}$, choosing the initial phases θ_i^0 and ξ_i^0 randomly from the intervals $[-2(0.95)\pi/3,0.95\pi/3]$ and $[0,0.90\pi]$ (see Figure 3.5a) so that

$$D(\Theta^0)=2.9801,\quad D(\Xi^0)=2.8244\quad\text{and}\quad D_{X^0}=3.8936,$$

with dual angles

$$D_1^\infty=0.1615,\quad D_2^\infty=0.3175$$

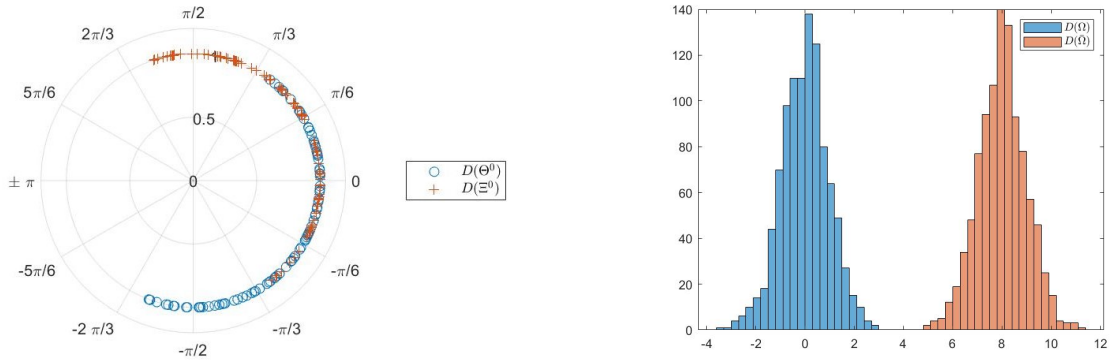

(a) Sample initial configuration

(b) Natural frequencies' histogram

Fig. 3.5 Initial configurations of X for the SIC model (3.3). Subfigure (a) Shows the initial configuration of X^0 with Θ^0 in blue and Ξ^0 in orange. Subfigure (b) shows the natural frequencies' histogram of Ω in blue and $\bar{\Omega}$ in orange.

the natural frequencies were chosen at random from a Lorentzian distribution centered in 0 with cut in $[-4,4]$ for Ω, and centered in 8 with cut in $[4,12]$ for $\bar{\Omega}$ (see Figure 3.5b). Then, considering the lemmas 3.4.4 and 3.4.1, the lower coupling bounds are:

$$\varepsilon = 0.8034, \quad K_1^c = 50.7421 \quad \text{and} \quad K_2^c = 27.2267$$

Our choices for $K_1 = 77$, $K_2 = 50$ and $\varepsilon = 1$ satisfy the assumptions. It is easy to see from Figure 3.6 that the phase diameters shrink to some positive number less than D_1^∞ and D_2^∞.

In fact, the limit of $D(\Theta(t))$ is around 0.0795 while for $D(\Xi(t))$ is around the value 0.1374. On the other hand, $D(X(t))$ shrinks until a certain time t_1 and then increases without any upper bound.

Moreover, if we consider the case where the natural frequencies' distance of the whole system is less than the sum of the distances of the natural frequencies of each layer, i.e., $D(\Omega,\bar{\Omega}) \leq D(\Omega) + D(\bar{\Omega})$ over the same coupling strength and initial conditions, the behavior of $D(X)$ is not guaranteed only with these conditions, the distance can start to grow after a certain time as in the previous case, or it can decrease to a specific value depending on $D(\Omega,\bar{\Omega})$ as in the case of Figure 3.7.

In order to test the results in Section 3.5 and point out the differences between the dynamics of the SIC model and the AIC model under similar conditions, we use the same

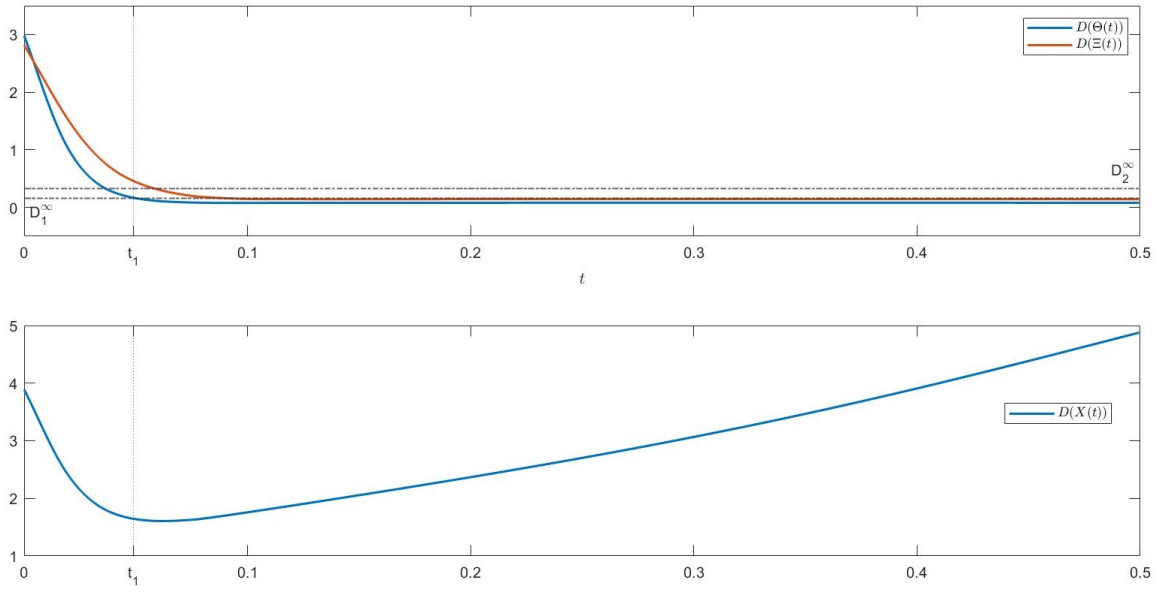

Fig. 3.6 Trajectories of $D(\Theta(t))$ and $D(\Xi(t))$. With their respective dual angles from the initial state D_1^{∞} and D_2^{∞} and the estimate times t in which the length of the diameters pass the dual angles.

setting on the fourth-order Runge-Kutta, and for the initial conditions of our first example, we choose a Cauchy distribution for the natural frequencies given by

$$g(\Omega) = \frac{1}{\pi}\frac{\lambda}{\lambda^2 + (\omega - \delta)^2}, \tag{3.64}$$

whit $\lambda = 1/2$ and $\delta = 0$ for the natural frequencies of Ω and $\delta = 8$ for the natural frequencies of $\bar{\Omega}$, in the same way, the initial phases Θ^0 are randomly picked from a uniform distribution in the interval $[-0.95\frac{2\pi}{3}, 0.95\frac{\pi}{3}]$ and Ξ^0 from $[0, 090\pi]$ (see Figure (3.8)), which means that we have adjusted this simulation to the same conditions imposed in the first example of the AIC model. For this case, we have that the diameters of the initial conditions are:

$$D(\Theta^0) = 2.9816, \quad D(\Xi^0) = 2.8068 \quad D(X) = 4.8019 \tag{3.65}$$

$$D(\Omega) = 7.6108 \quad \text{and} \quad D(\bar{\Omega}) = 7.8287 \tag{3.66}$$

Then, reviewing the Lemma 3.5.1 and the lower bounds necessary for the 2-cluster locked state, we take the following coupling strengths

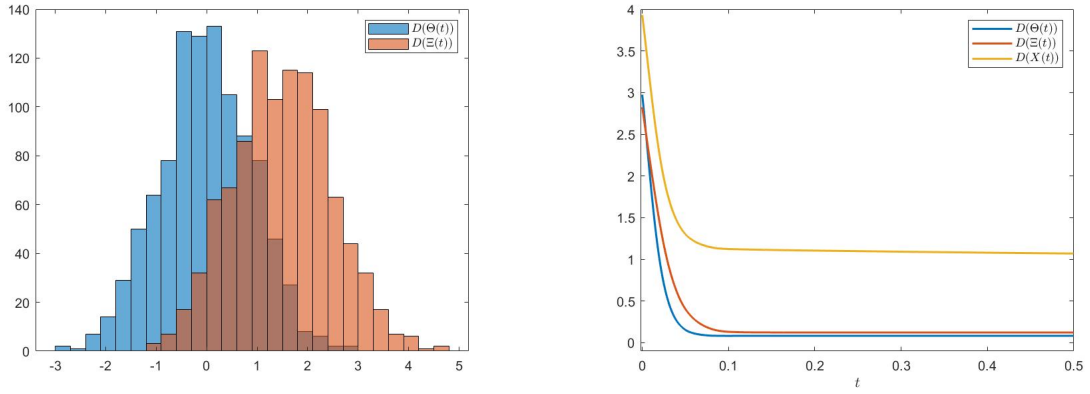

(a) Natural frequencies' histogram (b) Diameter's dynamics

Fig. 3.7 The behaviors of $D(\Theta)$, $D(\Xi)$ and $D(X)$ for non-identical oscillators with natural frequencies Ω and $\bar{\Omega}$ centered in 0 and 1.5 respectively.

$$K_1 = 44 > K_1^c = 42.7294, \quad K_2 = 22 > K_2^c = 21.0730 \quad \text{and} \quad \varepsilon = 1$$

Notice that the lower bounds required for the locked state can be visualized in Figure 3.9 are less than in the SIC case.

To compare the difference between Lemma 3.5.1 and Lemma 3.5.2, we take an identical natural frequency value $\omega_i = 2$ for the Θ layer, and we keep the natural frequencies of Ξ randomly chosen from a Cauchy distribution (3.64) with $\lambda = 1/2$ and $\delta = 8$ see Figs. 3.10a. For the coupling strengths, we choose the lower bound presented in equation(3.51) for the Θ layer and equation (3.51) for the Ξ layer. Notice that selecting equation (3.51) gives us a smaller coupling than the one given by (3.51); indeed, we have that

$$K_1^c = 2.57, \quad K_2^c = 12.06, \quad \bar{K}_1^c = 3.93 \quad \text{and} \quad \bar{K}_2^c = 12.16$$

We observe that the diameter of the Θ layer exponentially goes to zero, following the same argument presented in Lemma 3.5.2, while the $D(\Xi)$ decrease to a value bigger than zero.

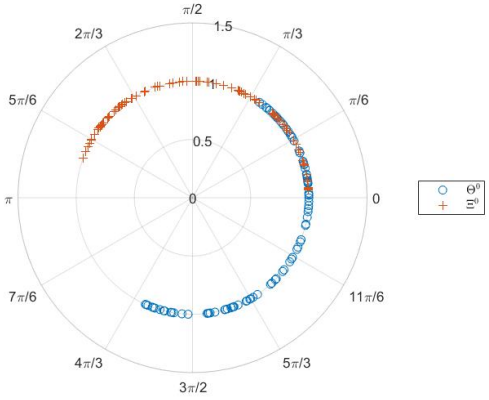

(a) X^0.

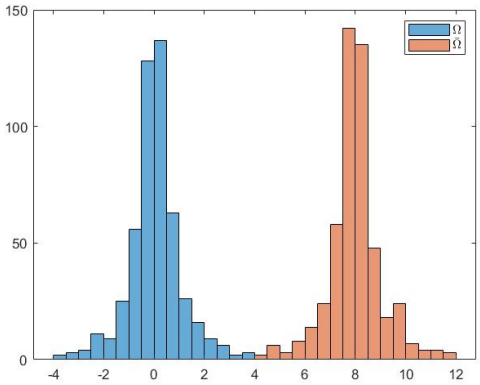

(b) Natural frequencies' histogram

Fig. 3.8 Initial setting for $N = 500$ oscillators in each layer. (a) Shows the initial configuration of X^0 with Θ^0 in blue and Ξ^0 in orange. (b) shows the natural frequencies' histogram of Ω in blue and $\bar{\Omega}$ in orange.

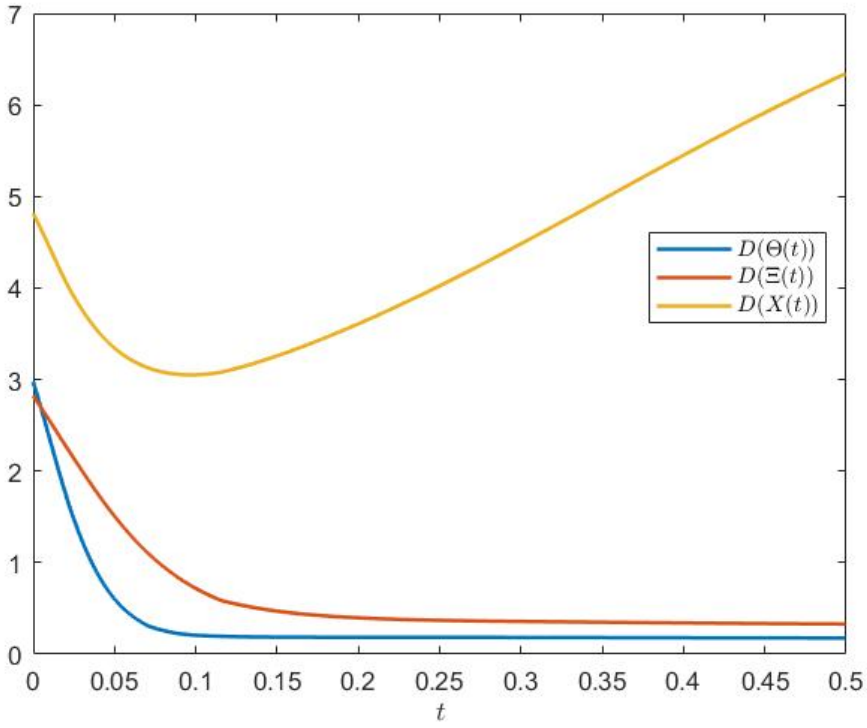

Fig. 3.9 The behaviors of $D(\Theta)$, $D(\Xi)$ and $D(X)$ for the initial configuration shown in equation (3.66) and coupling strengths $K_1 = 44$, $K_2 = 22$, and $\varepsilon = 1$ for the AIC model eq. (3.5).

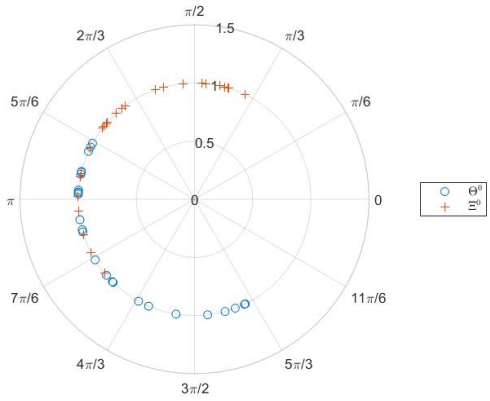

(a) The initial state of X^0.

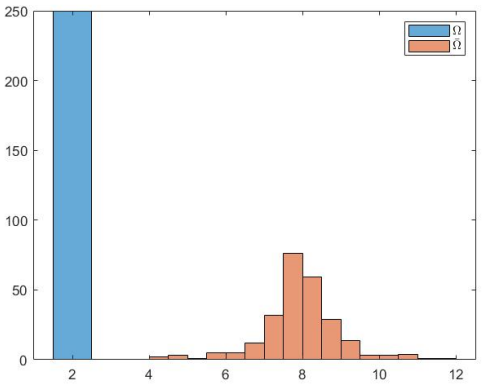

(b) Histogram of Ω and $\bar{\Omega}$.

Fig. 3.10 Initial configuration for Θ layer with identical natural frequencies $\omega_i = 2$.

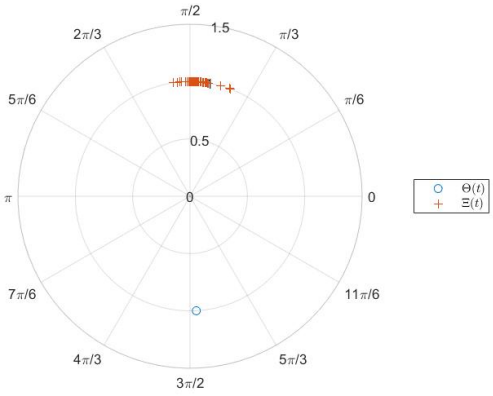

(a) State of $X(t)$ at time $t = 3$.

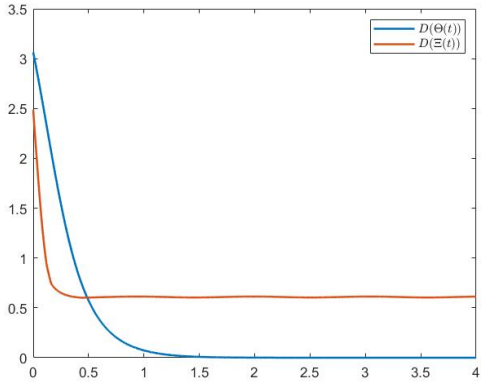

(b) Trajectories of $D(\Theta)$ and $D(\Xi)$.

Fig. 3.11 Comparison between $\Theta(t)$ and $\Xi(t)$. (a) shows at time $t = 3$ the polar coordinates of the oscillators, i.e., $e^{i\theta_j}$ in blue and $e^{i\xi_j}$ in orange. (b) shows the difference between the trajectories $D(\Theta)$ and $D(\Xi)$ when $t \to \infty$.

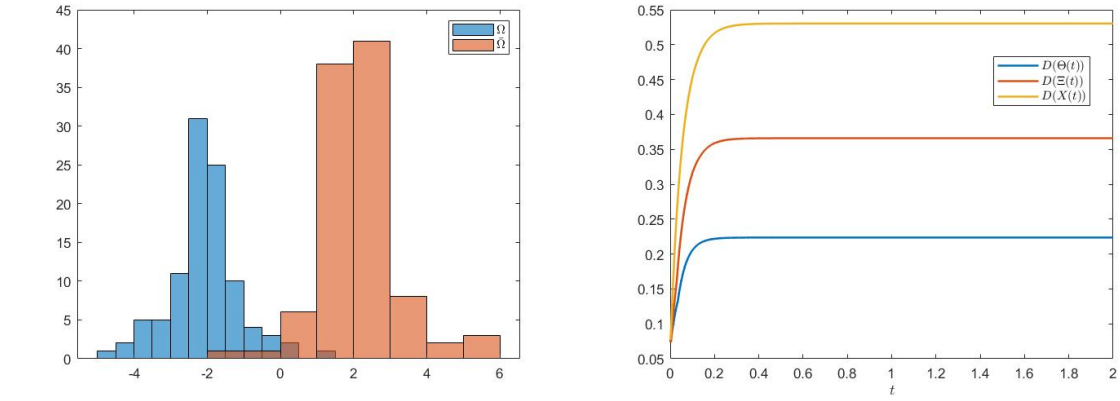

(a) Natural Frequency histogram for Ω and $\bar{\Omega}$

(b) Trajectory of $D(\Theta)$, $D(\Xi)$ and $D(X)$.

Fig. 3.12 Initial configuration and trajectories of layers diameters and the system diameter over the conditions given by (3.53) in Lemma 3.5.3.

The last example corresponds to the necessary conditions for reaching complete synchronization on an AIC topology. As we can observe from the Theorem 3.5.5, we have that, for $N = 100$ and $\lambda_0 = 2.83$, we need an initial energy $\mathscr{E}(X^0) \leq 0.078$

As we can see for

$$K_1 = 17, \quad K_2 = 13 \quad \text{and} \quad \varepsilon = 8.43,$$

following the condition given by (3.53) over ε, i.e. $\varepsilon > 7.5$ and the natural frequencies randomly picked from the Cauchy distribution (3.64) preserving the scale parameter used in the other examples, $\delta = -2$ for Ω and $\delta = 2$ for $\bar{\Omega}$ such that the average $\Omega_c = 0$, in the same way $X_c(0) = 0$. From the Figure 3.12b we can observe that $D(X(t)) < \lambda_0$ and for $t > 0.6$

$$\frac{dD(\Theta)}{dt} = \frac{dD(\Xi)}{dt} = \frac{dD(X)}{dt} = 0,$$

which means that $\dot{\theta} = \dot{\xi} = 0$.

The Figure 3.13 is a comparison between the trajectory of $\dot{\mathscr{E}}(t)$ in blue and the upper bound estimate exhibit in the equation (3.54) in orange.

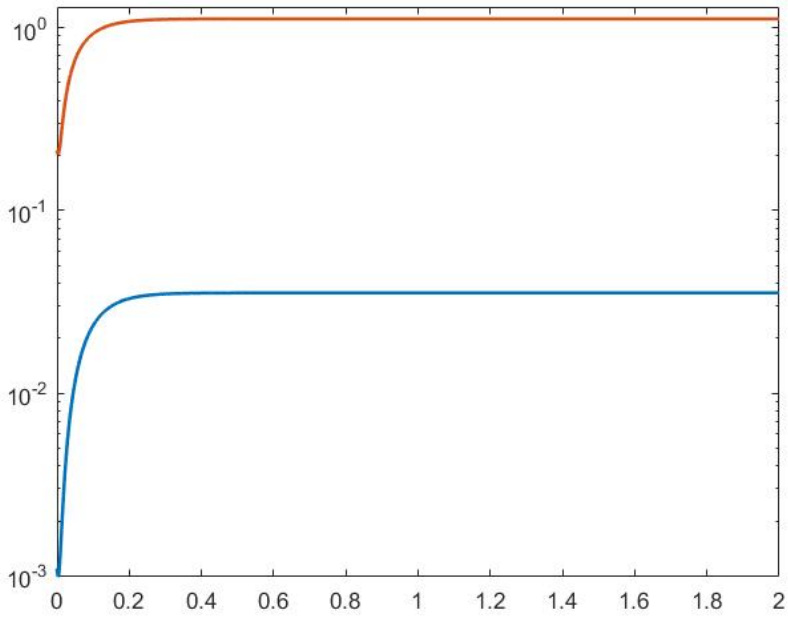

Fig. 3.13 Comparison between $\dot{\mathscr{E}}(t)$ in blue and the upper bound estimate given by the equation (3.54) in orange.

3.7 Summary of the chapter

In summary, we have analyzed two different multilayer networks, the so-called AIC and the SIC models. While multilayer networks have recently attracted a lot of attention in the fields of neuroscience and social networks, little is still known about the interplay between the structure of the layers and the synchronization patterns that can arise. We have aimed to fill this gap within a rigorous framework of theoretical analysis supported by numerical simulations. We have thus highlighted, in both examples, the dynamics of the center of mass and we also outlined a gradient flow formulation. Moreover, we studied the synchronization problem for the model of identical oscillators, and presented the corresponding stationary solution. We also considered the model with nonidentical oscillators, where we analyzed the phase diameter of each layer and the system. The AIC and SIC model are noteworthy because their study allowed us to understand how the fine tuning the different interaction strengths may produce different asymptotic states.

Chapter 4

Exact response theory for the Kuramoto model

> Thanks to chaos theory and its early pioneers, like Belgian chemist Ilya Prigogine, we now know that the conditions which give birth to structure are far from equilibrium. Though in some places and possibly even on average, things may drift toward dissolution, nothingness, and entropy, in other places there is a natural imbalance. Out of this imbalance, energised, highly chaotic activity spontaneously produces structure and complexity (Briggs,1992)

The response of a system with many degrees of freedom to an external stimulus is a central topic in nonequilibrium statistical mechanics. Its investigation has greatly progressed with the works of Callen, Green, Kubo, and Onsager, in particular, who contributed to the development of linear response theory [77, 86]. In the '90s, the derivation of the Fluctuation Relations [40, 42, 48], one of the few exact results about the behavior of non equilibrium dissipative dynamical systems, provided the framework for a more general response theory, applicable to both Hamiltonian as well as dissipative deterministic particle systems [20, 24, 26, 27, 30, 45, 86, 112]. The study of response in stochastic processes, with a special focus on diffusion and Markov jump processes, has also been inspired by fluctuation relations, and has been studied *e.g.* in [4, 8, 14, 25, 32]. Moreover, the role of causality, expressed by the Kramers-Kronig relations, in nonlinear extensions of the linear response theory has been discussed in [84].

The introduction of the Dissipation Function, first made explicit in [43], and developed as the observable of interest in Fluctuation Relations in [44, 115], paved the way to the construction of an exact response theory. Namely, a theory expected to hold in presence of arbitrarily large perturbations and modifications of states, which allows the study of the relaxation of particle systems to equilibrium or non-equilibrium steady states. The Dissipation Function is the main ingredient of the exact response theory, that we shall develop in the sequel for it possible to fully charaterize the nonequilibrium dynamics. In the sense, the Dissipation Function stands as the direct counterpart of the classical thermodynamic potentials, which describe equilibrium states.

In this chapter, we present and apply the Dissipation Function formalism to Kuramoto dynamics which undergo synchronization transitions. This is, in our opinion, an important step forward in nonequilibrium statistical mechanics. In fact, linear response theory does not apply, in general, to systems undergoing phase transitions, since even a small perturbation may in that case result in a large modification of the state. Thus, on the one hand, it is interesting to probe the exact response theory on a dissipative system with many degrees of freedom undergoing nonequilibrium phase transitions, which is in fact a challenging open problem. On the other hand, while a vast mathematical literature exists on the Kuramoto model, it is stimulating to analyze it from a new statistical mechanical perspective, in which some known results are reinterpreted, cf. e.g. Refs. [11, 34].

4.1 Mathematical framework of Response theory

Let us summarise the mathematical framework of the exact response theory originally derived in Ref.[45], and further developed in *e.g.* Refs.[20, 45, 46, 66, 115]. The starting point is a flow $S^t : \mathscr{M} \to \mathscr{M}$, with phase space $\mathscr{M} \subset \mathbb{R}^N$, $N \geq 1$, that is usually determined by an ODE system

$$\dot{\theta} = V(\theta), \quad \theta \in \mathscr{M} \tag{4.1}$$

with V a vector field on $\mathscr{M}$. Let $S^t\theta$ denote the solution at time $t \in \mathbb{R}$, with initial condition θ, of such ODEs. The second ingredient is a probability measure $d\mu_0(\theta) = f_0(\theta)d\theta$ on $\mathscr{M}$, with positive and continuously differentiable density f_0. A time evolution is induced on the simplex of probabilities on $\mathscr{M}$, defining the probability at a time $t \in \mathbb{R}$ as:

$$\mu_t(E) = \mu_0(S^{-t}E)$$

for each measurable set $E \subset \mathscr{M}$. This amounts to consider probability in a phase space like the mass of a fluid in real space. The corresponding continuity equation for the probability densities is the (generalised) Liouville equation:

$$\frac{\partial f}{\partial t} + \mathrm{div}_\theta(fV) = 0\,. \tag{4.2}$$

Denoting by f_t the solution of Eq.(4.2) with initial datum f_0, we can write $d\mu_t = f_t d\theta$. Letting $\Lambda = \mathrm{div}_\theta V$ be the phase space volumes variation rate, and introducing the *Dissipation Function* $\Omega^{f,V}$ [66, 115]:

$$\Omega^{f,V}(\theta) := -\Lambda(\theta) - V(\theta)\cdot\nabla \log f(\theta)\,,\ \ \nabla = (\partial_{\theta_1},\dots,\partial_{\theta_N}) \tag{4.3}$$

the Euler version of the Liouville equation (4.2) may be written as:

$$\frac{\partial f}{\partial t} = f\,\Omega^{f,V}\,. \tag{4.4}$$

which can also be cast in the Lagrangian form:

$$\frac{df}{dt} = -f\Lambda\,, \tag{4.5}$$

with $\frac{d}{dt} = \frac{\partial}{\partial t} + V\cdot\nabla_\theta$ the total derivative along the flow (4.1).

Direct integration of Eq.(4.5) yields

$$f_{s+t}(S^t\theta) = \exp\{-\Lambda_{0,t}(\theta)\} f_s(\theta)\,,\quad \forall t, s \geq 0 \tag{4.6}$$

where we used the notation

$$\mathscr{O}_{s,t}(\theta) := \int_s^t \mathscr{O}(S^\tau\theta)d\tau \tag{4.7}$$

for the phase functions, or *observables*, $\mathscr{O} : \mathscr{M} \to \mathbb{R}$, so that, in particular, $\Lambda_{0,t}(\theta) = \int_0^t \Lambda(S^\tau\theta)d\tau$.

In the following Proposition, this notation is used with the observable $\mathscr{O} = \Omega^{f,V}$, so that the time integral in (4.7) will correspondingly be denoted by $\Omega^{f,V}_{s,t}$.

Proposition 4.1.1. *For all t, $s \in \mathbb{R}$, the following identity holds:*

$$f_{s+t}(\theta) = \exp\left\{\Omega^{f_s,V}_{-t,0}(\theta)\right\} f_s(\theta)\,. \tag{4.8}$$

Proof. We start by claiming that

$$\Omega_{0,s}^{f_t,V}(\theta) = \log \frac{f_t(\theta)}{f_t(S^s\theta)} - \Lambda_{0,s}(\theta)\,. \tag{4.9}$$

Indeed, one has:

$$V(S^u\theta)\cdot\nabla \log f_t(S^u\theta) = \frac{d}{du}\log f_t(S^u\theta) \tag{4.10}$$

because t is fixed and f_t does not depend explicitly on u, hence Eqs.(4.3) and (4.10) imply:

$$\begin{aligned}\Omega_{0,s}^{f_t,V}(\theta) &= -\int_0^s \big[\Lambda(S^u\theta) + V\cdot\nabla\log f_t(S^u\theta)\big]du \\ &= -\Lambda_{0,s}(\theta) - \int_0^s \frac{d}{du}\log f_t(S^u\theta)d\theta = -\Lambda_{0,s}(\theta) - \log\frac{f_t(S^s\theta)}{f_t(\theta)}\end{aligned}$$

which leads to Eq.(4.9). Next, Eqs.(4.6) and Eq.(4.9) yield

$$\exp\Big\{\Omega_{s,s+t}^{f_s,V}(\theta)\Big\} f_s(S^{s+t}\theta) = \exp\Big\{-\Lambda_{s,s+t}(\theta)\Big\} f_s(S^s\theta) = f_{s+t}(S^{s+t}\theta) \tag{4.11}$$

which produces (4.8). □

As a consequence of Proposition 4.1.1, a probability density f is *invariant* under the dynamics if and only if $\Omega^{f,V}$ identically vanishes:

$$\Omega^{f,V}(\theta) = 0\,, \quad \forall\ \theta\in\mathscr{M}\,. \tag{4.12}$$

In the sequel, we shall use the notation

$$\langle\mathscr{O}\rangle_t := \int_{\mathscr{M}} \mathscr{O}(\theta) f_t(\theta) d\theta \tag{4.13}$$

to denote the average of an observable with respect to the probability measure $\mu_t = f_t\,d\theta$. The exact response theory based on the Dissipation Function states that the average $\langle\mathscr{O}\rangle_t$ can be expressed in terms of the known initial density f_0, as in linear response theory. The difference between the two theories lies in the correlation functions that must be integrated in time.

Lemma 4.1.2. (Exact response): *Given $\{S^t\}_{t\in\mathbb{R}}$ and an integrable observable $\mathscr{O}:\mathscr{M}\to\mathbb{R}$, the following identity holds:*

$$\langle\mathscr{O}\rangle_t = \langle\mathscr{O}\rangle_0 + \int_0^t \langle(\mathscr{O}\circ S^\tau)\ \Omega^{f_0,V}\rangle_0\ d\tau\,. \tag{4.14}$$

Proof. First of all, f_0 is smooth as a function of θ by assumption, and evolves according to the Liouville equation. Therefore, f_t is also smooth with respect to θ and t for every finite time t. In turn, $\Omega^{f_t,V}(\theta)$ is differentiable with respect to θ and t, if f_0 (that depends only on θ) is differentiable with respect to θ. These conditions are immediately verified for differentiable f_0, and smooth dynamics on a compact manifold. Therefore, two identities can be derived for integrable $\mathscr{O}$:

$$\begin{aligned}\mathscr{O}_{0,s}(\theta) &= \int_0^s \mathscr{O}(S^u\theta)du = \int_\tau^{s+\tau} \mathscr{O}(S^{u-\tau}\theta)du = \int_\tau^{s+\tau} \mathscr{O}(S^{-\tau}S^u\theta)du \\ &= \mathscr{O}_{\tau,s+\tau}(S^{-\tau}\theta)\end{aligned}$$

which is valid for every $\tau \in \mathbb{R}$, and

$$\begin{aligned}\langle\mathscr{O}\rangle_{t+s} &= \int \mathscr{O}(\theta) f_{t+s}(\theta)d\theta \\ &= \int \mathscr{O}(S^s(S^{-s}\theta)) f_{t+s}(S^s(S^{-s}\theta)) \left|\frac{\partial\theta}{\partial(S^{-s}\theta)}\right| d(S^{-s}\theta) \\ &= \int \mathscr{O}(S^s(S^{-s}\theta)) f_{t+s}(S^s(S^{-s}\theta)) \exp\left\{\Lambda_{-s,0}(\theta)\right\} d(S^{-s}\theta) \\ &= \int \mathscr{O}(S^s(S^{-s}\theta)) f_{t+s}(S^s(S^{-s}\theta)) \exp\left\{\Lambda_{0,s}(S^{-s}\theta)\right\} d(S^{-s}\theta) \\ &= \int \mathscr{O}(S^s\theta) f_{t+s}(S^s\theta) \exp\left\{\Lambda_{0,s}(\theta)\right\} d\theta \qquad (4.15) \\ &= \int \mathscr{O}(S^s\theta) f_t(\theta)d\theta \\ &= \langle\mathscr{O}\circ S^s\rangle_t \qquad (4.16)\end{aligned}$$

to obtain [66]:

$$\frac{d}{ds}\langle\mathscr{O}\rangle_s = \langle\mathscr{O}\ (\Omega^{f_r,V}\circ S^{r-s})\rangle_s \qquad (4.17)$$

which holds $\forall r \geq 0$. Note that in the equation (4.16) we used the relation

$$\left|\frac{\partial\theta}{\partial(S^{-s}\theta)}\right| = \exp\left\{\Lambda_{-s,0}(\theta)\right\} \qquad (4.18)$$

which is discussed in A.2, see Eq. (A.18). Choosing $r = 0$ in (4.17), one finds

$$\frac{d}{ds}\langle\mathscr{O}\rangle_s = \langle\mathscr{O}\ (\Omega^{f_0,V}\circ S^{-s})\rangle_s = \langle(\mathscr{O}\circ S^s)\ \Omega^{f_0,V}\rangle_0 \qquad (4.19)$$

where we used (4.16). Then, integrating over time from 0 to t, Eq.(4.19) yields (4.14). □

The apparently peculiar definition of the Dissipation Function is motivated by the fact that it can be associated with the energy dissipation of particle systems, if f_0 is properly chosen. In particular, this is the case for models of nonequilibrium molecular dynamics, such as the Gaussian and the Nosé - Hoover thermostatted systems, if f_0 is the invariant probability density for the corresponding equilibrium dynamics, *i.e.* the dynamics subjected to the same constraints of the nonequilibrium ones, in which the dissipative forces are switched off. In other words, $\Omega^{f_0,V}$ equals the energy dissipation if $\Omega^{f_0,V_0} \equiv 0$ and V_0 is the (non dissipative) vector field implementing the same constraints that V does [115]. Typical constraints are the constant internal energy, the constant kinetic energy, the constant temperature, the constant pressure etc.. The state characterised by f_0 may be prepared like that at start. Alternatively, one usually thinks that it is generated by the equilibrium dynamics:

$$\dot{\theta} = V_0(\theta) \tag{4.20}$$

started long before the time $t = 0$, so that at time 0 it is realised. While this is not mathematically required, it is physically convenient, and it helps our intuition to assume that μ_0 is invariant under the dynamics (4.20), which we call *unperturbed* or *reference* dynamics. At time $t = 0$, the dynamics (4.20) is perturbed and the perturbation remains in place for all $t > 0$. In general, the density f_0 is not invariant under the perturbed vector field V, cf. Eq.(4.1). Therefore, it will evolve as prescribed by Eq.(4.4) into a different density, f_t, at time $t > 0$. Nevertheless, Eq.(4.14) expresses the average $\langle \mathscr{O} \rangle_t$ in terms of a correlation function computed with respect to f_0, the non-invariant density, which is only invariant under the unperturbed dynamics. The full range of applicability of this theory is still to be identified. However, it obviously applies to smooth dynamics on smooth compact manifolds, such as the Kuramoto dynamics (2.8), which has $\mathscr{M} = \mathscr{T}^N$. One advantage of using the Dissipation Function, compared to other possible exact approaches to response, apart from molecular dynamics efficiency, is that $\Omega^{f_0,V}$ corresponds to a physically measurable quantity, *e.g.* proportional to a current, that is adapted to the initial state of the system of interest. Moreover, it provides necessary and sufficient conditions for relaxation of ensembles, as well as sufficient conditions for the single system relaxation, known as T-mixing [66, 115]. The analysis of the response theory for a specific example of the Kuramoto model is discussed in the next subsection.

4.2 Dissipation theory applied to the classic Kuramoto Model

4.2.1 Recap of the Kuramoto Model and his properties

For $\theta \in \mathscr{M}$, we can rewrite Eq.(2.10) as:

$$\dot{\theta} = W + V(\theta) = V_K(\theta), \tag{4.21}$$

where $W = (\omega_1, \ldots, \omega_N)$ is interpreted as an *equilibrium* vector field made of N natural frequencies that are drawn from some given distribution $g(\omega)$, while V represents a *nonequilibrium* vector perturbation with components:

$$V_i(\theta) = \frac{K}{N} \sum_{j=1}^{N} \sin(\theta_j - \theta_i) = KR \sin(\Phi - \theta_i), \qquad i = 1, \ldots, N. \tag{4.22}$$

where $K > 0$ and R is the order parameter defined in equation (2.9)

Lemma 4.2.1. *The divergence of the Kuramoto vector field V_K of Eq.*(4.21)*,* i.e. *the associated phase space volumes variation rate Λ, satisfies:*

$$\Lambda := \mathrm{div}_\theta V = K\left(1 - NR^2\right). \tag{4.23}$$

Proof. By means of (4.22), for $i = 1, \ldots, N$ one has

$$\begin{aligned} \partial_{\theta_i} V_i &= \frac{K}{N} \partial_{\theta_i} \left(\sum_{i \neq j = 1}^{N} \sin(\theta_j - \theta_i) \right) \\ &= -\frac{K}{N} \left(\sum_{i \neq j = 1}^{N} \cos(\theta_j - \theta_i) \right) = -\frac{K}{N} \left(\sum_{j=1}^{N} \cos(\theta_j - \theta_i) - 1 \right) \\ &= -KR \cos(\Phi - \theta_i) + \frac{K}{N} \end{aligned}$$

where we used (2.14). Summing over i, and using (2.11) , Eq.(4.23) follows. □

Therefore, the Kuramoto dynamics do not preserve the phase space volumes, and Λ actually varies in time, since R is a function of the dynamical variables $\theta(t)$.

4.2.2 Response theory for identical oscillators

Let us focus on the case of identical oscillators, namely the Kuramoto dynamics in which all the natural frequencies ω_i in Eq.(2.8) equal the same constant $\omega \in \mathbb{R}$. In particular, let the unperturbed dynamics be defined by the vector field $V_0(\theta) = W = (\omega, \dots, \omega)$, which corresponds to $K = 0$ in Eq.(2.8), *i.e.* to decoupled oscillators, equipped with the same natural frequency. Such dynamics are conservative, since $\mathrm{div}_\theta V_0 = 0$. The corresponding steady state can then be considered an equilibrium state. At time $t = 0$ the perturbation V is switched on, and we can write:

$$\dot{\theta} = \begin{cases} W & t < 0 \\ W + V(\theta) & t > 0\,. \end{cases} \tag{4.24}$$

The perturbed dynamics corresponds to the Kuramoto dynamics (2.8), which is not conservative, cf. Eq.(4.23). As an initial probability density, invariant under the unperturbed dynamics, we may take the factorized density:

$$f_0(\theta) = (2\pi)^{-N} \tag{4.25}$$

which, indeed, yields:

$$\Omega^{f_0,V_0} = -\left(\mathrm{div} V_0 + V_0 \cdot \nabla \log f_0\right) \equiv 0\,, \quad \text{and} \quad \frac{\partial f}{\partial t} = 0\,. \tag{4.26}$$

After the perturbation, the Dissipation Function takes the form:

$$\Omega^{f_0,V} = -\left(\mathrm{div}_\theta V + V \cdot \nabla \log f_0\right) = K\left(NR^2 - 1\right) = \frac{K}{N} \sum_{i,j=1}^{N} \cos(\theta_j - \theta_i) - K \tag{4.27}$$

and the density evolves as:

$$f_t(\theta) = \frac{1}{(2\pi)^N} \exp\Big[-K\left(t - NR^2_{-t,0}(\theta)\right) \Big] \tag{4.28}$$

where $R_{-t,0}$ denotes the integral of R from time $-t$ to 0, cf. Eq.(4.7).

Remark. *The Dissipation Function Eq.*(4.27) *is of class* C^∞.

Using the formula (4.14) to compute the response for the observable $\mathscr{O} = \Omega^{f_0,V}$, we obtain:

$$\langle \Omega^{f_0,V} \rangle_t = \langle \Omega^{f_0,V} \rangle_0 + \int_0^t \langle (\Omega^{f_0,V} \circ S^\tau) \Omega^{f_0,V} \rangle_0 \, d\tau \tag{4.29}$$

that is

$$\int_{\mathscr{M}} \Omega^{f_0,V}(\theta) f_t(\theta) d\theta$$
$$= (2\pi)^{-N} \int_{\mathscr{M}} \Omega^{f_0,V}(\theta) d\theta + (2\pi)^{-N} \int_0^t \int_{\mathscr{M}} \Omega^{f_0,V}(S^\tau(\theta)) \Omega^{f_0,V}(\theta)\, d\theta d\tau\,.$$

Moreover:

$$\langle R^2 \rangle_0 = \frac{1}{N}\,, \quad \text{hence} \;\; \langle \Omega^{f_0,V} \rangle_0 = K\big(N\langle R^2\rangle_0 - 1\big) = 0 \tag{4.30}$$

as expected.

Remark. *Note that the scalar field Ω^{f_0,V_0} is identically 0, while $\Omega^{f_0,V}$ is not, see Eq.*(4.27). *However, the phase space average $\left\langle \Omega^{f_0,V} \right\rangle_0$ vanishes.*

Therefore, using Eqs.(4.14) and (4.27) we can write:

$$\begin{aligned}
\left\langle \Omega^{f_0,V} \right\rangle_t &= \int_0^t \left\langle (\Omega^{f_0,V} \circ S^\tau) \Omega^{f_0,V} \right\rangle_0 d\tau \\
&= KN \int_0^t \left\langle \Omega^{f_0,V} \left[R^2 \circ S^\tau \right] \right\rangle_0 d\tau - K \int_0^t \left\langle \Omega^{f_0,V} \right\rangle_0 d\tau \\
&= KN \int_0^t \left\langle \Omega^{f_0,V} \left[R^2 \circ S^\tau \right] \right\rangle_0 d\tau \\
&= K^2 N^2 \int_0^t \left\langle R^2 \left[R^2 \circ S^\tau \right] \right\rangle_0 d\tau - K^2 N \int_0^t \left\langle R^2 \circ S^\tau \right\rangle_0 d\tau\,.
\end{aligned}$$

For the second integral we have:

$$\begin{aligned}
\int_0^t \left\langle R^2 \circ S^\tau \right\rangle_0 d\tau &= \frac{1}{(2\pi)^N} \int_0^t \int_{\mathscr{M}} R^2(S^\tau\theta) d\theta d\tau \\
&= \frac{1}{(2\pi)^N} \int_0^t \int_{\mathscr{M}} R^2(S^\tau\theta) \left| \frac{\partial \theta}{\partial S^\tau \theta} \right| dS^\tau\theta d\tau \\
&= \frac{1}{(2\pi)^N} \int_0^t \int_{\mathscr{M}} R^2(S^\tau\theta) \exp\Big\{ \Lambda_{0,\tau}(\theta) \Big\} dS^\tau\theta\,.
\end{aligned}$$

Explicit calculations can be carried out for $N = 2$ and will be discussed in Sec. 4.2.2.1, while the study of the general case with $N > 2$ is deferred to Sec. 4.2.2.2.

4.2.2.1 The case with two oscillators

For $N = 2$ and $\omega \geq 0$, consider the system for two oscillators:

$$\begin{cases} \dot{\theta}_1 = \dfrac{\omega}{2} + \dfrac{K}{2}\sin(\theta_2 - \theta_1) \\ \dot{\theta}_2 = -\dfrac{\omega}{2} + \dfrac{K}{2}\sin(\theta_1 - \theta_2)\,. \end{cases} \tag{4.31}$$

In the case in which all natural frequencies coincide, as in Eq.(4.31) for $\omega = 0$, the oscillators are referred to as *identical*. Setting $\psi = \theta_1 - \theta_2$, we obtain the following equation:

$$\frac{d\psi}{dt} = \omega - K\sin(\psi)\,. \tag{4.32}$$

With a slight abuse of notation, in the following we denote by $S^t\theta$, $S^t\psi$ the flows corresponding to (4.31), (4.32) respectively, with initial data $\theta = (\theta_1, \theta_2)$ and $\psi = \theta_1 - \theta_2$. Then, the solution of (4.32) can be explicitly expressed as

$$\tan\left(\frac{S^t\psi}{2}\right) = g(\psi, t) \tag{4.33}$$

where:

- if $K > \omega = 0$, then
$$g(\psi,t) = e^{-Kt}\tan\left(\frac{\psi}{2}\right);$$
- if $K > \omega > 0$, then
$$g(\psi,t) = \frac{K}{\omega} + \frac{\sqrt{K^2-\omega^2}}{\omega}\cdot\frac{1 + h_1(\psi)\,e^{t\sqrt{K^2-\omega^2}}}{1 - h_1(\psi)\,e^{t\sqrt{K^2-\omega^2}}}$$
$$h_1(\psi) = \frac{\omega\tan(\frac{\psi}{2}) - K - \sqrt{K^2-\omega^2}}{\omega\tan(\frac{\psi}{2}) - K + \sqrt{K^2-\omega^2}}\,.$$
The formulas here above can be deduced by [21, Lemma D.2], Case 1;
- if $0 \leq K < \omega$, then
$$g(\psi,t) = \frac{K}{\omega} + \frac{\sqrt{\omega^2-K^2}}{\omega}\tan\left(\frac{t\sqrt{\omega^2-K^2}}{2} + h_2(\psi)\right)$$

$$h_2(\psi) = \arctan \frac{\omega \tan\left(\frac{\psi}{2}\right) - K}{\sqrt{\omega^2 - K^2}},$$

see [21, Lemma D.2], Case 3 with $R^\infty = \omega/K$.

Recalling Eq.(2.15) and using the identity $1+\cos x = 2\left(1+\tan^2\left(\frac{x}{2}\right)\right)^{-1}$, we find that $(R^2 \circ S^t)$ can be written as

$$R^2(S^t\theta) = \frac{1}{2}\left[1+\cos(S^t\psi)\right] = \frac{1}{g^2(S^t\psi)+1}, \tag{4.34}$$

For $\omega = 0$, one explicitly obtains:

$$R^2(S^t\theta) = \left(\tan^2\left(\frac{\psi}{2}\right)e^{-2Kt}+1\right)^{-1} \tag{4.35}$$

and

$$\begin{aligned} &S^t\psi \to 0 \quad \text{for } t\to+\infty, \qquad \text{if } |\psi| \neq \pi \\ &|S^t\psi| \to \pi \quad \text{for } t\to-\infty, \qquad \text{if } \psi \neq 0. \end{aligned}$$

In particular, for $\theta_1 \neq \theta_2$ and $\theta_1, \theta_2 \in [0, 2\pi)$, the $t\to-\infty$ limit yields $S^t\psi \to -\pi$ if $\theta_1 < \pi$, and $S^t\psi \to \pi$ if $\theta_1 > \pi$. Then, the set

$$E_\infty = \{(\theta_1,\theta_2) \in \mathscr{T}^2 : \theta_1 = \theta_2\}$$

is invariant and attracting for the Kuramoto dynamics, while the set

$$E_{-\infty} = \{(\theta_1,\theta_2) \in \mathscr{T}^2 : |\theta_1 - \theta_2| = \pi\}$$

is invariant and repelling. This also implies that:

$$R^2(S^t\theta) \to 0, \quad \Omega^{f_0,V} \to -K, \qquad \text{for} \quad \psi \neq 0,\ t\to-\infty$$

while

$$R^2(S^t\theta) \to 1, \quad \Omega^{f_0,V} \to K, \qquad \text{for} \quad |\psi| \neq \pi,\ t\to\infty.$$

Consequently, Eq.(4.28) shows that the probability piles up on the zero Lebesgue measure sets E_∞ and $E_{-\infty}$, respectively for $t\to\infty$ and $t\to-\infty$.

For $\tau \geq 0$, the following relations also hold:

$$\left\langle R^2 \circ S^\tau \right\rangle_0 = \frac{1}{(2\pi)^2} \int_{\mathscr{M}} \frac{1}{\tan^2(\frac{\theta_1-\theta_2}{2}) e^{-2K\tau} + 1} d\theta = \frac{1}{e^{-K\tau}+1} \tag{4.36}$$

and

$$\left\langle R^2 (R^2 \circ S^\tau) \right\rangle_0 = \frac{1}{8\pi^2} \int_{\mathscr{M}} \frac{1+\cos(\theta_1-\theta_2)}{\tan^2(\frac{\theta_1-\theta_2}{2}) e^{-2K\tau} + 1} d\theta = \frac{2e^{-K\tau}+1}{2(e^{-K\tau}+1)^2}$$

which then yields

$$\int_0^t \left\langle R^2 \circ S^\tau \right\rangle_0 d\tau = t + \frac{\ln\left(e^{-Kt}+1\right)}{K} - \frac{\ln(2)}{K}$$

and

$$\begin{aligned} &\int_0^t \left\langle R^2 (R^2 \circ S^\tau) \right\rangle_0 d\tau \\ &\quad = \frac{t}{2} + \frac{1}{2K}\left[\frac{3}{2} + \ln\left(\frac{e^{-Kt}+1}{2}\right) - \frac{2}{e^{Kt}+1} - \frac{1}{e^{-Kt}+1}\right]. \end{aligned}$$

Thus, we finally obtain the explicit expressions

$$\left\langle \Omega^{f_0,V} \right\rangle_t = K \tanh\left(\frac{Kt}{2}\right) \tag{4.37}$$

and

$$\left\langle (\Omega^{f_0,V} \circ S^t) \Omega^{f_0,V} \right\rangle_0 = \frac{K^2}{1+\cosh(Kt)}. \tag{4.38}$$

In the limit $t \to +\infty$, we thus find the asymptotic values

$$\left\langle \Omega^{f_0,V} \right\rangle_t \to K \qquad \text{and} \qquad \left\langle (\Omega^{f_0,V} \circ S^t) \Omega^{f_0,V} \right\rangle_0 \to 0 \tag{4.39}$$

In particular, the two-time autocorrelation of $\Omega^{f_0,V}$ is monotonic as also shown in the two panels of Fig.4.1. Indeed, Eq.(4.38) yields, for $t \geq 0$:

$$\frac{\mathrm{d}}{\mathrm{d}t}\left\langle (\Omega^{f_0,V} \circ S^t) \Omega^{f_0,V} \right\rangle_0 = -K^2 \frac{\sinh Kt}{(1+\cosh Kt)^2} \leq 0.$$

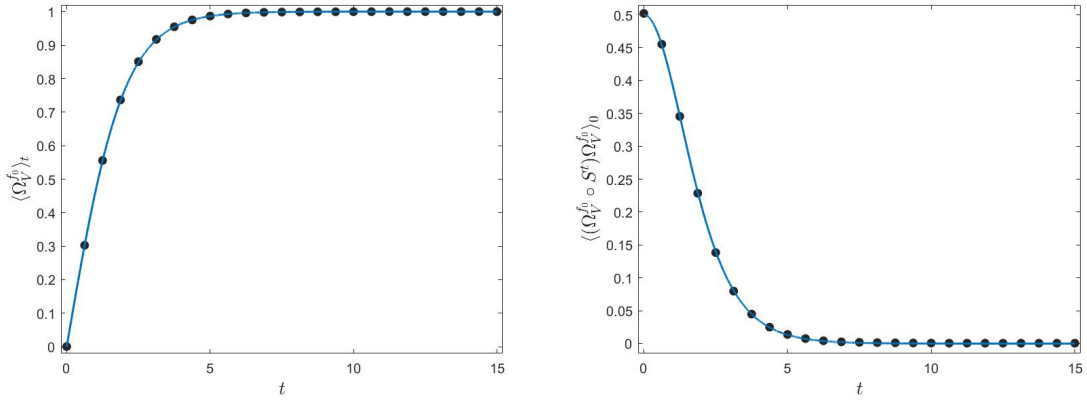

Fig. 4.1 Behavior of $\langle \Omega^{f_0,V} \rangle_t$ and $\langle (\Omega^{f_0,V} \circ S^t) \Omega^{f_0,V} \rangle_0$ as functions of time, for $N = 2$, $K = 1$ and $\omega = 0$. Disks and solid lines correspond to the numerical and analytical results, respectively. The averages were taken over a set of 5000 trajectories with initial data sampled from the uniform distribution on $[0, 2\pi)$ following the eq. (4.31) for the oscillator's dynamics and eq. (4.27) for $\Omega^{f_0,V}$.

4.2.2.2 General case

In this Subsection we assume $N \geq 2$ and $\omega = 0$, considering the following dynamics:

$$\dot{\theta}_i = \frac{K}{N} \sum_{j=1}^{N} \sin(\theta_j - \theta_i) = KR \sin(\Phi - \theta_i), \qquad i = 1, \ldots, N. \tag{4.40}$$

where R and Φ are defined in Eq.(2.9). We are going to prove that the observable $\left\langle \Omega^{f_0,V} \right\rangle_t$ is a monotonic function of time, and we can estimate the asymptotic value it attains in the large time limit.

We start by proving the following result.

Lemma 4.2.2. *For every $t > 0$, the time derivative of the expectation of the Dissipation Function obeys:*

$$\frac{d}{dt} \left(\Omega^{f_0,V}(S^t \theta) \right) \geq 0 \quad \textit{and} \quad \frac{d}{dt} \left\langle \Omega^{f_0,V} \right\rangle_t = \left\langle (\Omega^{f_0,V} \circ S^t) \Omega^{f_0,V} \right\rangle_0 \geq 0. \tag{4.41}$$

Proof. First, we note that by setting $\mathscr{O} = \Omega^{f_0,V}$ in Eq. (4.19), we find:

$$\frac{d}{dt} \langle \Omega^{f_0,V} \rangle_t = \langle (\Omega^{f_0,V} \circ S^t)\ \Omega^{f_0,V} \rangle_0 . \tag{4.42}$$

Moreover, Eq. (4.16) with $t = 0$ and $\mathscr{O} = \Omega^{f_0,V}$ yields:

$$\left\langle \Omega^{f_0,V} \right\rangle_t = \left\langle \Omega^{f_0,V} \circ S^t \right\rangle_0 . \tag{4.43}$$

Therefore, we can write:

$$\begin{aligned} \frac{d}{dt}\left\langle \Omega^{f_0,V} \circ S^t \right\rangle_0 &= \frac{d}{dt}\int_{\mathscr{M}} \Omega^{f_0,V}(S^t\theta) f_0(\theta) d\theta \\ &= \int_{\mathscr{M}} \frac{d}{dt}\left(\Omega^{f_0,V}(S^t\theta)\right) f_0(\theta) d\theta = \left\langle \frac{d}{dt}\left(\Omega^{f_0,V}(S^t\theta)\right)\right\rangle_0 \end{aligned} \tag{4.44}$$

Then, using Eq.(2.5) in Ref.[11] we find:

$$\frac{d}{dt}R^2(S^t\theta) = \frac{2K}{N}R^2(S^t\theta)\sum_{j=1}^{N}\sin^2\left(S^t\theta_j - \Phi\left(S^t\theta\right)\right) \tag{4.45}$$

where $S^t\theta_j$ denotes the $j-$th element of $S^t\theta$, and then

$$\frac{d}{dt}\left(\Omega^{f_0,V}(S^t\theta)\right) = 2K^2R^2(S^t\theta)\left[\sum_{j=1}^{N}\sin^2\left(S^t\theta_j - \Phi\left(S^t\theta\right)\right)\right] \geq 0 \tag{4.46}$$

for all $\theta \in \mathscr{M}$. By integrating over $\mathscr{M}$ we obtain (4.41). This completes the proof. □

Remark. *Unlike stationary current autocorrelations, that may fluctuate between positive and negative values, the two-time autocorrelation of $\Omega^{f_0,V}$, computed with respect to the initial probability measure, is non-negative.*

Theorem 2.3.4 shows that non stationary solutions of the system (4.40) converge, as $t \to +\infty$, either to a complete frequency synchronised state Θ^*, *i.e.* to a state denoted by $(N,0)$, that takes the form:

$$\Theta^* = (\varphi^*, \ldots, \varphi^*)$$

in which all phases are equal; or to a state denoted by $(N-1,1)$, that takes the form:

$$\Theta^\dagger = (\varphi^* + k_1\pi, \varphi^* + k_2\pi, \varphi^* + k_3\pi, \varphi^* + k_4\pi, \ldots, \varphi^* + k_N\pi)$$

where $k_i \in \{-1,+1\}$ for a single $i \in \{1,2,...,N\}$, and all $k_j = 0$ with $j \neq i$. This can be understood also in terms of the Dissipation Function. In the first place, without loss of generality, let us consider a fixed point $\bar{\theta}$ of type $(N-1,1)$ whose antipodal is in the

N-component, *i.e.*

$$\bar{\theta} = (\varphi^*, \dots, \varphi^*, (\varphi^* + \pi) \bmod 2\pi) \tag{4.47}$$

for a $\varphi^* \in [0, 2\pi)$. Then, the following holds:

Proposition 4.2.3. *The set of initial data such that the solution to* (4.40) *reaches a stationary* $(N-1,1)$*-state for* $t \to +\infty$ *has 0-measure.*

Proof. For $V(\theta)$ as in (4.21), the Jacobian matrix $A(\theta) \doteq \nabla V(\theta)$ is given by

$$A_{ij} = \begin{cases} \frac{\partial V_j}{\partial \theta_i} = \frac{1}{N}\cos(\theta_i - \theta_j), & i \neq j \\ \\ \frac{\partial V_j}{\partial \theta_j} = -\frac{1}{N}\sum_{k\neq j}^{N}\cos(\theta_j - \theta_k) & i = j\,. \end{cases}$$

For the fixed point $\bar{\theta}$ set in (4.47) we obtain a symmetric matrix $\bar{A} = A(\bar{\theta})$ whose entries are

$$\bar{A}_{ij} = \begin{cases} \frac{1}{N} & i \neq j \text{ and } i, j \neq N \\ -\frac{1}{N} & i \neq j \text{ and } i = N \text{ or } j = N \\ -\frac{N-3}{N} & i = j < N \\ \frac{N-1}{N} & i = j = N\,. \end{cases}$$

By the symmetry of $\bar{A}$, the extremal representation of the eigenvalues $\{\lambda_k\}_{k=1}^N$ of $\bar{A}$ are given by the optimisation problem:

$$\max_{1\leq k\leq N} \lambda_k = \max_{\|x\|=1} \{x'\bar{A}x\}, \qquad \min_{1\leq k\leq N} \lambda_k = \min_{\|x\|=1} \{x'\bar{A}x\}\,.$$

Setting x to be the standard-basis vectors $\mathbf{e}_i$, where $\mathbf{e}_i$ denotes the vector with a 1 in the ith coordinate and 0's elsewhere, we see that

$$\min_{1\leq k\leq N} \lambda_k \leq \min_{1\leq i\leq N} \{\bar{A}\}_{ii} = -\frac{N-3}{N} < 0\,, \qquad 0 < \frac{N-1}{N} = \max_{1\leq i\leq N} \{\bar{A}\}_{ii} \leq \max_{1\leq k\leq N} \lambda_k\,.$$

Therefore, there exists at least one positive eigenvalue and at least one negative eigenvalue. Indeed, the matrix $\bar{A}$ has the eigenvalues $\lambda_- = -(N-2)/N$ with algebraic multiplicity $N-2$, $\lambda_2 = 0$ and $\lambda_3 = 1$ with algebraic multiplicity 1. This can be checked considering the

proposed subspaces of the center, stable and unstable subspace of the linearised system at $\bar{\theta}$

$$E^c = \left\{ \begin{bmatrix} 1 \\ 1 \\ \vdots \\ 1 \\ \vdots \\ 1 \end{bmatrix} \right\}, E^s = \left\{ \begin{bmatrix} -1 \\ 1 \\ 0 \\ \vdots \\ 0 \\ 0 \end{bmatrix}, \begin{bmatrix} -1 \\ 0 \\ 1 \\ 0 \\ \vdots \\ 0 \end{bmatrix}, \ldots, \begin{bmatrix} -1 \\ 0 \\ \vdots \\ 0 \\ 1 \\ 0 \end{bmatrix} \right\} \text{ and } E^u = \left\{ \begin{bmatrix} -1 \\ -1 \\ \vdots \\ -1 \\ -1 \\ N-1 \end{bmatrix} \right\}.$$

Then, the Center Manifold Theorem [103, p.116] yields the existence of an $(N-2)$-dimensional stable manifold $W^s(\bar{\theta})$ tangent to the stable subspace E^s, and the existence of a 1-dimensional unstable manifold $W^u(\bar{\theta})$, and 1-dimensional center manifold $W^c(\bar{\theta})$ tangents to the E^u and E^c subspaces respectively. Consequently, the dimension of the center manifold conjoint with the stable manifold is smaller than N, which implies a null Lebesgue measure in $\mathbb{R}^n$. □

Moreover, we have:

Lemma 4.2.4. (Synchronization): *For any initial condition $\theta \in \mathscr{T}$, the Dissipation Function obeys:*

$$\lim_{t\to\infty} \Omega^{f_0,V}(S^t\theta) = \begin{cases} K(N-1), & \text{for } \theta \neq \Theta^\dagger \\ \\ K(N-1)\left(\frac{N-4}{N}\right) & \text{for } \theta = \Theta^\dagger \end{cases} \tag{4.48}$$

where $K(N-1)$, the maximum of $\Omega^{f_0,V}$ in $\mathscr{T}^N$, corresponds to $(N,0)$ synchronization.

Proof. Because of Theorem 2.4 in Ref.[11] and the continuity of $\Omega^{f_0,V}$, the long time limit of $\Omega^{f_0,V} \circ S^t$ in the case $\theta \neq \Theta^\dagger$ is given by $\Omega^{f_0,V}(\Theta^*)$. Then, Eq.(2.15) and Eq.(4.27), yield the first line of Eq.(4.48). The case $\theta = \Theta^\dagger$, gives, instead:

$$R^* e^{i\varphi^*} = \frac{1}{N}\left((N-1)e^{i\varphi^*} + e^{i(\varphi^*+\pi)}\right) = \frac{N-2}{N} e^{i\varphi^*}.$$

Substituting in Eq.(4.27) we obtain the second line of (4.48). □

Remark. *Equation* (4.48) *implies that*

$$\lim_{N\to\infty}\lim_{t\to\infty} \frac{\Omega^{f_0,V}(S^t\theta)}{N} = K. \tag{4.49}$$

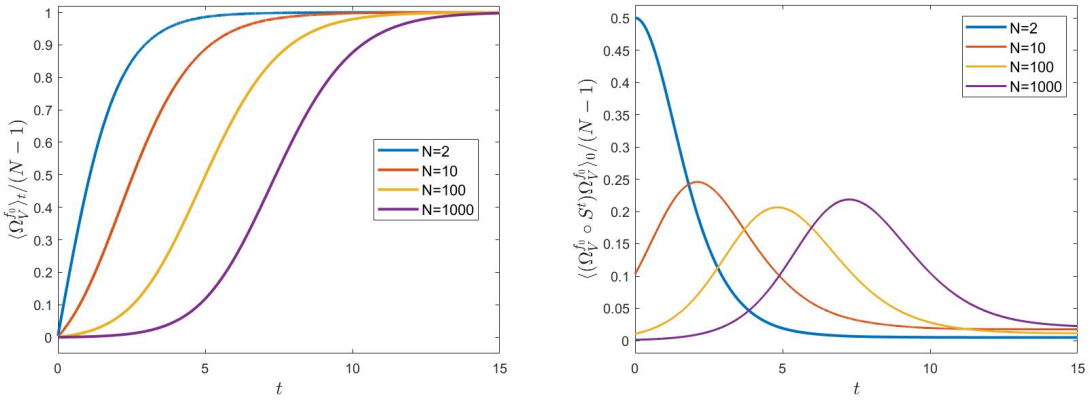

Fig. 4.2 Behavior of $\langle \Omega^{f_0,V} \rangle_t$ (left panel) and $\langle (\Omega^{f_0,V} \circ S^t)\Omega^{f_0,V} \rangle_0$ (right panel), both rescaled by $(N-1)$, as functions of time, for $K=1$, $\omega=0$ and for different values of N. The curves on the right panel represent the time derivative of those in the left panel. In particular, $t=0$ in the right panel represents K^2/N, cf. Eq.(4.50).

In other words, the large t limit followed by the large N limit implies that the coupling constant K, which drives the synchronization process in the Kuramoto dynamics (2.8)*, equals the average Dissipation per oscillator. For fixed N, synchronization is also evident from the fact that Eq.*(4.46) *must converge to 0, for* $\Omega^{f_0,V}$ *to become constant.*

This also implies $R^2(S^t\theta) \to 1$, as $t \to \infty$. It suffices to consider the definition (4.27) of $\Omega^{f_0,V}$ and (4.49). For different values of N, Fig. 4.2 illustrates the behavior of $\langle \Omega^{f_0,V} \rangle_t$ and of its time derivative, which is $\langle (\Omega^{f_0,V} \circ S^t)\Omega^{f_0,V} \rangle_0$, as functions of time. The initial growth of the autocorrelation may look unusual, since autocorrelations are commonly found to decrease. However, unlike standard calculations that rely on an invariant distribution,[1] our autocorrelation is computed with respect to the transient probability measure μ_0. The figure portrays the result of numerical simulations. The right panel of Fig. 4.2, shows that for sufficiently large N the autocorrelation function $\langle (\Omega^{f_0,V} \circ S^t)\Omega^{f_0,V} \rangle_0$ reaches a maximum before it decreases, as required for convergence to a steady state. An interesting result is the following.

Lemma 4.2.5. *For $N \geq 2$, the derivative of the time dependent average of $\Omega^{f_0,V}$, computed at time $t=0$ obeys:*

$$\frac{d}{dt}\left\langle \Omega^{f_0,V} \right\rangle_t \Big|_{t=0} = \left\langle \left(\Omega^{f_0,V}\right)^2 \right\rangle_0 = K^2 \frac{N-1}{N}. \tag{4.50}$$

[1] In linear response the initial distribution is considered invariant to first order in the perturbation.

Note that the derivative of the mean Dissipation Function equals its autocorrelation function, as expressed by Eq.(4.41). Therefore, Eq.(4.50) gives the value of this autocorrelation function at $t = 0$, as shown in the right panel of Fig. 4.2.

Proof. Using (4.43), (4.44) and (4.46) we find that

$$\frac{d}{dt}\left\langle \Omega^{f_0,V}\right\rangle_t = \frac{d}{dt}\left\langle \Omega^{f_0,V}\circ S^t\right\rangle_0 = 2K^2\left\langle R^2(S^t\theta)\sum_{j=1}^{N}\sin^2\left(S^t\theta_j-\Phi\left(S^t\theta\right)\right)\right\rangle_0 . \quad (4.51)$$

Thus, at $t = 0$, the integrand of (4.51) reads

$$R^2(\theta)\sum_{j=1}^{N}\sin^2(\Phi-\theta_j) = \frac{1}{N^2}\sum_{j=1}^{N}\left(\sum_{l=1}^{N}\sin(\theta_l-\theta_j)\right)^2 \quad (4.52)$$
$$= \frac{1}{N^2}\sum_{j=1}^{N}\left[\sum_{l=1}^{N}\sin^2(\theta_j-\theta_l)+\sum_{l=1}^{N}\sum_{\substack{k=1\\k\neq l}}^{N}\sin(\theta_l-\theta_j)\sin(\theta_k-\theta_j)\right].$$

Furthermore, we have:

$$\int_0^{2\pi}\int_0^{2\pi}\sin(\theta_l-\theta_j)\sin(\theta_k-\theta_j)d\theta_l d\theta_k$$
$$= \int_0^{2\pi}\sin(\theta_l-\theta_j)d\theta_l\int_0^{2\pi}\sin(\theta_k-\theta_j)d\theta_k = 0 . \quad (4.53)$$

Therefore, considering (4.52) and (4.53) over (4.51) at time $t = 0$ we have:

$$\begin{aligned}\frac{d}{dt}\langle\Omega^{f_0,V}\rangle_t\Big|_{t=0} &= 2K^2\int_{\mathscr{M}}R^2(\theta)\sum_{j=1}^{N}\sin^2(\Phi-\theta_j)f_0(\theta)d\theta\\ &= 2\frac{K^2}{N^2}\frac{1}{(2\pi)^N}\int_{\mathscr{M}}\sum_{j=1}^{N}\sum_{l=1}^{N}\sin^2(\theta_j-\theta_l)d\theta\\ &= 2\frac{K^2}{(2\pi)^2}\frac{N-1}{N}\int_0^{2\pi}\int_0^{2\pi}\sin^2(\theta_1-\theta_2)d\theta_1 d\theta_2\\ &= K^2\frac{N-1}{N}.\end{aligned}$$

This completes the proof of (4.50). □

4.2.3 Comparison with linear response

In this part, we compare the foregoing exact response formalism with the standard linear response. Our aim is, in fact, to highlight some remarkable differences between the two formalisms, which can be elucidated in full analytical detail with the present model.

$$V_\varepsilon(\theta) = V_0(\theta) + \varepsilon V_p(\theta)$$

where the parameter ε expresses the strength of the perturbation. Following subsection 4.2.2, we identify ε with K, and define:

$$V_0(\theta) = \omega \tag{4.54}$$

$$V_{p,j}(\theta) = R\sin(\Phi - \theta_j). \qquad j = 1,...,N \tag{4.55}$$

Correspondingly, we denote by S^t_ε and S^t_0 the perturbed and unperturbed flows, respectively. From Eq. (4.3), we obtain:

$$\Omega^{f_0}_\varepsilon = \Omega^{f_0}_0 + \varepsilon\Omega^{f_0}_p = \varepsilon\Omega^{f_0}_p \tag{4.56}$$

where $\Omega^{f_0}_0$ and $\Omega^{f_0}_p$ denote the Dissipation Function (4.27) evaluated in terms of the vector fields V_0 and V_p, respectively. In particular, we have:

$$\Omega^{f_0}_p = \frac{1}{N}\sum_{i,j=1}^{N}\cos(\theta_j - \theta_i) - 1 \tag{4.57}$$

The last equality in Eq.(4.56) derives from the fact that $\Omega^{f_0}_0 \equiv 0$ if, as assumed, f_0 is invariant under the unperturbed dynamics, cf. Eq.(4.26). We may then write the *exact* response Eq.(4.14) as:

$$\langle\mathscr{O}\rangle_{t,\varepsilon} = \langle\mathscr{O}\rangle_0 + \varepsilon\int_0^t \langle(\mathscr{O}\circ S^\tau_\varepsilon)\ \Omega^{f_0}_p\rangle_0\, d\tau\,, \tag{4.58}$$

where $\mathscr{O}\circ S^t_\varepsilon$ denotes the observable $\mathscr{O}$ composed with the perturbed flow. Because this formula is exact, the parameter ε in it does not need to be small, and it appears both as a factor multiplying the integral and as a subscript indicating the perturbed flow S^t_ε. Next, using Eq. (4.8), we can write

$$f_t(\theta) = \exp\left\{\varepsilon\int_{-t}^0 \Omega^{f_0}_p(S^\tau_\varepsilon\theta)\, d\tau\right\} f_0(\theta)\,. \tag{4.59}$$

which can be expanded about $\varepsilon = 0$, and truncated to first order, to obtain the linear approximation of the evolving probability density:

$$\begin{aligned} \bar{f}_t(\theta;\varepsilon) &= f_0(\theta)\left(1+\varepsilon\,\frac{d}{d\varepsilon}\exp\left\{\varepsilon\int_{-t}^{0}\Omega_p^{f_0}(S_\varepsilon^\tau\theta)\,d\tau\right\}\Big|_{\varepsilon=0}\right) \qquad (4.60)\\ &= f_0(\theta)\left(1+\varepsilon\int_{-t}^{0}\Omega_p^{f_0}(S_0^\tau\theta)\,d\tau\right)\\ &= f_0(\theta)\left(1+\varepsilon\int_{0}^{t}\Omega_p^{f_0}(S_0^{-\tau}\theta)\,d\tau\right). \qquad (4.61) \end{aligned}$$

Note that the expansion in the variable ε of the exponential in Eq.(4.59), requires computing the derivatives with respect to ε of the time integral in it. This, in turn, requires the derivatives of the Dissipation Function $\Omega_p^{f_0}(S_\varepsilon^\tau\theta)$, and of the evolved trajectory points $S_\varepsilon^\tau\theta$. Because both the Dissipation Function and the dynamics are smooth on a compact manifold, their derivatives are bounded, and their integral up to any time t computed at $\varepsilon = 0$ is also bounded. Multiplied by ε, this integral gives a vanishing contribution to the first derivative of the exponential in Eq.(4.59). There only remain the exponential and the integral computed at $\varepsilon = 0$, multiplied by the increment ε, which is the brackets in Eq.(4.61). We then define:

$$\overline{\langle\mathscr{O}\rangle}_{t,\varepsilon} = \int_{\mathscr{M}}\mathscr{O}(\theta)\bar{f}_t(\theta;\varepsilon)\,d\theta = \langle\mathscr{O}\rangle_0 + \varepsilon\int_0^t\left\langle\mathscr{O}\,\left(\Omega_p^{f_0}\circ S_0^{-\tau}\right)\right\rangle_0 d\tau \qquad (4.62)$$

which is the linear response result. At the same time, the invariance of the correlation function under time translations of the unperturbed dynamics, which is proven in Appendix A, yields:

$$\overline{\langle\mathscr{O}\rangle}_{t,\varepsilon} = \langle\mathscr{O}\rangle_0 + \varepsilon\int_0^t\left\langle(\mathscr{O}\circ S_0^\tau)\;\Omega_p^{f_0}\right\rangle_0 d\tau \qquad (4.63)$$

It is interesting to note that, unlike the Green-Kubo formulae, which are obtained from small Hamiltonian perturbations, here the perturbation is not Hamiltonian. Therefore, we may call (4.63) a *generalized* GK formula. It is worth comparing it with the exact response formula (4.58), as follows:

$$\langle\mathscr{O}\rangle_{t,\varepsilon} - \overline{\langle\mathscr{O}\rangle}_{t,\varepsilon} = \varepsilon\int_0^t\left\langle\left[(\mathscr{O}\circ S_\varepsilon^\tau) - (\mathscr{O}\circ S_0^\tau)\right]\Omega_p^{f_0}\right\rangle_0 d\tau \qquad (4.64)$$

which shows that the two formulae tend to be the same, in the small ε limit, as expected. Thanks to the use of the Dissipation Function, their difference lies only in the use of the perturbed rather than the unperturbed flow inside $\mathscr{O}$.

Let us dwell on the response of two relevant observables, in the case in which $V_0 = \omega = 0$, hence S_0^t is the identity operator, Id. First, taking $\mathscr{O} = \Omega_\varepsilon^{f_0} = \varepsilon\Omega_p^{f_0}$, we find

$$\begin{aligned}\langle\Omega_\varepsilon^{f_0}\rangle_{t,\varepsilon} - \overline{\langle\Omega_\varepsilon^{f_0}\rangle}_{t,\varepsilon} &= \int_0^t \left\langle \left[\left(\Omega_\varepsilon^{f_0}\circ S_\varepsilon^\tau\right) - \left(\Omega_\varepsilon^{f_0}\circ S_0^\tau\right)\right]\,\Omega_\varepsilon^{f_0}\right\rangle_0 d\tau \\ &= \int_0^t \left[\left\langle\left(\Omega_\varepsilon^{f_0}\circ S_\varepsilon^\tau\right)\Omega_\varepsilon^{f_0}\right\rangle_0 - \left\langle\left(\Omega_\varepsilon^{f_0}\right)^2\right\rangle_0\right] d\tau \end{aligned} \tag{4.65}$$

where we used the identity $\left(\Omega_\varepsilon^{f_0}\circ S_0^\tau\right) = \Omega_\varepsilon^{f_0}$, which derives from the fact that S_0^t =Id, and which yields, cf. Eq.(4.50):

$$\left\langle\left(\Omega_\varepsilon^{f_0}\right)^2\right\rangle_0 = \varepsilon^2\frac{N-1}{N} \tag{4.66}$$

For $N = 2$, we can also use the explicit expression (4.38) for the autocorrelation function:

$$\left\langle\left(\Omega_\varepsilon^{f_0}\circ S_\varepsilon^\tau\right)\Omega_\varepsilon^{f_0}\right\rangle_0 = \frac{\varepsilon^2}{1+\cosh(\varepsilon\tau)} \tag{4.67}$$

which leads to:

$$\langle\Omega_\varepsilon^{f_0}\rangle_{t,\varepsilon} = \varepsilon\tanh\left(\frac{\varepsilon t}{2}\right), \quad \text{and} \quad \overline{\langle\Omega_\varepsilon^{f_0}\rangle}_{t,\varepsilon} = \frac{\varepsilon^2 t}{2} \tag{4.68}$$

so that

$$\langle\Omega_\varepsilon^{f_0}\rangle_{t,\varepsilon} = \overline{\langle\Omega_\varepsilon^{f_0}\rangle}_{t,\varepsilon} + o(\varepsilon^2)t \tag{4.69}$$

In other words, for any $\varepsilon > 0$, the difference of the two responses is small at small times, but it diverges linearly as time passes.

As a second instance, let us take $\mathscr{O} = \psi = \theta_1 - \theta_2$. From (4.27) and (4.34) we have:

$$\Omega_\varepsilon^{f_0} = 2\varepsilon R^2(\psi) - \varepsilon = \frac{2\varepsilon}{\tan^2\left(\frac{\psi}{2}\right)+1} - \varepsilon = \varepsilon\cos(\psi) \tag{4.70}$$

Moreover, Eq.(4.33) yields:

$$(\psi\circ S_\varepsilon^t) = 2\arctan\left[\tan\left(\frac{\psi}{2}\right)e^{-\varepsilon t}\right] \tag{4.71}$$

and we can write:

$$\langle\psi\rangle_{t,\varepsilon} - \overline{\langle\psi\rangle}_{t,\varepsilon} = \int_0^t \left[\left\langle(\psi\circ S_\varepsilon^\tau)\,\Omega_\varepsilon^{f_0}\right\rangle_0 - \left\langle(\psi\circ S_0^\tau)\,\Omega_\varepsilon^{f_0}\right\rangle_0\right] d\tau$$

$$= \int_0^t \left[\left\langle (\psi \circ S_\varepsilon^\tau)\, \Omega_\varepsilon^{f_0} \right\rangle_0 - \left\langle \psi\, \Omega_\varepsilon^{f_0} \right\rangle_0 \right] d\tau \tag{4.72}$$

where we used $S_0^t = \mathrm{Id}$, which implies $\left(\psi \circ S_0^\tau\right) \equiv \psi$. Therefore, using (4.70) and (4.71) in (4.72), we obtain:

$$\begin{aligned} \langle \psi \rangle_{t,\varepsilon} - \overline{\langle \psi \rangle}_{t,\varepsilon} = & \frac{\varepsilon}{(2\pi)^2} \int_0^t \int_{\mathscr{M}} 2 \arctan \left[\tan\left(\frac{\theta_1 - \theta_2}{2} \right) e^{-\varepsilon\tau} \right] \cos(\theta_1 - \theta_2) d\theta d\tau \\ & - \frac{\varepsilon}{(2\pi)^2} \int_0^t \int_{\mathscr{M}} (\theta_1 - \theta_2) \cos(\theta_1 - \theta_2) d\theta d\tau = 0 \end{aligned} \tag{4.73}$$

The last equality follows from the fact that the integrands in Eq. (4.73) are odd continuous and periodic functions, that are integrated over a whole period, so that in fact one has:

$$\langle \psi \rangle_{t,\varepsilon} = \overline{\langle \psi \rangle}_{t,\varepsilon} \equiv 0 \quad , \quad \forall t > 0 \,. \tag{4.74}$$

Clearly, there are observables for which the difference of responses is irrelevant, since they do not evolve in time, and others for which the difference is substantial, even under small perturbations. In any event, the exact response characterizes the synchronization transition, while the linear response does not. This provides an example in which a successful theory in providing expression to the phenomenological coefficients of a dynamic as it is the linear response fails to describe the synchronization transition of a system.

4.3 Dissipation theory for coupled Kuramoto models

To continue the program started in [5], consider a system endowed with the AIC topology (3.5)-(3.15). Therefore, let $\mathscr{T} = \mathbb{R}/(2\pi\mathbb{Z})$, with $N \geq 1$, and

$$X = [\Theta, \Xi] \in \mathscr{T}^{2N},$$

where Θ and Ξ represent the two layers. As in Chapter 4.2, we introduce an *equilibrium* vector field W, whose components are given by:

$$W_i := \begin{cases} \omega & i \in \{1, N\} \\ \bar{\omega} & i \in \{N+1, 2N\} \end{cases} \tag{4.75}$$

where ω and $\bar{\omega}$ are the natural frequencies of the two layers. At time $t = 0$, the system is assumed to be perturbed by a nonequilibrium vector field $V(X)$ with components

$$V_i(X) = \begin{cases} \dfrac{K_1}{N}\displaystyle\sum_{j=1}^{N}\sin(\theta_j-\theta_i)+\dfrac{\varepsilon}{N}\sum_{j=1}^{N}\sin(\xi_j-\theta_i), & i=1,\dots,N \\ \dfrac{K_2}{N}\displaystyle\sum_{j=1}^{N}\sin(\xi_j-\xi_i)+\dfrac{\varepsilon}{N}\sum_{j=1}^{N}\sin(\theta_j-\xi_i), & i=N+1,\dots,2N. \end{cases} \tag{4.76}$$

The dynamical system takes hence the form:

$$\dot{X}(t) = \begin{cases} V^-(X) = W & t<0 \\ V^+(X) = W+V(X) & t>0 \end{cases} \tag{4.77}$$

Adapting the notation introduced in (3.8), we can rewrite the vector field V as follows:

$$V_i(\theta) = \begin{cases} K_1 r_1 \sin(\varphi_1-\theta_i)+\varepsilon r_2\sin(\varphi_2-\theta_i), & i=1,\dots,N \\ \\ K_2 r_2 \sin(\varphi_2-\xi_i)+\varepsilon r_1\sin(\varphi_1-\xi_i), & i=N+1,\dots,2N. \end{cases}$$

In the following proposition we express the phase space volumes variation rate $\Lambda(X)$ as a function of the order parameters r_1 and r_2.

Proposition 4.3.1. *The divergence of the vector field defined in Eq.*(4.76)*, reads:*

$$\Lambda = \mathrm{div}_X V = K_1(1-Nr_1^2)+K_2(1-Nr_2^2)-2\varepsilon N r_1 r_2\cos(\varphi_1-\varphi_2).$$

Proof. For $i = 1,\dots,N$ one has

$$\begin{aligned} \partial_{\theta_i}V_i &= \frac{K_1}{N}\partial_{\theta_i}\left(\sum_{i\neq j=1}^{N}\sin(\theta_j-\theta_i)\right)+\frac{\varepsilon}{N}\partial_{\theta_i}\left(\sum_{j=1}^{N}\sin(\xi_j-\theta_i)\right) \\ &= -\frac{K_1}{N}\left(\sum_{i\neq j=1}^{N}\cos(\theta_j-\theta_i)\right)-\frac{\varepsilon}{N}\left(\sum_{j=1}^{N}\cos(\xi_j-\theta_i)\right) \\ &= -K_1 r_1\cos(\varphi_1-\theta_i)+\frac{K_1}{N}-\varepsilon r_2\cos(\varphi_2-\theta_i)\,. \end{aligned}$$

Analogously for $i = N+1,\ldots,2N$ it holds:

$$\partial_{\xi_i} V_i = -K_2 r_2 \cos(\varphi_2 - \xi_i) + \frac{K_2}{N} - \varepsilon r_1 \cos(\varphi_1 - \xi_i)\,.$$

Then

$$\begin{aligned}
\mathrm{div}_X V &= \sum_{i=1}^{N} \partial_{\theta_i} V_i + \sum_{i=1}^{N} \partial_{\xi_i} V_{N+i} \\
&= K_1 - K_1 r_1 \sum_{i=1}^{N} \cos(\varphi_1 - \theta_i) - \varepsilon r_2 \sum_{i=1}^{N} \cos(\varphi_2 - \theta_i) \\
&+ K_2 - K_2 r_2 \sum_{i=1}^{N} \cos(\varphi_2 - \xi_i) - \varepsilon r_1 \sum_{i=1}^{N} \cos(\varphi_1 - \xi_i) \\
&= K_1(1 - N r_1^2) + K_2(1 - N r_2^2) - 2N\varepsilon r_1 r_2 \cos(\varphi_1 - \varphi_2)\,.
\end{aligned}$$

□

We take the uniform probability density (cf. Eq. (4.25)) as the probability density at time $t = 0$:

$$f_0(X) = (2\pi)^{-2N} \tag{4.78}$$

which is invariant under the equilibrium dynamics. We immediately find:

$$\Omega^{f_0, V^-} = 0. \tag{4.79}$$

and:

$$\begin{aligned}
\Omega^{f_0, V^+} &= -\mathrm{div}_X V - V \cdot \nabla \log f_0 \\
&= K_1(N r_1^2 - 1) + K_2(N r_2^2 - 1) + 2N\varepsilon r_1 r_2 \cos(\varphi_1 - \varphi_2)\,.
\end{aligned} \tag{4.80}$$

Using the identity

$$\left\langle \Omega^{f_0, V^+} \right\rangle_0 = \left\langle \Omega^{f_0, V^-} \right\rangle_0 + \left\langle \Omega^{f_0, V} \right\rangle_0,$$

and because

$$\left\langle r_1^2 \right\rangle_0 = \frac{1}{N}, \quad \left\langle r_2^2 \right\rangle_0 = \frac{1}{N}, \quad \left\langle r_1 r_2 \cos(\varphi_1 - \varphi_2) \right\rangle_0 = 0$$

we obtain:

$$\left\langle \Omega^{f_0,V} \right\rangle_0 = K_1(N\left\langle r_1^2 \right\rangle_0 - 1) + K_2(N\left\langle r_2^2 \right\rangle_0 - 1) + 2N\varepsilon \left\langle r_1 r_2 \cos(\varphi_1 - \varphi_2) \right\rangle_0 = 0, \quad (4.81)$$

and consequently

$$\left\langle \Omega^{f_0,V^+} \right\rangle_0 = 0$$

The foregoing result can be proved in greater generality. Let use define the vector field V in Eq. (4.76) as follows:

$$V_i(X) = \sum_{j=1}^{N} \Psi_{ij} \sin(x_j - x_i), \quad i = 1, \ldots, N,$$

where $X = [x_1, \ldots, x_N] \in \mathscr{T}^N \in \mathscr{M}$ and Ψ_{ij} a connectivity matrix such that $\Psi_{ii} \neq 0$ for $i = 1, \ldots, N$. We find:

$$\partial_{x_i} V_i = -\sum_{j=1}^{N} \Psi_{ij} \cos(x_j - x_i) + \Psi_{ii}$$

and hence:

$$\mathrm{div}_X V = -\sum_{i,j=1}^{N} \Psi_{ij} \cos(x_j - x_i) + \sum_{i=1}^{N} \Psi_{ii}$$

By taking the factorized uniform density (see (4.25)) as the initial probability density, we have that

$$\begin{aligned} \Omega^{f_0,V} &= -\mathrm{div}_X V - V \cdot \nabla \log f_0 \\ &= \sum_{i,j=1}^{N} \Psi_{ij} \cos(x_j - x_i) - \sum_{i=1}^{N} \Psi_{ii} \\ &= \sum_{i \neq j=1}^{N} \Psi_{ij} \cos(x_j - x_i). \end{aligned} \quad (4.82)$$

which yields:

$$\left\langle \Omega^{f_0,V} \right\rangle_0 := \frac{1}{(2\pi)^N} \left[\int_{\mathscr{M}} \sum_{i,j=1}^{N} \Psi_{ij} \cos(x_j - x_i) dx - \int_{\mathscr{M}} \sum_{i=1}^{N} \Psi_{ii} dx \right] = 0.$$

We now aim at deriving an equation for the time evolution of $\left\langle \Omega^{f_0,V} \right\rangle_t$. We note, first, that the following relations hold:

$$\frac{d}{dt} r_1^2(\theta) = \frac{2K_1}{N} r_1^2 \sum_{j=1}^{N} \sin^2(\varphi_1 - \theta_j) + \frac{2\varepsilon}{N} r_2 r_1 \sum_{j=1}^{N} \sin(\varphi_1 - \theta_j)\sin(\varphi_2 - \theta_j), \tag{4.83}$$

$$\frac{d}{dt} r_2^2(\theta) = \frac{2K_2}{N} r_2^2 \sum_{j=1}^{N} \sin^2(\varphi_2 - \xi_j) - \frac{2\varepsilon}{N} r_1 r_2 \sum_{j=1}^{N} \sin(\xi_j - \varphi_1)\sin(\varphi_2 - \xi_j) \tag{4.84}$$

It is also possible to establish the following relation:

$$\frac{d}{dt} z_1 \bar{z}_2 = \frac{1}{N^2} \frac{d}{dt} \left(\sum_{j,k=1}^{N} e^{i(\theta_j - \xi_k)} \right), \tag{4.85}$$

which can equivalently be written as:

$$\frac{d}{dt} \left(r_1 r_2 \left(\cos(\varphi_1 - \varphi_2) + i \sin(\varphi_1 - \varphi_2) \right) \right) = \frac{1}{N^2} \frac{d}{dt} \left(\sum_{j,k=1}^{N} \cos(\theta_j - \xi_k) + i \sin(\theta_j - \xi_k) \right)$$

In particular, we have that

$$\begin{aligned}
\frac{d}{dt} \left(r_1 r_2 \cos(\varphi_1 - \varphi_2) \right) &= \frac{d}{dt} \left(\frac{1}{N^2} \sum_{j,k=1}^{N} \cos(\theta_j - \xi_k) \right) \\
&= -\frac{1}{N^2} \sum_{j,k=1}^{N} \sin(\theta_j - \xi_k)(\dot{\theta}_j - \dot{\xi}_k) \\
&= -\frac{1}{N^2} \left(\sum_{j,k=1}^{N} \sin(\theta_j - \xi_k)\dot{\theta}_j - \sum_{j,k=1}^{N} \sin(\theta_j - \xi_k)\dot{\xi}_k \right) \\
&= -\frac{1}{N} \left(r_2 \sum_{j=1}^{N} \sin(\theta_j - \varphi_2)\dot{\theta}_j - r_1 \sum_{k=1}^{N} \sin(\varphi_1 - \xi_k)\dot{\xi}_k \right).
\end{aligned}$$

Therefore, we find that the real part of $z_1\bar{z}_2$ obeys the dynamics

$$\begin{aligned}\frac{dRe(z_1\bar{z}_2)}{dt} = -\frac{1}{N}\Bigg[r_2 \Bigg(& Nr_1\omega_1 \sin(\varphi_1-\varphi_2) + K_1 r_1 \sum_{j=1}^{N} \sin(\varphi_1-\theta_j)\sin(\theta_j-\varphi_2) \\ & -\varepsilon r_2 \sum_{j=1}^{N} \sin^2(\varphi_2-\theta_j)\Bigg) - r_1 \Big(Nr_2\omega_2 \sin(\varphi_1-\varphi_2) \\ & + K_2 r_2 \sum_{k=1}^{N} \sin(\varphi_1-\xi_k)\sin(\varphi_2-\xi_k) + \varepsilon r_1 \sum_{k=1}^{N} \sin^2(\varphi_1-\xi_k)\Bigg)\Bigg],\end{aligned}$$

which, due to Eqs. (3.10) to (3.13), leads to:

$$\frac{dRe(z_1\bar{z}_2)}{dt} = r_1 r_2 \sin(\varphi_1-\varphi_2)(\omega_2-\omega_1) + \frac{K_1}{N} r_1 r_2 \sum_{j=1}^{N} \sin(\varphi_1-\theta_j)\sin(\varphi_2-\theta_j) \tag{4.86}$$

$$+ \frac{K_2}{N} r_2 r_1 \sum_{k=1}^{N} \sin(\varphi_1-\xi_k)\sin(\varphi_2-\xi_k) \tag{4.87}$$

$$+ \frac{\varepsilon}{N}\left(r_2^2 \sum_{j=1}^{N} \sin^2(\varphi_2-\theta_j) + r_1^2 \sum_{k=1}^{N} \sin^2(\varphi_1-\xi_k)\right) \tag{4.88}$$

Then, using (4.83), (4.84) and (4.88), we get

$$\begin{aligned}\frac{d}{dt}\Omega^{f_0,V} &= K_1 N \frac{d}{dt} r_1^2 + K_2 N \frac{d}{dt} r_2^2 + 2N\varepsilon \frac{d}{dt}\left(r_1 r_2 \cos(\varphi_1-\varphi_2)\right) \\ &= K_1 N \left(\frac{2K_1}{N} r_1^2 \sum_{j=1}^{N} \sin^2(\varphi_1-\theta_j) + \frac{2\varepsilon}{N} r_2 r_1 \sum_{j=1}^{N} \sin(\varphi_1-\theta_j)\sin(\varphi_2-\theta_j)\right) \\ &+ K_2 N \left(\frac{2K_2}{N} r_2^2 \sum_{j=1}^{N} \sin^2(\varphi_2-\xi_j) + \frac{2\varepsilon}{N} r_1 r_2 \sum_{j=1}^{N} \sin(\varphi_1-\xi_j)\sin(\varphi_2-\xi_j)\right) \\ &+ 2N\varepsilon \Bigg[r_1 r_2 \sin(\varphi_1-\varphi_2)(\omega_2-\omega_1) + \frac{K_1}{N} r_1 r_2 \sum_{j=1}^{N} \sin(\varphi_1-\theta_j)\sin(\varphi_2-\theta_j) \\ &+ \frac{K_2}{N} r_2 r_1 \sum_{k=1}^{N} \sin(\varphi_1-\theta_k^2)\sin(\varphi_2-\theta_k^2) + \frac{\varepsilon}{N}\Bigg(r_2^2 \sum_{j=1}^{N} \sin^2(\varphi_2-\theta_j) \\ &+ r_1^2 \sum_{k=1}^{N} \sin^2(\varphi_1-\theta_k^2)\Bigg)\Bigg]\end{aligned}$$

$$= 2Nr_1r_2\varepsilon\,(\omega_2-\omega_1)\sin(\varphi_1-\varphi_2)+2K_1^2r_1^2\sum_{j=1}^{N}\sin^2(\varphi_1-\theta_j)$$
$$+2K_2^2r_2^2\sum_{j=1}^{N}\sin^2(\varphi_2-\xi_j)+2\varepsilon^2\left(r_2^2\sum_{j=1}^{N}\sin^2(\varphi_2-\theta_j)+r_1^2\sum_{k=1}^{N}\sin^2(\varphi_1-\theta_k^2)\right)$$
$$+4\varepsilon r_1r_2\left(K_1\sum_{j=1}^{N}\sin(\varphi_1-\theta_j)\sin(\varphi_2-\theta_j)+K_2\sum_{j=1}^{N}\sin(\varphi_1-\xi_j)\sin(\varphi_2-\xi_j)\right).$$

We hence arrive at the following time evolution equation for the Dissipation Function:

$$\frac{d}{dt}\Omega^{f_0,V}=2Nr_1r_2\varepsilon\,(\omega_2-\omega_1)\sin(\varphi_1-\varphi_2)+2\sum_{j=1}^{N}\big[K_1r_1\sin(\varphi_1-\theta_j)$$
$$+\varepsilon r_2\sin(\varphi_2-\theta_j)\big]^2+\big[K_2r_2\sin(\varphi_2-\xi_j)+\varepsilon r_1\sin(\varphi_1-\xi_j)\big]^2 \quad (4.89)$$

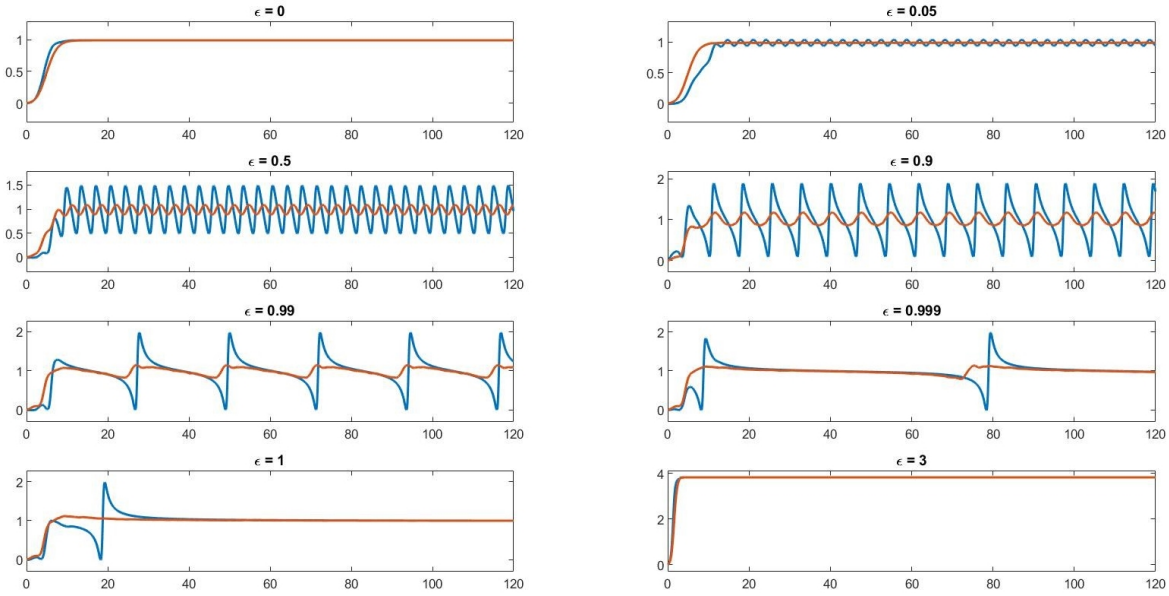

Fig. 4.3 Behavior of $\Omega^{f_0,V}/(2N)$ and $\langle\Omega^{f_0,V}\rangle_t/(2N)$ (blue and orange lines, respectively) as functions of time, for $N=100$, $K_1=K_2=1$, $\omega_1=-\omega_2=1$ and different values of $\varepsilon=\{0,0.05,0.5,0.98,0.99,1,3\}$. The averages were taken over a set of 1000 trajectories with initial data sampled from the uniform distribution on $[0,2\pi)$ in a time $t\in[0,120]$.

From the last equation we can see that if $\omega_2=\omega_1$ then $\dot{\Omega}^{f_0,V}\geq 0$.

Lemma 4.3.2. *For every $t > 0$, and for every $\varepsilon \geq 0$, if $\omega_1 = \omega_2$, then the time derivative of the expectation of the Dissipation Function obeys:*

$$\frac{d}{dt}\left\langle \Omega^{f_0,V} \right\rangle_t \geq 0\,. \tag{4.90}$$

Proof. First we note that we may write

$$\left\langle \Omega^{f_0,V} \right\rangle_t = \left\langle \Omega^{f_0,V} \circ S^t \right\rangle_0\,, \tag{4.91}$$

an identity coming from the exact response theory. Therefore, we also have:

$$\begin{aligned}\frac{d}{dt}\left\langle \Omega^{f_0,V} \circ S^t \right\rangle_0 &= \frac{d}{dt}\int_{\mathscr{M}} \Omega^{f_0,V}(S^t\theta) f_0(\theta) d\theta \\ &= \int_{\mathscr{M}} \frac{d}{dt}\left(\Omega^{f_0,V}(S^t\theta)\right) f_0(\theta) d\theta = \left\langle \frac{d}{dt}\left(\Omega^{f_0,V}(S^t\theta)\right)\right\rangle_0 .\end{aligned} \tag{4.92}$$

Then, using Eq. (4.89), we find:

$$\begin{aligned}\frac{d}{dt}\left\langle \Omega^{f_0,V} \right\rangle_t = 2\Bigg[\sum_{j=1}^{N} \Big\langle \big(K_1 r_1(S^t\theta)\sin(S^t\varphi_1 - S^t\theta_j) \\ +\varepsilon r_2(S^t\xi)\sin(S^t\varphi_2 - S^t\theta_j)\big)^2 \Big\rangle_0 + \sum_{j=1}^{N} \Big\langle \big(K_2 r_2(S^t\xi)\sin(S^t\varphi_2 - S^t\xi_j) \\ +\varepsilon r_1(S^t\theta)\sin(S^t\varphi_1 - S^t\xi_j)\big)^2 \Big\rangle_0\Bigg] \\ \geq 0.\end{aligned}$$

□

The behavior of $\Omega^{f_0,V}$ and $\langle\Omega^{f_0,V}\rangle$ as functions of time, for different values of the coupling constant ε, for the models with $\omega_1 \neq \omega_2$ and $\omega_1 = \omega_2$, is illustrated in Figs. 4.3 and 4.4. The behavior shown in Figs. 4.4 demonstrates the statement already made in Lemma 4.3.2 while the behavior in Figs. 4.3 shows that this statement cannot be transferred to the case where $\omega_1 \neq \omega_2$.

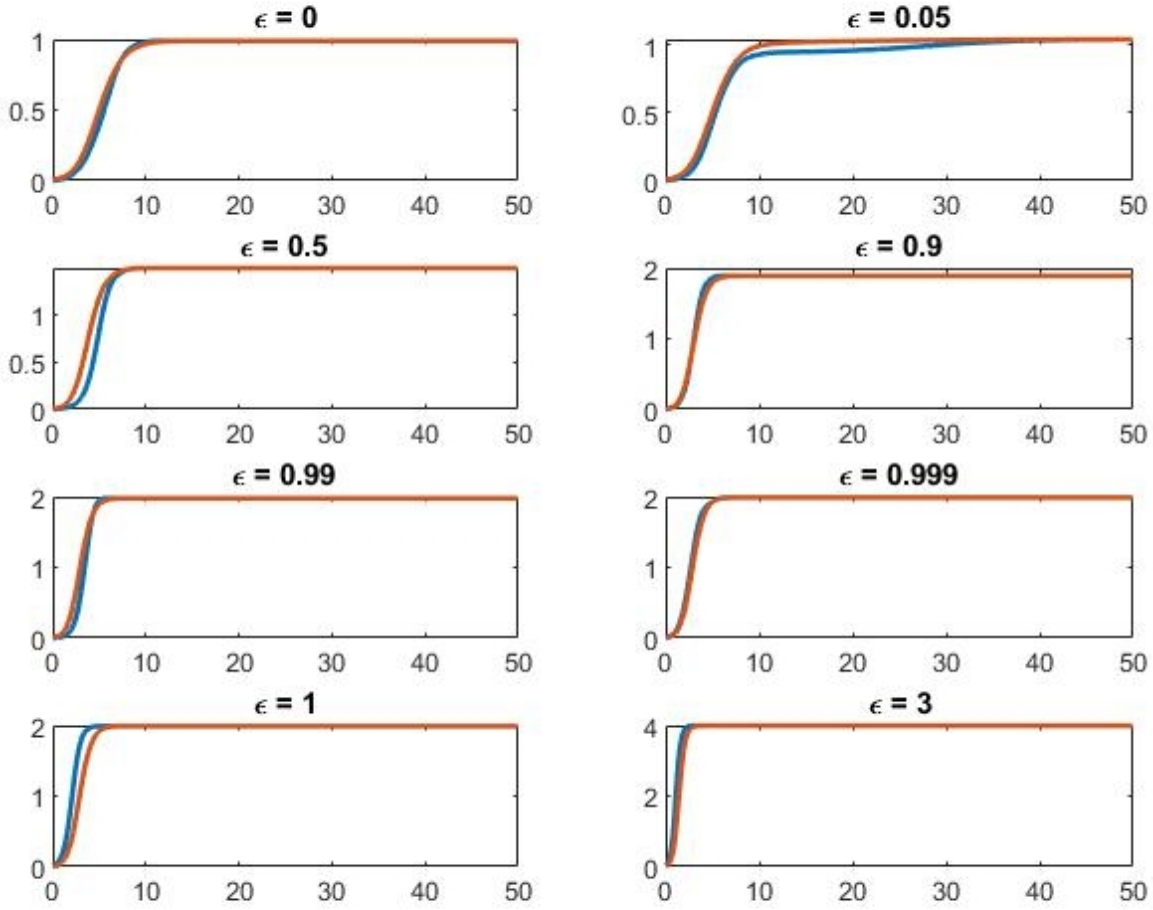

Fig. 4.4 Dynamics of $\Omega^{f_0,V}/(2N)$ and $\langle \Omega^{f_0,V} \rangle_t/(2N)$ as functions of t blue and orange lines, respectively, for $N = 100$, $K_1 = K_2 = 1$, $\omega_1 = \omega_2 = 0$ and different values of $\varepsilon = \{0, 0.05, 0.5, 0.98, 0.99, 1, 3\}$. The averages were taken over a set of 1000 trajectories with initial data sampled from the uniform distribution on $[0, 2\pi)$ in a time $t \in [0, 50]$.

Appendix A

Mathematical tools

In this Appendix, we recover some useful lemmas that we used for the analysis of our dynamics.

A.1 Useful mathematical results

Lemma A.1.1. *Suppose that θ_l, $l \in \{1,\dots,N\}$ satisfy $\theta_l \in [0,2\pi)$ and*

$$\left|\theta_i - \theta_j\right| < \pi, \quad 1 \leq i,j \leq N. \tag{A.1}$$

Then:

- *For all $i,j,l \in \{1,\dots,N\}$ one has that*

$$\sin(\theta_i - \theta_j) + \sin(\theta_l - \theta_i) - \sin(\theta_l - \theta_j) = C_{ij}^l \sin(\theta_i - \theta_j) \tag{A.2}$$

  where C_{ij}^l is given by the following:

$$C_{ij}^l := 1 - \frac{\cos(\frac{\theta_l-\theta_i}{2} + \frac{\theta_l-\theta_j}{2})}{\cos(\frac{\theta_j-\theta_i}{2})}. \tag{A.3}$$

- *For all $l = 1,\dots,N$ one has that*

$$\sin(\theta_M - \theta_m) + \sin(\theta_l - \theta_M) + \sin(\theta_m - \theta_l) \leq 0 \tag{A.4}$$

where M, m are defined by

$$M = \arg\max_{1\le l\le N} \theta_l \quad \textit{and} \quad m = \arg\min_{1\le l\le N} \theta_l \tag{A.5}$$

Proof. To prove (A.2), we use the standard sum-to-product and double-angle formulae to obtain

$$\begin{aligned}\sin(\theta_l-\theta_i)-\sin(\theta_l-\theta_j) &= 2\sin\left(\frac{\theta_j-\theta_i}{2}\right)\cos(\theta_l-\frac{\theta_i+\theta_j}{2})\\ &= -\frac{\sin(\theta_i-\theta_j)}{\cos\left(\frac{\theta_j-\theta_i}{2}\right)}\cos(\theta_l-\frac{\theta_i+\theta_j}{2})\end{aligned}$$

where, thanks to assumption (A.1),

$$\left|\frac{\theta_j-\theta_i}{2}\right| < \frac{\pi}{2} \tag{A.6}$$

and hence the $\cos(\frac{\theta_j-\theta_i}{2}) \neq 0$. Therefore

$$\begin{aligned}\sin(\theta_i-\theta_j)+\sin(\theta_l-\theta_i)-\sin(\theta_l-\theta_j) &= \sin(\theta_i-\theta_j)\left[1-\frac{\cos(\frac{\theta_l-\theta_i}{2}+\frac{\theta_l-\theta_j}{2})}{\cos(\frac{\theta_j-\theta_i}{2})}\right]\\ &= C_{ij}^l \sin(\theta_i-\theta_j).\end{aligned}$$

This completes the proof of (A.2). To prove (A.4), we apply (A.2) with $i=M$, $j=m$. The right hand side of (A.2) becomes:

$$C_{Mm}^l \sin(\theta_M-\theta_m). \tag{A.7}$$

By assumption (A.1) we have

$$0 \le \theta_M-\theta_m < \pi \tag{A.8}$$

and hence $\sin(\theta_M-\theta_m) \ge 0$. Therefore, to prove (A.4), we need to prove that $C_{Mn}^l \le 0$, that is,

$$\cos\left(\frac{\theta_M-\theta_m}{2}\right) \le \cos\left(\frac{\theta_l-\theta_M}{2}+\frac{\theta_l-\theta_m}{2}\right). \tag{A.9}$$

For this, we use the elementary inequality

$$\left|x-\frac{a+b}{2}\right| \le \frac{b-a}{2} \quad \forall a<b, \quad x\in[a,b] \tag{A.10}$$

to obtain that

$$\left|\theta_l - \frac{\theta_M + \theta_m}{2}\right| \leq \frac{\theta_M - \theta_m}{2} < \frac{\pi}{2}. \tag{A.11}$$

Therefore,

$$1 \geq \cos\left(\frac{\theta_l - \theta_M}{2} + \frac{\theta_l - \theta_m}{2}\right) \geq \cos\left(\frac{\theta_M - \theta_m}{2}\right) > 0, \tag{A.12}$$

That implies $C^l_{Mm} \leq 0$. In conclusion (A.7) is non negative and with that the proof of (A.4) is complete.

□

Lemma A.1.2. *Let f be a C^1 function $f : [0,\infty) \to \mathbb{R}$, with $\|f'(t)\| \leq C$. If the integral*

$$\int_0^\infty f(s)ds, \tag{A.13}$$

exist finite, then $f(t) \underset{t\to\infty}{\longrightarrow} 0$.

Lemma A.1.3. *If f and g are real analytic functions on an open interval U and there is an open set $W \subset U$ such that*

$$f(x) = g(x), \quad \text{for all } x \in W$$

then

$$f(x) = g(x), \quad \text{for all } x \in U$$

Proof. See [76], p. 13. □

Theorem A.1.4. *Let $U \subset \mathbb{R}^d$ be open, $f : U \to R$ be real analytic, and $a \in U$. Then there exist constants $\gamma \in (0, \frac{1}{2}]$, c, $\lambda > 0$ such that for every $z \in U$, $\|z - a\| \leq \lambda$,*

$$|f(z) - f(a)|^{1-\gamma} \leq c\|\nabla f(z)\|. \tag{A.14}$$

Proof. See Theorem 17, [82]. □

The above inequality is called Łojasiewicz inequality and thanks to that Łojasiewicz obtained:

Theorem A.1.5. *Consider the gradient system*

$$\dot{x}(t) = -\nabla f(x) \tag{A.15}$$

where $x(t) \in R^n$ and $f : R^n \to R$ is real analytic function. If $x(t)$ has a limit point x_0, i.e., $x(t_n) \to x_0$ for some sequence $t_n \to \infty$, then we have $x(t) \to x_0$ as $t \to \infty$. Moreover, $x_0 \in M = \{x : \nabla f(x) = 0\}$, and therefore $\frac{dx}{dt} \to 0$ as $t \to \infty$.

A.2 Stationary correlation functions

Given a vector field V_0, let f_0 be an invariant probability density under the flow S_0^t generated by V_0. With the notation set by Eq.(4.7), let $\Lambda^0_{0,t}$ be the time integral over a trajectory segment, from time 0 to time t, of the phase space volume variation rate Λ^0, which is the divergence of the vector field V_0. Two-time correlation functions between two generic observables $\mathscr{A}, \mathscr{B} : \mathscr{M} \to \mathbb{R}$, evaluated with the density f_0, are invariant under the time translations determined by S_0^t. This can be shown as follows. First we note that, proceeding as in Eq. (4.9), one finds

$$\begin{aligned} \Omega^{f_s,V_0}_{-t,0} &= \int_{-t}^{0} \Omega^{f_s,V_0}(S_0^\tau\theta)d\tau = -\Lambda^0_{-t,0} - \int_{-t}^{0} \frac{d}{d\tau}\left(\log f_s(S_0^\tau\theta)\right) d\tau \\ &= -\Lambda^0_{-t,0} - \log \frac{f_s(\theta)}{f_s(S_0^{-t}\theta)}\,. \end{aligned} \tag{A.16}$$

Upon setting $s = 0$ in (A.16) and using Eq.(4.12), we find $\left(\Omega^{f_0,V_0}\right)_{-t,0} \equiv 0$, from which we obtain the following useful relation

$$f_0(\theta) = \exp\Big\{ -\Lambda^0_{-t,0}(\theta)\Big\} f_0(S_0^{-t}\theta) \tag{A.17}$$

where the exponential term is related to the Jacobian determinant of the dynamics as [66]:

$$\left| \frac{\partial\left(S_0^{-t}\theta\right)}{\partial\theta} \right| = \exp\Big\{ -\Lambda^0_{-t,0}(\theta)\Big\}\,. \tag{A.18}$$

Let us look, next, at time correlation functions of the form

$$\langle \left(\mathscr{A}\circ S_0^{s+\tau}\right)\ \left(\mathscr{B}\circ S_0^t\right)\rangle_0 = \int_{\mathscr{M}} \mathscr{A}(S_0^{s+\tau}\theta)\ \mathscr{B}(S_0^t\theta) f_0(\theta) d\theta$$

for any $s,t,\tau \in \mathbb{R}$. By a change of variables, one finds

$$\begin{aligned}
\langle \left(\mathscr{A}\circ S_0^{s+\tau}\right)\ \left(\mathscr{B}\circ S_0^t\right)\rangle_0 &= \int_{\mathscr{M}} \mathscr{A}(S_0^s\theta)\ \mathscr{B}(S_0^{t-\tau}\theta) f_0(S_0^{-\tau}\theta) d\left(S_0^{-\tau}\theta\right) \\
&= \int_{\mathscr{M}} \mathscr{A}(S_0^s\theta)\ \mathscr{B}(S_0^{t-\tau}\theta) f_0(S_0^{-\tau}\theta) \left|\frac{\partial\left(S_0^{-\tau}\theta\right)}{\partial\theta}\right| d\theta \\
&= \int_{\mathscr{M}} \mathscr{A}(S_0^s\theta)\ \mathscr{B}(S_0^{t-\tau}\theta) \exp\left\{-\Lambda^0_{-\tau,0}\right\} f_0(S_0^{-\tau}\theta) d\theta \\
&= \int_{\mathscr{M}} \mathscr{A}(S_0^s\theta)\ \mathscr{B}(S_0^{t-\tau}\theta) f_0(\theta) d\theta \\
&= \langle (\mathscr{A}\circ S_0^s)\ \left(\mathscr{B}\circ S_0^{t-\tau}\right)\rangle_0 \qquad \text{(A.19)}
\end{aligned}$$

where we used (A.18) and, in the last line, the formula (A.17).

Appendix B

Stuart-Landau oscillators on 2-layer models

The Stuart-Landau oscillators is an equation in normal form, which means that the limit cycle dynamics of many other oscillators can be transformed onto or can be approximated by the dynamics given by equation [100]:

$$\dot{z} = \left(1 - |z|^2 + i\Omega\right) z, \tag{B.1}$$

where $z \in \mathrm{C}$ denotes the position of the Stuart-Landau oscillator and $\Omega \in \mathrm{R}$ is the natural frequency of the Stuart-Landau oscillator. We set $z = re^{i\theta}$, then the equatio above can be retritten as follows

$$\dot{r} = r(1 - r^2), \quad \dot{\theta} = \Omega. \tag{B.2}$$

Then, it is easy to see that Stuart-Landau oscillator has a stable limit cycle $r = 1$, on which it moves at its natural frequency Ω. Now, let's consider a weakly coupled system of 2 layers with N Stuart-Landau oscillators in each layer and a SIC linear coupling:

$$\begin{cases} \frac{dz_j}{dt} = \left(1 - |z_j|^2 + i\Omega_j\right) z_j + \frac{K_1}{N} \sum_{i=1} (z_i - z_j) + \varepsilon(\bar{z}_j - z_j) \\ \\ \frac{d\bar{z}_j}{dt} = \left(1 - |\bar{z}_j|^2 + i\Omega_j\right) \bar{z}_j + \frac{K_2}{N} \sum_{i=1} (\bar{z}_i - \bar{z}_j) + \varepsilon(z_j - \bar{z}_j) \end{cases} \tag{B.3}$$

where K_1, K_2 are the positive coupling strength between oscillators from the same layer and ε is the positive coupling strength between a pair of oscillators from different layers. A similar result was give it by [49]. We set z_c and $\bar{z}_c$ the centroid of the oscillators:

$$z_c := \frac{1}{N}\sum_{j=1}^{N} z_j \quad \bar{z}_c := \frac{1}{N}\sum_{j=1}^{N} \bar{z}_j. \tag{B.4}$$

Then, the system (B.3) can be rewritten as

$$\begin{cases} \frac{dz_j}{dt} = \left(1-|z_j|^2+i\Omega_j\right) z_j + K_1(z_c - z_j) + \varepsilon(\bar{z}_j - z_j) \\ \\ \frac{d\bar{z}_j}{dt} = \left(1-|\bar{z}_j|^2+i\bar{\Omega}_j\right) \bar{z}_j + K_2(\bar{z}_c - \bar{z}_j) + \varepsilon(z_j - \bar{z}_j) \end{cases} \tag{B.5}$$

we now introduce polar forms for $z_j, \bar{z}_j, z_c$ and $\bar{z}_c$:

$$z_j = r_j e^{i\theta_j}, \quad \bar{z}_j = \bar{r}_j e^{i\xi_j} \quad z_c = r_1 e^{i\phi_1} \quad \bar{z}_c = r_2 e^{i\phi_2} \tag{B.6}$$

Thus, system (B.5) is equivalent to

$$\begin{cases} \dot{r}_j = \left(1-r_j^2\right) r_j + K_1\left(r_1\cos(\phi_1-\theta_j) - r_j\right) + \varepsilon\left(\bar{r}_j\cos(\xi_j-\theta_j) - r_j\right) & \text{(B.7a)} \\ \dot{\theta}_j = \Omega_j + K_1\frac{r_1}{r_j}\sin(\varphi_1-\theta_j) + \varepsilon\frac{\bar{r}_j}{r_j}\sin(\xi_j-\theta_j) & \text{(B.7b)} \\ \dot{\bar{r}}_j = \left(1-\bar{r}_j^2\right)\bar{r}_j + K_2\left(\bar{r}_1\cos(\phi_2-\xi_j) - \bar{r}_j\right) + \varepsilon\left(r_j\cos(\theta_j-\xi_j) - \bar{r}_j\right) & \text{(B.7c)} \\ \dot{\xi}_j = \bar{\Omega}_j + K_2\frac{r_2}{\bar{r}_j}\sin(\varphi_2-\xi_j) + \varepsilon\frac{r_j}{\bar{r}_j}\sin(\theta_j-\xi_j) & \text{(B.7d)} \end{cases}$$

For the limit-cycle oscillators where $r_j = 1$ and $\bar{r}_j = 1$, the equations (B.7b) and (B.7d) becomes our AIC system in terms of r_1, r_2 φ_1 and φ_2:

$$\begin{cases} \dot{\theta}_j = \Omega_j + K_1 r_1 \sin(\varphi_1-\theta_j) + \varepsilon\sin(\xi_j-\theta_j) \\ \dot{\xi}_j = \bar{\Omega}_j + K_2 r_2 \sin(\varphi_2-\xi_j) + \varepsilon\sin(\theta_j - xi_j) \end{cases} \tag{B.8}$$

The case of oscillators with an AIC linear coupling is analogous to SIC, we have the dynamic

$$\begin{cases} \frac{dz_j}{dt} = \left(1-|z_j|^2+i\Omega_j\right)z_j + \frac{K_1}{N}\sum_{i=1}(z_i-z_j) + \varepsilon\sum_{i=1}^{N}(\bar{z}_i-z_j) \\ \\ \frac{d\bar{z}_j}{dt} = \left(1-|\bar{z}_j|^2+i\Omega_j\right)\bar{z}_j + \frac{K_2}{N}\sum_{i=1}(\bar{z}_i-\bar{z}_j) + \varepsilon\sum_{i=1}^{N}(z_i-\bar{z}_j) \end{cases} \tag{B.9}$$

considering the centroid of the oscillators defined in (B.4) and the polar forms in (B.6) the system can be rewritten as

$$\begin{cases} \dot{r}_j = \left(1-r_j^2\right)r_j + K_1\left(r_1\cos(\phi_1-\theta_j)-r_j\right) + \varepsilon\left(r_2\cos(\varphi_2-\theta_j)-r_j\right) & \text{(B.10a)} \\ \dot{\theta}_j = \Omega_j + K_1\frac{r_1}{r_j}\sin(\varphi_1-\theta_j) + \varepsilon\frac{r_2}{r_j}\sin(\varphi_2-\theta_j) & \text{(B.10b)} \\ \dot{\bar{r}}_j = \left(1-\bar{r}_j^2\right)\bar{r}_j + K_2\left(\bar{r}_1\cos(\phi_2-\xi_j)-\bar{r}_j\right) + \varepsilon\left(r_1\cos(\varphi_1-\xi_j)-\bar{r}_j\right) & \text{(B.10c)} \\ \dot{\xi}_j = \bar{\Omega}_j + K_2\frac{r_2}{\bar{r}_j}\sin(\varphi_2-\xi_j) + \varepsilon\frac{r_1}{\bar{r}_j}\sin(\varphi_1-\xi_j) & \text{(B.10d)} \end{cases}$$

which also reach the form of the SIC equation when $r_j = 1$ and $\bar{r}_j = 1$.

List of figures

References

[1] Abrams, D. M., Mirollo, R., Strogatz, S. H., and Wiley, D. A. (2008). Solvable model for chimera states of coupled oscillators. *Phys. Rev. Lett.*, 101:084103.

[2] Abrams, D. M. and Strogatz, S. H. (2004). Chimera states for coupled oscillators. *Phys. Rev. Lett.*, 93:174102.

[3] Acebrón, J., Bonilla, L., Pérez, C., Ritort, F., and Spigler, R. (2005). The Kuramoto model: A simple paradigm for synchronization phenomena. *Rev. Mod. Phys.*, 77:137–185.

[4] Agarwal, G. S. (1972). Fluctuation-Dissipation Theorems for Systems in Non-Thermal Equilibrium and Applications. *Z. Physik*, 252:25–38.

[5] Amadori, D., Colangeli, M., Correa, A., and Rondoni, L. (2022). Exact response theory and Kuramoto dynamics. *Physica D: Nonlinear Phenomena*, 429:133076.

[6] Ariaratnam, J. T. and Strogatz, S. H. (2001). Phase diagram for the winfree model of coupled nonlinear oscillators. *Physical Review Letters*, 86(19):4278.

[7] Bag, B. C., Petrosyan, K. G., and Hu, C.-K. (2007). Influence of noise on the synchronization of the stochastic Kuramoto model. *Phys. Rev. E*, 76:056210.

[8] Baiesi, M., Maes, C., and Wynants, B. (2009). Nonequilibrium Linear Response for Markov Dynamics, I: Jump Processes and Overdamped Diffusions. *J. Stat. Phys.*, 137(5):1094.

[9] Barreto, E., Hunt, B., Ott, E., and So, P. (2008). Synchronization in networks of networks: The onset of coherent collective behavior in systems of interacting populations of heterogeneous oscillators. *Phys. Rev. E*, 77:036107.

[10] Bassett, D. S., Zurn, P., and Gold, J. I. (2018). On the nature and use of models in network neuroscience. *Nature Reviews Neuroscience*, 19(9):566–578.

[11] Benedetto, D., Caglioti, E., and Montemagno, U. (2015). On the complete phase synchronization for the Kuramoto model in the mean-field limit. *Commun. Math. Sci.*, 13(7):1775–1786.

[12] Blekhman, I. I. (1988). *Synchronization in science and technology*. ASME press.

[13] Boccaletti, S., Bianconi, G., Criado, R., Del Genio, C. I., Gómez-Gardenes, J., Romance, M., Sendina-Nadal, I., Wang, Z., and Zanin, M. (2014). The structure and dynamics of multilayer networks. *Physics reports*, 544(1):1–122.

[14] Bodineau, T., Derrida, B., and Lebowitz, J. L. (2010). A diffusive system driven by a battery or by a smoothly varying field. *J. Stat. Phys.*, 140:648–675.

[15] Briggs, J. (1992). *Fractals: The patterns of chaos: A new aesthetic of art, science, and nature*. Simon and Schuster.

[16] Brummitt, C. D., D'Souza, R. M., and Leicht, E. A. (2012). Suppressing cascades of load in interdependent networks. *Proceedings of the national academy of sciences*, 109(12):E680–E689.

[17] Buck, J. and Buck, E. (1968). Mechanism of rhythmic synchronous flashing of fireflies: Fireflies of southeast asia may use anticipatory time-measuring in synchronizing their flashing. *Science*, 159(3821):1319–1327.

[18] Carareto, R., Baptista, M. S., and Grebogi, C. (2013). Natural synchronization in power-grids with anti-correlated units. *Communications in Nonlinear Science and Numerical Simulation*, 18(4):1035–1046.

[19] Cardillo, A., Zanin, M., Gómez-Gardenes, J., Romance, M., García del Amo, A. J., and Boccaletti, S. (2013). Modeling the multi-layer nature of the european air transport network: Resilience and passengers re-scheduling under random failures. *The European Physical Journal Special Topics*, 215(1):23–33.

[20] Caruso, S., Giberti, C., and Rondoni, L. (2020). Dissipation Function: Nonequilibrium Physics and Dynamical Systems. *Entropy*, **22**:835.

[21] Choi, Y.-P., Ha, S.-Y., Jung, S., and Kim, Y. (2012). Asymptotic formation and orbital stability of phase-locked states for the Kuramoto model. *Physica D: Nonlinear Phenomena*, 241(7):735–754.

[22] Choi, Y.-P., Li, Z., Ha, S.-Y., Xue, X., and Yun, S.-B. (2014). Complete entrainment of kuramoto oscillators with inertia on networks via gradient-like flow. *Journal of Differential Equations*, 257(7):2591–2621.

[23] Chopra, N. and Spong, M. W. (2009). On exponential synchronization of kuramoto oscillators. *IEEE transactions on Automatic Control*, 54(2):353–357.

[24] Colangeli, M. and Lucarini, V. (2014). Elements of a unified framework for response formulae. *J. Stat. Mech. Theory Exp.*, 2014:P01002.

[25] Colangeli, M., Maes, C., and Wynants, B. (2011). A meaningful expansion around detailed balance. *J. Phys. A*, 44(9):095001, 13.

[26] Colangeli, M. and Rondoni, L. (2012). Equilibrium, fluctuation relations and transport for irreversible deterministic dynamics. *Physica D: Nonlinear Phenomena*, **241**(6):681–691.

[27] Colangeli, M., Rondoni, L., and Vulpiani, A. (2012). Fluctuation-dissipation relation for chaotic non-Hamiltonian systems. *J. Stat. Mech. Theory Exp.*, 2012:L04002.

[28] Coutinho, B. C., Goltsev, A. V., Dorogovtsev, S. N., and Mendes, J. F. F. (2013). Kuramoto model with frequency-degree correlations on complex networks. *Phys. Rev. E*, 87:032106.

[29] Cumin, D. and Unsworth, C. (2007). Generalizing the Kuramoto model for the study of neuronal synchronization in the brain. *Physica D: Nonlinear Phenomena*, 226(2):181–196.

[30] Dal Cengio, S. and Rondoni, L. (2016). Broken versus non-broken time reversal symmetry: irreversibility and response. *Symmetry*, 8(8):Art. 73, 20.

[31] De Domenico, M., Granell, C., Porter, M. A., and Arenas, A. (2016). The physics of spreading processes in multilayer networks. *Nature Physics*, 12(10):901–906.

[32] Derrida, B. (2007). Non-equilibrium steady states: fluctuations and large deviations of the density and of the current. *J. Stat. Mech. Theory Exp.*, 2007(7):P07023, 45.

[33] Dickison, M. E., Magnani, M., and Rossi, L. (2016). *Multilayer Social Networks*. Cambridge University Press.

[34] Dong, J.-G. and Xue, X. (2013). Synchronization analysis of Kuramoto oscillators. *Commun. Math. Sci.*, 11(2):465–480.

[35] Donges, J. F., Schultz, H. C., Marwan, N., Zou, Y., and Kurths, J. (2011). Investigating the topology of interacting networks. *The European Physical Journal B*, 84(4):635–651.

[36] Dörfler, F. and Bullo, F. (2014). Synchronization in complex networks of phase oscillators: A survey. *Automatica*, 50(6):1539–1564.

[37] Dörfler, F., Chertkov, M., and Bullo, F. (2013). Synchronization in complex oscillator networks and smart grids. *Proceedings of the National Academy of Sciences*, 110(6):2005–2010.

[38] Eckhorn, R., Bauer, R., Jordan, W., Brosch, M., Kruse, W., Munk, M., and Reitboeck, H. (1988). Coherent oscillations: A mechanism of feature linking in the visual cortex? *Biological cybernetics*, 60(2):121–130.

[39] Ermentrout, B. (1991). An adaptive model for synchrony in the firefly pteroptyx malaccae. *Journal of Mathematical Biology*, 29(6):571–585.

[40] Evans, D., Cohen, E., and Morriss, G. (1993). Probability of second law violations in shearing steady flows. *Phys. Rev. Lett.*, 71:2401.

[41] Evans, D. and Morriss, G. (2008). *Statistical Mechanics of Nonequilibrium Liquids*. Cambridge University Press.

[42] Evans, D. and Searles, D. (1994). Equilibrium microstates which generate second law violating steady states. *Phys. Rev. E*, 50:1645–1648.

[43] Evans, D. and Searles, D. (2002). The Fluctuation Theorem. *Advances in Physics*, 51(7):1529–1585.

[44] Evans, D., Searles, D., and Rondoni, L. (2005). Application of the Gallavotti–Cohen fluctuation relation to thermostated steady states near equilibrium. *Phys. Rev. E*, 71:056120.

[45] Evans, D., Searles, D., and Williams, S. (2008). On the fluctuation theorem for the dissipation function and its connection with response theory. *J. Chem. Phys.*, 128(014504).

[46] Evans, D., Williams, S., Searles, D., and Rondoni, L. (2016). On typicality in nonequilibrium steady states. *J. Chem. Phys.*, 128(014504).

[47] Filatrella, G., Nielsen, A. H., and Pedersen, N. F. (2008). Analysis of a power grid using a Kuramoto-like model. *The European Physical Journal B*, 61(4):485–491.

[48] Gallavotti, G. and Cohen, E. (1995). Dynamical ensembles in stationary states. *J. Statist. Phys.*, **80**:931–970.

[49] Gambuzza, L. V., Frasca, M., and Gomez-Gardenes, J. (2015). Intra-layer synchronization in multiplex networks. *EPL (Europhysics Letters)*, 110(2):20010.

[50] Gómez-Gardeñes, J., Moreno, Y., and Arenas, A. (2007). Synchronizability determined by coupling strengths and topology on complex networks. *Physical Review E*, 75(6):066106.

[51] Gómez-Gardenes, J., Reinares, I., Arenas, A., and Floría, L. M. (2012). Evolution of cooperation in multiplex networks. *Scientific reports*, 2(1):1–6.

[52] Granell, C., Gómez, S., and Arenas, A. (2013a). Dynamical interplay between awareness and epidemic spreading in multiplex networks. *Phys. Rev. Lett.*, 111:128701.

[53] Granell, C., Gómez, S., and Arenas, A. (2013b). Dynamical interplay between awareness and epidemic spreading in multiplex networks. *Physical review letters*, 111(12):128701.

[54] Gray, C. M., König, P., Engel, A. K., and Singer, W. (1989). Oscillatory responses in cat visual cortex exhibit inter-columnar synchronization which reflects global stimulus properties. *Nature*, 338(6213):334–337.

[55] Gupta, S., Campa, A., and Ruffo, S. (2014). Nonequilibrium first-order phase transition in coupled oscillator systems with inertia and noise. *Phys. Rev. E*, 89:022123.

[56] Ha, S., Ko, D., Park, J., and Zhang, X. (2016a). Collective synchronization of classical and quantum oscillators. *EMS Surv. Math. Sci.*, 3(2):209–267.

[57] Ha, S.-Y., Ha, T., and Kim, J.-H. (2010). On the complete synchronization of the Kuramoto phase model. *Physica D: Nonlinear Phenomena*, 239(17):1692–1700.

[58] Ha, S.-Y., Ko, D., Park, J., and Ryoo, S. W. (2016b). Emergent dynamics of Winfree oscillators on locally coupled networks. *Journal of Differential Equations*, 260(5):4203–4236.

[59] Ha, S.-Y., Lattanzio, C., Rubino, B., and Slemrod, M. (2011). Flocking and synchronization of particle models. *Quarterly of applied mathematics*, 69(1):91–103.

[60] Ha, S.-Y. and Li, Z. (2014). Complete synchronization of kuramoto oscillators with hierarchical leadership. *Communications in Mathematical Sciences*, 12(3):485–508.

[61] Ha, S.-Y., Li, Z., and Xue, X. (2013). Formation of phase-locked states in a population of locally interacting Kuramoto oscillators. *J. Differential Equations*, 255(10):3053–3070.

[62] Ha, S.-Y., Noh, S. E., and Park, J. (2015). Practical synchronization of generalized Kuramoto systems with an intrinsic dynamics. *Networks & Heterogeneous Media*, 10(4):787.

[63] Hong, H., Choi, M. Y., and Kim, B. J. (2002). Synchronization on small-world networks. *Phys. Rev. E*, 65:026139.

[64] Horvát, E.-Á. and Zweig, K. A. (2013). A fixed degree sequence model for the one-mode projection of multiplex bipartite graphs. *Social Network Analysis and Mining*, 3(4):1209–1224.

[65] Huygens, C. (1888). *Oeuvres complètes de Christiaan Huygens*, volume 5, page 456. Societe Hollandaise DesSciences, Martinus Nijhoff, La Haye.

[66] Jepps, O. and Rondoni, L. (2016). A dynamical-systems interpretation of the dissipation function, T-mixing and their relation to thermodynamic relaxation. *J. Phys. A: Math. Theor.*, **49**:154002.

[67] Jiang, X., Li, M., Zheng, Z., Ma, Y., and Ma, L. (2015). Effect of externality in multiplex networks on one-layer synchronization. *Journal of the Korean Physical Society*, 66(11):1777–1782.

[68] Kachhvah, A. D. and Jalan, S. (2017). Multiplexing induced explosive synchronization in Kuramoto oscillators with inertia. *EPL (Europhysics Letters)*, 119(6):60005.

[69] Kawamura, Y., Nakao, H., Arai, K., Kori, H., and Kuramoto, Y. (2010). Phase synchronization between collective rhythms of globally coupled oscillator groups: Noiseless nonidentical case. *Chaos: An Interdisciplinary Journal of Nonlinear Science*, 20(4):043110.

[70] Khanra, P. and Pal, P. (2021). Explosive synchronization in multilayer networks through partial adaptation. *Chaos, Solitons and Fractals*, 143:110621.

[71] Kim, J., Yang, J., Kim, J., and Shim, H. (2012). Practical consensus for heterogeneous linear time-varying multi-agent systems. In *2012 12th International Conference on Control, Automation and Systems*, pages 23–28.

[72] Kiss, I. Z., Zhai, Y., and Hudson, J. L. (2002). Emerging coherence in a population of chemical oscillators. *Science*, 296(5573):1676–1678.

[73] Kivelä, M., Arenas, A., Barthelemy, M., Gleeson, J. P., Moreno, Y., and Porter, M. A. (2014). Multilayer networks. *Journal of complex networks*, 2(3):203–271.

[74] Kopell, N. and Ermentrout, G. (1986). Symmetry and phaselocking in chains of weakly coupled oscillators. *Communications on Pure and Applied Mathematics*, 39(5):623–660.

[75] Krackhardt, D. (1987). Cognitive social structures. *Social networks*, 9(2):109–134.

[76] Krantz, S. G. and Parks, H. R. (2002). *A primer of real analytic functions*. Springer Science & Business Media.

[77] Kubo, R. (1966). The fluctuation-dissipation theorem. *Rep. Prog. Phys.*, **29**:255–284.

[78] Kuramoto, Y. (1975). Self-entrainment of a population of coupled non-linear oscillators. In *International Symposium on Mathematical Problems in Theoretical Physics*, pages 420–422. Springer-Verlag.

[79] Kuramoto, Y. (1984). *Chemical oscillations, waves, and turbulence*. Springer Series in Synergetics. Springer-Verlag, Berlin.

[80] León, I. and Pazó, D. (2019). Phase reduction beyond the first order: The case of the mean-field complex ginzburg-landau equation. *Physical Review E*, 100(1):012211.

[81] Lewis, K., Kaufman, J., Gonzalez, M., Wimmer, A., and Christakis, N. (2008). Tastes, ties, and time: A new social network dataset using facebook. com. *Social networks*, 30(4):330–342.

[82] Łojasiewicz, S. (1963). Une propriété topologique des sous-ensembles analytiques réels. *Les équations aux dérivées partielles*, 117:87–89.

[83] Lu, W. and Atay, F. M. (2018). Stability of phase difference trajectories of networks of kuramoto oscillators with time-varying couplings and intrinsic frequencies. *SIAM Journal on Applied Dynamical Systems*, 17(1):457–483.

[84] Lucarini, V. and Colangeli, M. (2012). Beyond the linear fluctuation-dissipation theorem: the role of causality. *J. Stat. Mech. Theory Exp.*, 2012:P05013.

[85] Maksimenko, V. A., Makarov, V. V., Bera, B. K., Ghosh, D., Dana, S. K., Goremyko, M. V., Frolov, N. S., Koronovskii, A. A., and Hramov, A. E. (2016). Excitation and suppression of chimera states by multiplexing. *Phys. Rev. E*, 94:052205.

[86] Marconi, U., Puglisi, A., Rondoni, L., and Vulpiani, A. (2008). Fluctuation–dissipation: Response theory in statistical physics. *Physics Reports*, **461**:111–195.

[87] Menara, T., Baggio, G., Bassett, D. S., and Pasqualetti, F. (2019). Stability conditions for cluster synchronization in networks of heterogeneous kuramoto oscillators. *IEEE Transactions on Control of Network Systems*, 7(1):302–314.

[88] Michaels, D. C., Matyas, E. P., and Jalife, J. (1987). Mechanisms of sinoatrial pacemaker synchronization: a new hypothesis. *Circulation research*, 61(5):704–714.

[89] Mirollo, R. E. and Strogatz, S. H. (1990). Synchronization of pulse-coupled biological oscillators. *SIAM Journal on Applied Mathematics*, 50(6):1645–1662.

[90] Montbrió, E., Kurths, J., and Blasius, B. (2004). Synchronization of two interacting populations of oscillators. *Physical Review E*, 70(5):056125.

[91] Monzón, P. and Paganini, F. (2005). Global considerations on the kuramoto model of sinusoidally coupled oscillators. In *Proceedings of the 44th IEEE Conference on Decision and Control*, pages 3923–3928. IEEE.

[92] Motter, A. E., Myers, S. A., Anghel, M., and Nishikawa, T. (2013). Spontaneous synchrony in power-grid networks. *Nature Physics*, 9(3):191–197.

[93] Motter, A. E., Zhou, C., and Kurths, J. (2005). Network synchronization, diffusion, and the paradox of heterogeneity. *Physical Review E*, 71(1):016116.

[94] Nase, G., Singer, W., Monyer, H., and Engel, A. K. (2003). Features of neuronal synchrony in mouse visual cortex. *Journal of Neurophysiology*, 90(2):1115–1123.

[95] Néda, Z., Ravasz, E., Brechet, Y., Vicsek, T., and Barabási, A.-L. (2000). The sound of many hands clapping. *Nature*, 403(6772):849–850.

[96] Okuda, K. and Kuramoto, Y. (1991). Mutual entrainment between populations of coupled oscillators. *Progress of theoretical physics*, 86(6):1159–1176.

[97] Ott, E. and Antonsen, T. M. (2008). Low dimensional behavior of large systems of globally coupled oscillators. *Chaos: An Interdisciplinary Journal of Nonlinear Science*, 18(3):037113.

[98] Ott, E. and Antonsen, T. M. (2009). Long time evolution of phase oscillator systems. *Chaos: An interdisciplinary journal of nonlinear science*, 19(2):023117.

[99] Panaggio, M. J. and Abrams, D. M. (2015). Chimera states: coexistence of coherence and incoherence in networks of coupled oscillators. *Nonlinearity*, 28(3):R67.

[100] Panteley, E., Loria, A., and El Ati, A. (2015). On the stability and robustness of stuart-landau oscillators. *IFAC-PapersOnLine*, 48(11):645–650.

[101] Pazó, D. and Montbrió, E. (2014). Low-dimensional dynamics of populations of pulse-coupled oscillators. *Phys. Rev. X*, 4:011009.

[102] Pazó, D., Montbrió, E., and Gallego, R. (2019). The winfree model with heterogeneous phase-response curves: analytical results. *Journal of Physics A: Mathematical and Theoretical*, 52(15):154001.

[103] Perko, L. (2006). *Differential equations and dynamical systems*. Springer-Verlag New York.

[104] Peron, T. D. and Rodrigues, F. A. (2011). Collective behavior in financial markets. *EPL (Europhysics Letters)*, 96(4):48004.

[105] Petkoski, S. and Stefanovska, A. (2012). Kuramoto model with time-varying parameters. *Phys. Rev. E*, 86:046212.

[106] Pikovsky, A., Kurths, J., Rosenblum, M., Kurths, J., Chirikov, B., Press, C. U., Cvitanovic, P., Moss, F., and Swinney, H. (2001). *Synchronization: A Universal Concept in Nonlinear Sciences*. Cambridge Nonlinear Science Series. Cambridge University Press.

[107] Pikovsky, A. and Rosenblum, M. (2008). Partially integrable dynamics of hierarchical populations of coupled oscillators. *Phys. Rev. Lett.*, 101:264103.

[108] Pluchino, A., Boccaletti, S., Latora, V., and Rapisarda, A. (2006). Opinion dynamics and synchronization in a network of scientific collaborations. *Physica A: Statistical Mechanics and its Applications*, 372(2):316–325.

[109] Pluchino, A., Latora, V., and Rapisarda, A. (2005). Changing opinions in a changing world: A new perspective in sociophysics. *International Journal of Modern Physics C*, 16(04):515–531.

[110] Ren, X., Brodovskaya, A., Hudson, J. L., and Kapur, J. (2021). Connectivity and neuronal synchrony during seizures. *Journal of Neuroscience*, 41(36):7623–7635.

[111] Rodrigues, F. A., Peron, T. K. D., Ji, P., and Kurths, J. (2016). The kuramoto model in complex networks. *Physics Reports*, 610:1–98.

[112] Ruelle, D. (1998). General linear response formula in statistical mechanics, and the fluctuation-dissipation theorem far from equilibrium. *Physics Letters A*, **245**:220–224.

[113] Saxena, G., Prasad, A., and Ramaswamy, R. (2012). Amplitude death: The emergence of stationarity in coupled nonlinear systems. *Physics Reports*, 521(5):205–228. Amplitude Death: The Emergence of Stationarity in Coupled Nonlinear Systems.

[114] Schaub, M. T., O'Clery, N., Billeh, Y. N., Delvenne, J.-C., Lambiotte, R., and Barahona, M. (2016). Graph partitions and cluster synchronization in networks of oscillators. *Chaos: An Interdisciplinary Journal of Nonlinear Science*, 26(9):094821.

[115] Searles, D., Rondoni, L., and Evans, D. (2007). The steady state fluctuation relation for the dissipation function. *J. Stat. Phys.*, 128(6):1337–1363.

[116] Sheeba, J. H., Chandrasekar, V., Stefanovska, A., and McClintock, P. V. (2009). Asymmetry-induced effects in coupled phase-oscillator ensembles: Routes to synchronization. *Physical Review E*, 79(4):046210.

[117] Singer, W. (1999). Neuronal synchrony: a versatile code for the definition of relations? *Neuron*, 24(1):49–65.

[118] Singer, W. (2018). The role of oscillations and synchrony in the development of the nervous system. In *Emergent Brain Dynamics. Prebirth to Adolescence. Strüngmann Forum Reports*, pages 15–32. MIT Press.

[119] Sorrentino, F. and Ott, E. (2007). Network synchronization of groups. *Physical Review E*, 76(5):056114.

[120] Strogatz, S. (2000). From Kuramoto to Crawford: exploring the onset of synchronization in populations of coupled oscillators. *Physica D: Nonlinear Phenomena*, 143(1):1–20.

[121] Strogatz, S. (2012). *Sync: How Order Emerges from Chaos In the Universe, Nature, and Daily Life*. Hachette Books.

[122] Strogatz, S. H. and Mirollo, R. E. (1991). Stability of incoherence in a population of coupled oscillators. *Journal of Statistical Physics*, 63(3):613–635.

[123] Strogatz, S. H. and Stewart, I. (1993). Coupled oscillators and biological synchronization. *Scientific American*, 269(6):102–109.

[124] Tanaka, H.-A., Lichtenberg, A. J., and Oishi, S. (1997). First order phase transition resulting from finite inertia in coupled oscillator systems. *Phys. Rev. Lett.*, 78:2104–2107.

[125] Tang, Y., Qian, F., Gao, H., and Kurths, J. (2014). Synchronization in complex networks and its application–a survey of recent advances and challenges. *Annual Reviews in Control*, 38(2):184–198.

[126] Telenczuk, B., Nikulin, V. V., and Curio, G. (2010). Role of neuronal synchrony in the generation of evoked eeg/meg responses. *Journal of neurophysiology*, 104(6):3557–3567.

[127] Tiberi, L., Favaretto, C., Innocenti, M., Bassett, D. S., and Pasqualetti, F. (2017). Synchronization patterns in networks of kuramoto oscillators: A geometric approach for analysis and control. In *2017 IEEE 56th Annual Conference on Decision and Control (CDC)*, pages 481–486. IEEE.

[128] Tong, D., Rao, P., Chen, Q., Ogorzalek, M. J., and Li, X. (2018). Exponential synchronization and phase locking of a multilayer Kuramoto-oscillator system with a pacemaker. *Neurocomputing*, 308:129–137.

[129] Tsuda, S. and Jones, J. (2011). The emergence of synchronization behavior in physarum polycephalum and its particle approximation. *Biosystems*, 103(3):331–341.

[130] Vasudevan, K., Cavers, M., and Ware, A. (2015). Earthquake sequencing: Chimera states with kuramoto model dynamics on directed graphs. *Nonlinear Processes in Geophysics*, 22(5):499–512.

[131] Verheijck, E. E., Wilders, R., Joyner, R. W., Golod, D. A., Kumar, R., Jongsma, H. J., Bouman, L. N., and Ginneken, A. C. v. (1998). Pacemaker synchronization of electrically coupled rabbit sinoatrial node cells. *The Journal of general physiology*, 111(1):95–112.

[132] Wasserman, S., Faust, K., et al. (1994). Social network analysis: Methods and applications.

[133] Watts, D. J. and Strogatz, S. H. (1998). Collective dynamics of 'small-world'networks. *nature*, 393(6684):440–442.

[134] Winfree, A. T. (1967). Biological rhythms and the behavior of populations of coupled oscillators. *Journal of theoretical biology*, 16(1):15–42.

[135] Winfree, A. T. (1980). *The geometry of biological time*, volume 2. Springer.

[136] Woo, J. H., Honey, C. J., and Moon, J.-Y. (2020). Phase and amplitude dynamics of coupled oscillator systems on complex networks. *Chaos: An Interdisciplinary Journal of Nonlinear Science*, 30(12):121102.

[137] Wu, J. and Li, X. (2020). Collective synchronization of Kuramoto-oscillator networks. *IEEE Circuits and Systems Magazine*, 20(3):46–67.

[138] Wu, L., Pota, H. R., and Petersen, I. R. (2019). Synchronization conditions for a multirate kuramoto network with an arbitrary topology and nonidentical oscillators. *IEEE Transactions on Cybernetics*, 49(6):2242–2254.

[139] Wu, Y. (2017). Weak synchronization and large-scale collective oscillation in dense bacterial suspensions. In *APS March Meeting Abstracts*, volume 2017, pages A6–010.

[140] Yeung, M. S. and Strogatz, S. H. (1999). Time delay in the Kuramoto model of coupled oscillators. *Physical Review Letters*, 82(3):648.

[141] Zhang, J. and Zhu, J. (2021). Synchronization of high-dimensional Kuramoto models with nonidentical oscillators and interconnection digraphs. *IET Control Theory & Applications*.

[142] Zhang, X., Boccaletti, S., Guan, S., and Liu, Z. (2015). Explosive synchronization in adaptive and multilayer networks. *Physical review letters*, 114(3):038701.